

THE POLARIZATION PROPERTIES OF THE FINAL STATE PARTICLES IN
THE RARE RADIATIVE B-MESON DECAYS

A THESIS SUBMITTED TO
THE GRADUATE SCHOOL OF NATURAL AND APPLIED SCIENCES
OF
MIDDLE EAST TECHNICAL UNIVERSITY

BY

ÜMİT OKTAY YILMAZ

IN PARTIAL FULFILLMENT OF THE REQUIREMENTS

FOR

THE DEGREE OF DOCTOR OF PHILOSOPHY

IN

PHYSICS

MAY 2005

Approval of the Graduate School of Natural and Applied Sciences.

Prof. Dr. Canan ÖZGEN
Director

I certify that this thesis satisfies all the requirements as a thesis for the degree of Doctor of Philosophy.

Prof. Dr. Sinan BİLİKMEN
Head of Department

This is to certify that we have read this thesis and that in our opinion it is fully adequate, in scope and quality, as a thesis for the degree of Doctor of Philosophy.

Prof. Dr. Gürsevil TURAN
Supervisor

Examining Committee Members

Prof. Dr. Mehmet ABAK (Hacettepe University, PHYS) _____

Prof.Dr. Gürsevil TURAN (METU, PHYS) _____

Prof.Dr.Mustafa SAVCI (METU, PHYS) _____

Prof. Dr. Saleh SULTANSOY (Gazi University, PHYS) _____

Assoc. Prof. Dr. Meltem SERIN ZEYREK (METU, PHYS) _____

I hereby declare that all information in this document has been obtained and presented in accordance with academic rules and ethical conduct. I also declare that, as required, I have fully cited and referenced all material and results that are not original to this work.

Name Lastname : Ümit Oktay YILMAZ

Signature :

ABSTRACT

THE POLARIZATION PROPERTIES OF THE FINAL STATE PARTICLES IN THE RARE RADIATIVE B-MESON DECAYS

YILMAZ, Ümit Oktay

Ph. D., Department of Physics

Supervisor: Prof. Dr. Gürsevil TURAN

May 2005, 83 pages.

A general analysis of the photon and lepton polarizations in the rare $B_s \rightarrow \gamma \ell^+ \ell^-$ decay by using the most general model independent form of the effective Hamiltonian is presented. The total and the differential branching ratios for these decays, when photon is in the positive and negative helicity states, are studied. The sensitivity of "photon polarization asymmetry" and the longitudinal, transverse and normal polarization asymmetries of final state leptons, as well as lepton-antilepton combined asymmetries in $B_s \rightarrow \gamma \ell^+ \ell^-$ decay to the new Wilson coefficients are also investigated.

It is shown that all these physical observables are very sensitive to the existence of new physics beyond SM and their experimental measurements can give valuable information about it.

Keywords: Flavor Changing Neutral Current, Semileptonic Decay, Rare Radiative Decay, Photon Polarization, Lepton Polarization

ÖZ

NADİR IŞINIMLI B-MESON BOZUNUMLARINDA ORTAYA ÇIKAN PARÇACIKLARIN POLARİZASYON ÖZELLİKLERİ

YILMAZ, Ümit Oktay

Doktora, Fizik Bölümü

Tez Yöneticisi: Prof. Dr. Gürsevil TURAN

Mayıs 2005, 83 sayfa.

Etkin Hamiltonun modelden bağımsız en genel formunu kullanarak nadir $B_s \rightarrow \gamma \ell^+ \ell^-$ bozunmasındaki foton ve lepton polarizasyonlarının genel bir çözümlemesi sunuldu. Bu bozunmaların, fotonun pozitif ve negatif helisite durumundaki toplam ve difransiyel dallanma oranları çalışıldı. Ayrıca $B_s \rightarrow \gamma \ell^+ \ell^-$ bozunmasında "foton polarizasyon asimetrisinin" ve son durum leptonlarının paralel, çapraz ve dik polarizasyon asimetrisi, bunun yanı sıra lepton-antilepton birleşik asimetrisinin yeni Wilson katsayılarına hassasiyetleri incelendi.

Tüm bu fiziksel gözlenebilirlerin SM ötesinde var olan yeni fiziğe hassas oldukları ve deneysel ölçümlerinin değerli bilgiler verebileceği gösterildi.

Anahtar Sözcükler: Çeşni Değiştiren Nötr Akımlar, Yarıleptonik Bozunum, Nadir Işınımlı Bozunma, Foton Polarizasyonu, Lepton Polarizasyonu.

ACKNOWLEDGMENTS

I am grateful to my supervisor Prof. Dr. Gürsevil TURAN; first of all for introducing me to the subject matter of this thesis and her stimulating guidance as well as critical comments, advices and patience throughout all stages of my thesis.

I am also grateful to Prof. Dr. Saleh SULTANSOY for his valuable support, suggestions and encouragement.

I am thankful to Dr. B. Berin ŞİRVANLI for her effective collaborations and friendly attitude.

My thanks are for the members of Middle East Technical University Department of Physics for their helps throughout my education.

My special thanks are for the director, the administrative staff and the teachers of Demetevler Mimar Sinan High School, Ankara for their patience and understanding during my studies.

And my friends, who I have ever found nearby anytime I need, thanks for your friendship and sorry for not being able to write all your names here.

At the end, but not least, I want to express my grateful sense to my wife Müjgan ERGÜL YILMAZ for her patience and supports.

This thesis was partially supported by Middle East Technical University, The School of Natural and Applied Science Grant No: BAP-2002-07-02-00-21.

TABLE OF CONTENTS

	PLAGIARISM	iii
	ABSTRACT	iv
	ÖZ	v
	ACKNOWLEDGMENTS	vi
	TABLE OF CONTENTS	vii
	LIST OF TABLES	ix
	LIST OF FIGURES	x
CHAPTER		
1	INTRODUCTION	1
2	RARE B-MESON DECAYS	6
2.1	The Structure of Standard Model	6
2.1.1	Flavor Mixing	14
2.1.2	Neutral Current and Flavor Changing Neutral Current	17
2.1.3	Unsatisfactory Features of the SM	19
2.2	Rare B Meson Decays	21
2.3	The Effective Hamiltonian Theory	22
3	MODEL INDEPENDENT ANALYSIS OF $B_S \rightarrow \gamma \ell^+ \ell^-$ DECAYS	31
3.1	Effective Hamiltonian	33
3.2	Matrix Elements and the Decay Rate	34

4	PHOTON POLARIZATIONS IN $B_S \rightarrow \gamma \ell^+ \ell^-$ DECAY	41
4.1	Photon Polarization	41
4.2	Numerical Analysis and Discussion	45
5	LEPTON POLARIZATIONS IN $B_S \rightarrow \gamma \ell^+ \ell^-$ DECAY	57
5.1	Lepton Polarization Asymmetry	57
5.2	Lepton Anti-lepton Combined Asymmetries	62
5.3	Numerical Analysis	65
6	DISCUSSION AND CONCLUSION	74
	REFERENCES	78
	APPENDIX	
A	INPUT PARAMETERS	82

LIST OF TABLES

2.1	The $SU(3)_C$ matrices.	7
2.2	Lepton quantum numbers	8
2.3	Quark quantum numbers	9
2.4	Values of the SM Wilson coefficients at $\mu \sim m_b$ scale.	29
2.5	Charmonium ($\bar{c}c$) masses and widths [32].	30

LIST OF FIGURES

2.1	The basic vertices representing the interactions of the quarks with the gauge bosons. The labels i and j represent the flavour quantum number ($i, j = u, d, c, s, t, b$).	17
2.2	Examples of penguin diagrams which contribute to the FCNC process $b \rightarrow s$. Diagrams (a) and (b) are electroweak penguins graphs, and diagram (c) is a gluonic penguin graph.	18
2.3	Examples of box diagrams.	19
2.4	Typical leading logarithmic order penguin and box diagrams in the SM.	25
4.1	The dependence of the integrated branching ratio for the $B_s \rightarrow \gamma \mu^+ \mu^-$ decay with photon in positive helicity state on the new Wilson coefficients with LD effects	50
4.2	The dependence of the integrated branching ratio for the $B_s \rightarrow \gamma \mu^+ \mu^-$ decay with photon in negative helicity state on the new Wilson coefficients with LD effects	50
4.3	The dependence of the differential branching ratio for the $B_s \rightarrow \gamma \mu^+ \mu^-$ decay with photon in the positive helicity state on the dimensionless variable $x = 2E_\gamma/m_B$ at different values of vector interaction with coefficient C_{LL} without LD effects.	51
4.4	The same as Fig.(4.3), but with photon in the negative helicity state.	51
4.5	The dependence of the differential branching ratio for the $B_s \rightarrow \gamma \mu^+ \mu^-$ decay with photon in the positive helicity state on the dimensionless variable $x = 2E_\gamma/m_B$ at different values of tensor interaction with coefficient C_{TE} without LD effects.	52
4.6	The same as Fig.(4.5), but with photon in the negative helicity state.	52
4.7	The dependence of the differential branching ratio for the $B_s \rightarrow \gamma \mu^+ \mu^-$ decay with photon in the positive helicity state on the dimensionless variable $x = 2E_\gamma/m_B$ at different values of scalar interaction with coefficient C_{RLRL} without LD effects.	53
4.8	The same as Fig.(4.7), but with photon in the negative helicity state.	53
4.9	The dependence of the integrated photon polarization asymmetry for the $B_s \rightarrow \gamma \mu^+ \mu^-$ decay on the new Wilson coefficients with LD effects.	54

4.10	The dependence of the differential photon polarization asymmetry for the $B_s \rightarrow \gamma \mu^+ \mu^-$ decay on the dimensionless variable $x = 2E_\gamma/m_B$ for different values of C_{RL} without LD effects.	54
4.11	The dependence of the integrated branching ratio for the $B_s \rightarrow \gamma \tau^+ \tau^-$ decay with photon in the positive helicity state on the new Wilson coefficients with LD effects.	55
4.12	The same as Fig.(4.11), but with photon in negative helicity state.	55
4.13	The dependence of the integrated photon polarization asymmetry for the $B_s \rightarrow \gamma \tau^+ \tau^-$ decay on the new Wilson coefficients with LD effects.	56
4.14	The dependence of the differential photon polarization asymmetry for the $B_s \rightarrow \gamma \tau^+ \tau^-$ decay on the dimensionless variable $x = 2E_\gamma/m_B$ for different values of C_{LRRL} without LD effects.	56
5.1	The dependence of the averaged longitudinal polarization $\langle P_L^- \rangle$ of ℓ^- for the $B_s \rightarrow \gamma \mu^+ \mu^-$ decay on the new Wilson coefficients .	68
5.2	The dependence of the combined averaged longitudinal lepton polarization $\langle P_L^- + P_L^+ \rangle$ for the $B_s \rightarrow \gamma \mu^+ \mu^-$ decay on the new Wilson coefficients	68
5.3	The same as Fig.(5.1), but for the $B_s \rightarrow \gamma \tau^+ \tau^-$ decay	69
5.4	The same as Fig.(5.2), but for the $B_s \rightarrow \gamma \tau^+ \tau^-$ decay.	69
5.5	The dependence of the averaged transverse polarization $\langle P_T^- \rangle$ of ℓ^- for the $B_s \rightarrow \gamma \mu^+ \mu^-$ decay on the new Wilson coefficients. The line convention is the same as before.	70
5.6	The dependence of the combined averaged transverse lepton polarization $\langle P_T^- - P_T^+ \rangle$ for the $B_s \rightarrow \gamma \mu^+ \mu^-$ decay on the new Wilson coefficients. The line convention is the same as before. . .	70
5.7	The same as Fig.(5.5), but for the $B_s \rightarrow \gamma \tau^+ \tau^-$ decay.	71
5.8	The same as Fig.(5.6), but for the $B_s \rightarrow \gamma \tau^+ \tau^-$ decay.	71
5.9	The dependence of the averaged normal polarization $\langle P_N^- \rangle$ of ℓ^- for the $B_s \rightarrow \gamma \mu^+ \mu^-$ decay on the new Wilson coefficients . . .	72
5.10	The dependence of the combined averaged normal lepton polarization $\langle P_N^- + P_N^+ \rangle$ for the $B_s \rightarrow \gamma \mu^+ \mu^-$ decay on the new Wilson coefficients.	72
5.11	The same as Fig.(5.10), but for the $B_s \rightarrow \gamma \tau^+ \tau^-$ decay.	73
5.12	The same as Fig. (5.10), but for the $B_s \rightarrow \gamma \tau^+ \tau^-$ decay.	73

CHAPTER 1

INTRODUCTION

The "Standard Model" (SM) of elementary particle physics [1], which is a renormalizable relativistic quantum field theory based on non-Abelian gauge symmetry of the gauge group $SU(3)_C \times SU(2)_L \times U(1)_Y$, leads the progress of understanding the weak, electromagnetic, and strong interactions in the past half-century. It has been very successful phenomenologically and all experiments confirm its predictions within the existing experimental and theoretical uncertainties, with the exception of neutrino oscillations. Therefore, in the experimental sense there is not much motivation for moving beyond the SM. However, there are some conceptual problems with the structure of the SM, such as, number of free parameters, the origin of mass and Higgs sector of the theory, the "hierarchy" problem, not including the gravity, origin of CP violation, etc. Therefore, it is widely believed that when the precision of experiments and also theoretical tools improve, signals of new physics beyond the SM will appear. There are several classes of extended models which address the conceptual open questions of the SM, such as the minimal supersymmetric model (MSSM), the two Higgs doublet model (2HDM), left-right symmetric models, fourth generation models, extra dimensions, etc.

Rare B decays have always a special place for providing the essential information about the structure of the SM and particle physics in general. By rare decays, it is meant decays which do not include the release of a c quark into the final state. These may include both the so-called Cabibbo-suppressed decays, such as those mediated by the transition $b \rightarrow uW^-$ and flavor changing neutral current (FCNC) decays; that is, decays via the currents that change the flavor but not the charge of the quark. In the SM, the neutral currents are mediated through the gauge bosons Z^0, γ, g , and do not change flavor. Therefore, FCNC processes

are absent in the SM at tree level. However, they may appear at the loop level through the box and penguin diagrams. These loop effects are sensitive to the masses and other properties of the internal particles. Other massive particles which are not present in the SM, like a fourth generation fermions, supersymmetric particles, or others, may also contribute to these decays in the same way therefore can be studied in a rare B decay at energies which are much lower than the direct production energies of such particles. Then, it becomes possible to compare the SM predictions for such a rare B decay with the experimental result. Any possible discrepancy between them signals the existence and the structure of the new physics beyond the SM. Thus, rare B-decays are very useful tools for extracting new physics beyond SM, as well as providing the essential information about the poorly studied aspects of it, particularly Cabibbo-Kobayashi-Maskawa (CKM) matrix elements, leptonic decay constants, etc.

The experimental situation concerning rare B decays is also quite promising. Some rare decays have already been measured. CLEO [2], BaBar [3] and BELLE [4] experiments determined the inclusive $B \rightarrow X_s \gamma$ and the exclusive $B \rightarrow K^* \gamma$ channels with the world average branching ratio (BR) [5, 6]

$$\begin{aligned}
BR(B \rightarrow X_s \gamma) &= (3.34 \pm 0.38) \times 10^{-4}, \\
BR(B^0 \rightarrow K^{*0} \gamma) &= (4.17 \pm 0.23) \times 10^{-5}, \\
BR(B^+ \rightarrow K^{*+} \gamma) &= (4.18 \pm 0.32) \times 10^{-5}.
\end{aligned}
\tag{1.1}$$

More recently, both BELLE [7] and BaBar [8] have announced a clear evidence of the $B \rightarrow X_s \ell^+ \ell^-$ and $B \rightarrow K^{(*)} \ell^+ \ell^-$ decays, whose average BRs are [6]

$$\begin{aligned}
BR(B \rightarrow X_s \ell^+ \ell^-) &= (6.2 \pm 1.1) \times 10^{-6}, \\
BR(B \rightarrow K \ell^+ \ell^-) &= (5.85 \pm 0.4) \times 10^{-7}, \\
BR(B \rightarrow K^* \ell^+ \ell^-) &= (10.2 \pm 1.2) \times 10^{-7},
\end{aligned}
\tag{1.2}$$

Among the rare B-meson decays, the semileptonic $B_s \rightarrow \gamma \ell^+ \ell^-$ ($\ell = e, \mu, \tau$) decays are especially interesting due to their relative cleanliness and sensitivity to new physics. $B_s \rightarrow \gamma \ell^+ \ell^-$ decay is induced by $B \rightarrow \ell^+ \ell^-$ one, which can

in principle serve as a useful process to determine the fundamental parameters of the SM since the only non-perturbative quantity in its theoretical calculation is the decay constant f_{B_s} , which is reliably known. However, in the SM, matrix element of $B \rightarrow \ell^+\ell^-$ decay is proportional to the lepton mass and therefore corresponding branching ratio will be helicity suppressed. Although $\ell = \tau$ channel is free from this suppression, its experimental observation is quite difficult due to low efficiency. In the radiative $B_s \rightarrow \gamma\ell^+\ell^-$ decay, photon emitted from any of the charged lines in addition to the lepton pair makes it possible to overcome the helicity suppression which in turn makes its branching ratio to be larger than purely leptonic modes. For that reason, the investigation of the $B_s \rightarrow \gamma\ell^+\ell^-$ decays becomes interesting.

The main tool to calculate rare B decays by including the perturbative QCD corrections is the effective Hamiltonian, $\mathcal{H}_{eff} \sim \sum C_i O_i$, method. In this program starting with an operator product expansion (OPE) and performing a renormalization group equation (RGE) analysis, the heavy degrees of freedom, W^\pm, H, t quark, are integrated out [9]-[17]. In this way it becomes possible to factorize low energy weak processes in terms of perturbative short-distance Wilson coefficients C_i from the long-distance operator matrix elements $\langle O_i \rangle$.

In this work, we will investigate the new physics effects in the $B_s \rightarrow \gamma\ell^+\ell^-$ decay. In rare B-meson decays, the new physics effects can appear in two different ways: one way is through new contributions to the Wilson coefficients that are already present in the SM, and the other is through the new operators in the effective Hamiltonian, which is absent in the SM. Here, we use the most general effective Hamiltonian that combines both these approaches and includes the scalar and tensor type interactions as well as the vector types.

As an exclusive process, the theoretical calculation of $B_s \rightarrow \gamma\ell^+\ell^-$ decay requires the additional knowledge about the decay form factors. These are the matrix elements of the effective Hamiltonian between the initial B and final photon states, when a photon is released from the initial quark lines, which give rise to the so called "structure dependent" (SD) contributions to the amplitude, and

between the B and the vacuum states for the "internal Bremsstrahlung" (IB) part, which arises when a photon is radiated from final leptons. Finding these hadronic transition matrix elements is related to the nonperturbative sector of the QCD and should be calculated by means of a nonperturbative approach. Thus, their theoretical calculation yields the main uncertainty in the prediction of the exclusive rare decays. The form factors for B decays into γ and a vacuum state have been calculated in the framework of light-cone QCD sum rules in [18, 19] and in the framework of the light front quark model in [20]. In addition, a model has been proposed a model in [21] for the $B \rightarrow \gamma$ form factors which obey all the restrictions obtained from the gauge invariance combined with the large energy effective theory.

In this work, we have mainly focused on polarization properties of the final state particles, namely photon and lepton pairs in $B_s \rightarrow \gamma \ell^+ \ell^-$ decay, and their effects to the observable quantities of the same decay. In this connection, we have studied the photon and lepton polarization asymmetries as well as the polarized branching ratios of $B_s \rightarrow \gamma \ell^+ \ell^-$ decay as a function of various new Wilson coefficients. Along this line, the polarization asymmetries of the final state lepton in $B_s \rightarrow \gamma \ell^+ \ell^-$ decays have been studied in MSSM in [22] and concluded that they can be very useful for accurate determination of various Wilson coefficients.

The thesis is organized as follows: In Chapter 2, after a brief overview of the SM, we present an introduction to rare B decays. There, we have also briefly discuss the effective Hamiltonian theory. In Chapter 3, we start our model independent analysis of the radiative rare $B_s \rightarrow \gamma \ell^+ \ell^-$ decay. After presenting the most general effective Hamiltonian, we give the hadronic matrix elements and then calculate some analytical expressions like the decay rate, etc., that are necessary in the next two chapters. In Chapter 4, we consider the photon polarizations in $B_s \rightarrow \gamma \ell^+ \ell^-$ decay and calculate the differential decay width and the photon polarization asymmetry for this decay when the photon is in positive and negative helicity states. In Chapter 5, a general analysis of the lepton polarizations in the rare $B_s \rightarrow \gamma \ell^+ \ell^-$ decay is given. We mainly investigate the

sensitivity of the longitudinal, transverse and normal polarizations of final state leptons, as well as lepton-antilepton combined asymmetries, on the new Wilson coefficients. Finally, Chapter 6 is devoted to a summary and the conclusion of the thesis.

CHAPTER 2

RARE B-MESON DECAYS

In this chapter we first outline the structure of the SM. We discuss the CKM mixing matrix and the importance of studying FCNC transitions. We then discuss the motivation and the method for studying the rare B-meson decays and introduce the effective Hamiltonian as a necessary tool to include QCD perturbative corrections in weak decays. Finally, we give the explicit form of the effective Hamiltonian and the corresponding Wilson coefficients for the quark level $b \rightarrow s\ell^+\ell^-$ transition in the SM together with a discussion about the possible long distance effects.

2.1 The Structure of Standard Model

The Standard model [1] is a renormalizable relativistic quantum field theory based on non-Abelian gauge symmetry of the gauge group $SU(3)_C \times SU(2)_L \times U(1)_Y$. It has two sectors: The first is Quantum Chromodynamics (QCD)[23], which is a vector gauge theory describing the $SU(3)_C$ color interactions of quarks and gluons. The second sector is the Electroweak Theory (EW) describing the electromagnetic and weak interactions of the quarks and leptons as a non-Abelian weak isospin (T) and an Abelian hypercharge (Y) gauge symmetry $SU(2)_L \times U(1)_Y$.

The strong interaction part is described by the Lagrangian

$$\mathcal{L}_{QCD} = -\frac{1}{4}F_{\mu\nu}^i F^{i\mu\nu} + \sum_r \bar{q}_{r\alpha} i \not{D}_\beta^\alpha q_r^\beta, \quad (2.1)$$

where g_s is the QCD gauge coupling constant and

$$F_{\mu\nu}^i = \partial_\mu G_\nu^i - \partial_\nu G_\mu^i - g_s f_{ijk} G_\mu^j G_\nu^k, \quad (2.2)$$

Table 2.1: The $SU(3)_C$ matrices.

$\lambda^1 = \begin{pmatrix} \tau_1 & 0 \\ 0 & 0 \end{pmatrix}$	$\lambda^2 = \begin{pmatrix} \tau_2 & 0 \\ 0 & 0 \end{pmatrix}$	$\lambda^3 = \begin{pmatrix} \tau_3 & 0 \\ 0 & 0 \end{pmatrix}$
$\lambda^4 = \begin{pmatrix} 0 & 0 & 1 \\ 0 & 0 & 0 \\ 1 & 0 & 0 \end{pmatrix}$	$\lambda^5 = \begin{pmatrix} 0 & 0 & -i \\ 0 & 0 & 0 \\ i & 0 & 0 \end{pmatrix}$	$\lambda^6 = \begin{pmatrix} 0 & 0 & 0 \\ 0 & 0 & 1 \\ 0 & 1 & 0 \end{pmatrix}$
$\lambda^7 = \begin{pmatrix} 0 & 0 & 0 \\ 0 & 0 & -i \\ 0 & i & 0 \end{pmatrix}$	$\lambda^8 = \frac{1}{\sqrt{3}} \begin{pmatrix} 1 & 0 & 0 \\ 0 & 1 & 0 \\ 0 & 0 & -2 \end{pmatrix}$	

is the field strength tensor for the gluon fields G_μ^i , $i = 1, \dots, 8$ where the structure constants f_{ijk} ($i, j, k = 1, \dots, 8$) are defined by

$$[\lambda^i, \lambda^j] = 2if_{ijk}\lambda^k, \quad (2.3)$$

and the $SU(3)_C$ λ matrices are defined in Table 2.1.

The $F \cdot F$ term in Eq.(2.1) leads to three and four-point gluon self-interactions. In the second term in \mathcal{L}_{QCD} , q_r is the r^{th} quark flavor, $\alpha, \beta = 1, 2, 3$ are color indices, and

$$D_{\mu\beta}^\alpha = (D_\mu)_{\alpha\beta} = \partial_\mu \delta_{\alpha\beta} + ig_s G_\mu^i L_{\alpha\beta}^i, \quad (2.4)$$

is the gauge covariant derivative for the quarks. Here, the quarks transform according to the triplet representation matrices, $\lambda^i/2$. The color interactions are diagonal in the flavor indices, but in general, change the quark colors. They are purely vector and therefore parity conserving. There are no mass terms for the quarks in Eq. (2.1). These would be allowed by QCD alone, but are forbidden by the chiral symmetry of the electroweak part of the theory. The quark masses will be generated later by spontaneous symmetry breaking.

Let us now review the essential elements of the $SU(2)_L \times U(1)_Y$ electroweak theory [24]-[27]. The matter fields of the SM, which are the leptons and quarks

carrying spin-1/2, are classified as left-handed (LH) isospin doublets and right-handed (RH) isospin singlets:

$$\begin{aligned} \ell_L &= \begin{pmatrix} \nu_e \\ e \end{pmatrix}_L, \quad \begin{pmatrix} \nu_\mu \\ \mu \end{pmatrix}_L, \quad \begin{pmatrix} \nu_\tau \\ \tau \end{pmatrix}_L, \quad \ell_R = e_R, \quad \mu_R, \quad \tau_R, \\ q_L &= \begin{pmatrix} u \\ d \end{pmatrix}_L, \quad \begin{pmatrix} c \\ s \end{pmatrix}_L, \quad \begin{pmatrix} t \\ b \end{pmatrix}_L, \quad q_R = u_R, \quad d_R, \quad c_R. \end{aligned} \tag{2.5}$$

As the gauge sector, there are four vector bosons as carriers of the electroweak force, and the corresponding spin-1 gauge vector fields are the $SU(2)_L$ isotriplet, $W_\mu^1, W_\mu^2, W_\mu^3$ and $U(1)_Y$ hypercharge B_μ . The $SU(2)_L \times U(1)_Y$ group has then four generators, three of which are the $SU(2)_L$ generators, $T_i = \frac{\tau_i}{2}$, where τ_i are Pauli matrices with $i = 1, 2, 3$, and the fourth one is the $U(1)_Y$ generator, $\frac{Y}{2}$. The commutation relations for the total group are:

$$[T_i, T_j] = i\epsilon_{ijk}T_k \ ; \ [T_i, Y] = 0 \ ; \ i, j, k = 1, 2, 3$$

where ϵ_{ijk} is totally antisymmetric symbol. The fermion quantum numbers are as in Tables 2 and 3, and the relation

$$Q = T_3 + \frac{Y}{2}$$

is also incorporated in the SM.

Table 2.2: Lepton quantum numbers

Lepton	T	T_3	Q	Y
ν_L	$\frac{1}{2}$	$\frac{1}{2}$	0	-1
e_L	$\frac{1}{2}$	$-\frac{1}{2}$	-1	-1
e_R	0	0	-1	-2

The building of the SM Lagrangian is done by following the same steps as in any gauge theory. In particular, the $SU(2)_L \times U(1)_Y$ symmetry is promoted from global to local by replacing the derivatives of the fields by the corresponding covariant derivatives. For a generic fermion field f , its covariant derivative

Table 2.3: Quark quantum numbers

Quark	T	T_3	Q	Y
u_L	$\frac{1}{2}$	$\frac{1}{2}$	$\frac{2}{3}$	$\frac{1}{3}$
d_L	$\frac{1}{2}$	$-\frac{1}{2}$	$-\frac{1}{3}$	$\frac{1}{3}$
u_R	0	0	$\frac{2}{3}$	$\frac{4}{3}$
d_R	0	0	$-\frac{1}{3}$	$-\frac{2}{3}$

corresponding to the $SU(2)_L \times U(1)_Y$ gauge symmetry is,

$$D_\mu f = \left(\partial_\mu - ig\vec{T} \cdot \vec{W}_\mu - ig' \frac{Y}{2} B_\mu \right) f, \quad (2.6)$$

where $g(g')$ is the $SU(2)_L(U(1)_Y)$ gauge coupling. For example, the covariant derivatives for a left-handed and a right-handed electron are respectively,

$$\begin{aligned} D_\mu e_L &= \left(\partial_\mu - ig \frac{\vec{\sigma}}{2} \cdot \vec{W}_\mu + ig' \frac{1}{2} B_\mu \right) e_L, \\ D_\mu e_R &= (\partial_\mu + ig' B_\mu) e_R. \end{aligned} \quad (2.7)$$

The SM total Lagrangian can be written as,

$$\mathcal{L}_{SM} = \mathcal{L}_f + \mathcal{L}_G + \mathcal{L}_{SBS} + \mathcal{L}_{YW},$$

where the fermion Lagrangian is given by

$$\mathcal{L}_f = \sum_{f=l,q} \bar{f} i \not{D} f, \quad (2.8)$$

while the Lagrangian for the gauge fields has the form

$$\mathcal{L}_G = -\frac{1}{4} W_{\mu\nu}^i W_i^{\mu\nu} - \frac{1}{4} B_{\mu\nu} B^{\mu\nu}, \quad (2.9)$$

which is written in terms of the field strength tensors

$$\begin{aligned} W_{\mu\nu}^i &= \partial_\mu W_\nu^i - \partial_\nu W_\mu^i + g\epsilon^{ijk} W_\mu^j W_\nu^k, \\ B_{\mu\nu} &= \partial_\mu B_\nu - \partial_\nu B_\mu. \end{aligned} \quad (2.10)$$

The last two terms, \mathcal{L}_{SBS} and \mathcal{L}_{YW} , are the Symmetry Breaking Sector Lagrangian and the Yukawa Lagrangian, respectively, which are needed in order to

provide the wanted gauge boson masses m_W and m_Z and fermion masses m_f . For spontaneous breaking of the $SU(2)_L \times U(1)_Y$ symmetry leaving the electromagnetic gauge subgroup $U(1)_{em}$ unbroken, a single complex scalar doublet field with hypercharge $Y = 1$

$$\Phi(x) = \begin{pmatrix} \phi^+(x) \\ \phi_0(x) \end{pmatrix} \quad (2.11)$$

is coupled to the gauge fields. Then the spontaneous symmetry breaking and the Higgs Mechanism provide indeed this mass generation through the scalar part of the SM Lagrangian:

$$\mathcal{L}_{SBS} = (D_\mu \Phi)^\dagger (D_\mu \Phi) - V(\Phi), \quad (2.12)$$

where

$$V(\Phi) = \mu^2 \Phi^\dagger \Phi + \lambda (\Phi^\dagger \Phi)^2,$$

and the Higgs-fermion Yukawa couplings are given by

$$L_{YW} = \lambda_e \bar{\ell}_L \Phi e_R + \lambda_u \bar{q}_L \tilde{\Phi} u_R + \lambda_d \bar{q}_L \Phi d_R + \text{h.c} + 2^{nd} \text{ and } 3^{rd} \text{ families.} \quad (2.13)$$

The following steps summarize the procedure to get the spectrum from \mathcal{L}_{SM} :

1. A non-symmetric vacuum must be fixed. Let's choose

$$\langle \Phi \rangle_0 \equiv \langle 0 | \Phi | 0 \rangle = \begin{pmatrix} 0 \\ \frac{v}{\sqrt{2}} \end{pmatrix}. \quad (2.14)$$

2. The physical spectrum is built by performing small oscillations around this vacuum. These are parameterized by

$$\Phi(x) = \exp\left(\frac{i\vec{\xi}(x) \cdot \vec{\sigma}}{v}\right) \begin{pmatrix} 0 \\ \frac{v+H(x)}{\sqrt{2}} \end{pmatrix}, \quad (2.15)$$

where $\vec{\xi}(x)$ is a small field and $H(x)$ describes the neutral Higgs boson.

3. The unphysical field $\vec{\xi}(x)$ is eliminated through the following gauge transformation

$$\Phi' = U(\xi)\Phi = \begin{pmatrix} 0 \\ \frac{v+H}{\sqrt{2}} \end{pmatrix}, \quad (2.16)$$

where

$$U(\xi) = \exp\left(-i\frac{\vec{\xi} \cdot \vec{\sigma}}{v}\right). \quad (2.17)$$

The fermion and the gauge fields are transformed accordingly;

$$\begin{aligned} \ell'_L &= U(\xi)\ell_L, \quad e'_R = e_R, \\ q'_L &= U(\xi)q_L, \quad u'_R = u_R, \quad d'_R = d_R, \\ \frac{\vec{\sigma} \cdot \vec{W}'_\mu}{2} &= U(\xi)\left(\frac{\vec{\sigma} \cdot \vec{W}_\mu}{2}\right)U^{-1}(\xi) - \frac{i}{g}(\partial_\mu U(\xi))U^{-1}(\xi), \\ B'_\mu &= B_\mu, \end{aligned} \quad (2.18)$$

and we rewrite the Lagrangian for them in a new gauge.

The physical bosons consist of the charged particles W_μ^\pm and the neutrals Z_μ and A_μ (the photon). The latter are taken as a linear combinations of W_μ^3 and B_μ . Thus, one can set

$$\begin{aligned} W_\mu^\pm &= \frac{1}{\sqrt{2}}(W_\mu^1 \pm iW_\mu^2), \\ Z_\mu &= \frac{gW_\mu^3 - g'B_\mu}{\sqrt{g^2 + g'^2}}, \quad A_\mu = \frac{g'W_\mu^3 + gB_\mu}{\sqrt{g^2 + g'^2}}. \end{aligned} \quad (2.19)$$

It is possible to relate the coupling constants of $SU(2)_L$ and $U(1)_Y$ to the so-called the Weinberg angle θ_W by using the definition $g/g' = \tan \theta_W$,

$$\sin \theta_W = \frac{g'}{\sqrt{g^2 + g'^2}}, \quad \cos \theta_W = \frac{g}{\sqrt{g^2 + g'^2}}. \quad (2.20)$$

The photon field A_μ couples via the electric charge $e = \sqrt{4\pi\alpha}$ to the electron, thus e can be expressed in term of the gauge couplings in the following way

$$e = \frac{gg'}{\sqrt{g^2 + g'^2}} \quad \text{or} \quad e = g \sin \theta_W = g' \cos \theta_W. \quad (2.21)$$

It is now easy to read the masses from the following terms of \mathcal{L}_{SM} :

$$\begin{aligned}
D_\mu \Phi' D^\mu \Phi' &= \frac{g^2 v^2}{4} W_\mu^+ W^{\mu-} + \frac{1}{2} \frac{(g^2 + g'^2) v^2}{4} Z^\mu + \dots \\
V(\Phi') &= \frac{1}{2} 2\mu^2 H^2 + \dots \\
\mathcal{L}_{YW} &= \lambda_e \frac{v}{\sqrt{2}} \bar{e}'_L e'_R + \lambda_u \frac{v}{\sqrt{2}} \bar{u}'_L u'_R + \lambda_d \frac{v}{\sqrt{2}} \bar{d}'_L d'_R + \dots
\end{aligned} \tag{2.22}$$

and get finally the tree level predictions

$$\begin{aligned}
m_W &= \frac{gv}{\sqrt{2}}, & m_Z &= \frac{\sqrt{g^2 + g'^2}}{2} v, & m_H &= \sqrt{2}\mu, \\
m_e &= \lambda_e \frac{v}{\sqrt{2}}, & m_u &= \lambda_u \frac{v}{\sqrt{2}}, & m_d &= \lambda_d \frac{v}{\sqrt{2}},
\end{aligned} \tag{2.23}$$

where

$$v = \sqrt{\frac{\mu^2}{\lambda}}, \tag{2.24}$$

and photon remains massless, $m_A = 0$.

The SM does not predict a numerical value for m_W and m_Z but provides some relations among the relevant parameters. Then it is possible to obtain their numerical values in terms of three experimentally well known quantities; namely the fine structure constant $\alpha^{-1} = (e^2/4\pi)^{-1} = 137.035$, the Fermi coupling constant $G_F = 1.166 \times 10^{-5} \text{ GeV}^{-2}$, and the weak mixing angle θ_W given by $\sin^2 \theta_W = 0.231 \pm 0.014$. In particular, the following relations hold in the SM:

$$\frac{G_F}{\sqrt{2}} = \frac{g^2}{8m_W^2} = \frac{1}{2v^2} \Rightarrow v = 2^{-1/4} G_F^{-1/2} = 246 \text{ GeV}. \tag{2.25}$$

Then,

$$\begin{aligned}
m_W^2 &= \frac{e^2 v^2}{4 \sin^2 \theta_W} \simeq \left(\frac{\pi \alpha}{\sin^2 \theta_W} \right) v^2 \simeq \left(\frac{37.2 \text{ GeV}}{\sin \theta_W} \right)^2 \\
m_W &\sim 80 \text{ GeV},
\end{aligned} \tag{2.26}$$

$$m_Z^2 \simeq \left(\frac{37.2}{\sin \theta_W \cos \theta_W} \text{ GeV} \right)^2 \Rightarrow m_Z \simeq 90 \text{ GeV}, \tag{2.27}$$

which are in a good agreement with the experimentally measured masses [28].

The mass of the Higgs boson is determined by the coupling in the self energy part of the potential

$$m_H = \sqrt{2}\mu = \sqrt{2v^2\lambda} \quad (2.28)$$

and it can not be predicted in the SM either since the coupling λ is an unknown parameter. Therefore, m_H can take any value in the SM. However, there are some arguments to constrain the Higgs mass that comes from the consistency of the theory, that is from unitarity, triviality, and vacuum stability arguments:

- Unitarity of the scattering matrix together with the elastic approximation for the total cross-section and the Optical Theorem imply certain elastic unitarity conditions for the partial wave amplitudes. These, in turn, when applied in the SM to scattering processes involving the Higgs particle, imply an upper limit on the Higgs mass, $m_H < 860$ GeV.
- If we want the SM to be a sensible effective theory, we must keep all the renormalized masses \approx the cut-off in the renormalized coupling at one-loop level, $\Lambda \sim 1$ TeV. Since we want to keep the Higgs mass below the physical cut-off, it implies an upper bound, $m_H < 1$ TeV.
- A different perturbative upper limit on m_H can be found by analysing the renormalization group equations in the SM to one-loop. By requiring the theory to be perturbative (i.e. all the couplings be sufficiently small) at all energy scales below some fixed high energy, one finds a maximum allowed m_H value [29]. For instance, by fixing this energy scale to 10^{16} GeV and for $m_t = 170$ GeV one gets: $m_H < 170$ GeV.
- A lower bound on the Higgs mass is obtained by the requirement of the stability of the Higgs potential when quantum corrections are taken into account. By the assumptions that the SM is valid up to an energy scale of $\Lambda \sim 1$ TeV, it may be established that $m_H \geq 55$ GeV. This is for $m_t = 175$ GeV.

- Finally, the direct Higgs boson searches in the $e^+e^- \rightarrow H^0 Z^0$ process at CERNs LEP experiment constrains the Higgs mass from below [30], and indicates that $m_H > 114$ GeV. A new machine at CERN, Large Hadron Collider, is expected to operate in 2005 and its main goal is to search for the Higgs particles.

2.1.1 Flavor Mixing

In the SM quarks acquire mass through a gauge invariant way called Yukawa coupling of the quarks with the Higgs field, Φ , whose Lagrangian is given by Eq.(2.13). After spontaneous symmetry breaking, by inserting the vacuum expectation values of Φ and $\tilde{\Phi}$, we obtain mass terms for the quarks,

$$\mathcal{L}_{\text{mass}} = M_{ij}^u \bar{u}'_{Li} u'_{Rj} + M_{ij}^d \bar{d}'_{Li} d'_{Rj} + \text{h.c.}, \quad (2.29)$$

where the superscript $'$ denote the quark fields in the weak interaction basis, and $M^u = (v/\sqrt{2}) \lambda_u$ and $M^d = (v/\sqrt{2}) \lambda_d$ stand for the mass matrices for up- and down-type quarks, respectively. To obtain the physical mass eigenstates, we must diagonalize the matrices M^d and M^u . As any complex matrix, they can be diagonalized by two unitary matrices, $U_{L,R}$ and $D_{L,R}$, respectively:

$$\begin{aligned} M_{\text{diag}}^u &\equiv U_L M^u U_R^\dagger, \\ M_{\text{diag}}^d &\equiv D_L M^d D_R^\dagger. \end{aligned} \quad (2.30)$$

One can rewrite the up-quarks mass term from Eq. (2.29) as

$$\begin{aligned} \bar{u}'_{Li} M_{ij}^u u'_{Rj} + \text{h.c.} &\equiv \bar{u}'_L U_L^\dagger U_L M^u U_R^\dagger U_R u'_R + \text{h.c.} \\ &= \bar{u}_L M_{\text{diag}}^u u_R + \text{h.c.} = \bar{u} M_{\text{diag}}^u u, \end{aligned}$$

where the mass eigenstates u_L and d_R are identified according to the following formulas:

$$u_L = U_L u'_L, \quad u_R = U_R u'_R. \quad (2.31)$$

Applying the same procedure to matrix M^d , we observe that it becomes diagonal as well in the new rotated basis:

$$d_L = D_L d'_L, \quad d_R = D_R d'_R. \quad (2.32)$$

In summary, starting from the quark fields in the weak interaction basis it is found that they should be rotated by four unitary matrices U_L , U_R , D_L and D_R in order to obtain mass eigenstates with diagonal masses. Since kinetic energies and interactions with the vector fields W_μ^3 , B_μ and gluons are diagonal in the quark fields, these terms remain diagonal in the new basis, too. The only term in the SM Lagrangian \mathcal{L}_{SM} where the matrices U and D show up is charged current interaction with the emission of W-boson:

$$\mathcal{L}_{CC} = -\frac{g}{2\sqrt{2}}(J_W^\mu W_\mu^- + J_W^{\mu\dagger} W_\mu^+) \quad (2.33)$$

where

$$J_W^{\mu\dagger} = (\bar{\nu}_e, \bar{\nu}_\mu, \bar{\nu}_\tau) \gamma^\mu (1 - \gamma_5) \begin{pmatrix} e^- \\ \mu^- \\ \tau^- \end{pmatrix} + (\bar{u}', \bar{c}', \bar{t}') \gamma^\mu (1 - \gamma_5) \begin{pmatrix} d' \\ s' \\ b' \end{pmatrix},$$

which becomes in the new basis

$$J_W^{\mu\dagger} = (\bar{\nu}_e, \bar{\nu}_\mu, \bar{\nu}_\tau) \gamma^\mu (1 - \gamma_5) \begin{pmatrix} e^- \\ \mu^- \\ \tau^- \end{pmatrix} + (\bar{u}, \bar{c}, \bar{t}) \gamma^\mu (1 - \gamma_5) V_{CKM} \begin{pmatrix} d \\ s \\ b \end{pmatrix},$$

where the unitary matrix $V_{CKM} \equiv U_L^\dagger D_L$ is called the Cabibbo-Kobayashi-Maskawa (CKM) quark mixing matrix [26], which appears due to the mismatch between the weak and the Yukawa interactions. With two quark generations, V_{CKM} is defined by a single real parameter, the Cabibbo angle θ . However, with three quark generations, four parameters are required. The real rotations may be taken to be three Euler angles, and the remaining extra parameter is an irreducible complex phase. This phase is the only source of CP violation in flavor changing transitions in the SM.

In the "standard parametrization" [31] recommended by the Particle Data Group [32], the three-generation CKM matrix takes the form

$$V_{CKM} = \begin{pmatrix} V_{ud} & V_{us} & V_{ub} \\ V_{cd} & V_{cs} & V_{cb} \\ V_{td} & V_{ts} & V_{tb} \end{pmatrix}$$

$$= \begin{pmatrix} c_{12}c_{13} & s_{12}c_{13} & s_{13}e^{-i\delta_{13}} \\ -s_{12}c_{23} - c_{12}s_{23}s_{13}e^{i\delta_{13}} & c_{12}c_{23} - s_{12}s_{23}s_{13}e^{i\delta_{13}} & s_{23}c_{13} \\ s_{12}s_{23} - c_{12}c_{23}s_{13}e^{i\delta_{13}} & -c_{12}s_{23} - s_{12}c_{23}s_{13}e^{i\delta_{13}} & c_{23}c_{13} \end{pmatrix},$$

where $c_{ij} = \cos \theta_{ij}$ and $s_{ij} = \sin \theta_{ij}$. It has been observed experimentally that the CKM matrix has a hierarchical structure reflected by

$$s_{12} = 0.22 \gg s_{23} = \mathcal{O}(10^{-2}) \gg s_{13} = \mathcal{O}(10^{-3}). \quad (2.34)$$

Thus, if in the standard parametrization above, we introduce new parameters λ , A , ρ and η by imposing the relations

$$s_{12} \equiv \lambda = 0.22, \quad s_{23} \equiv A\lambda^2, \quad s_{13}e^{-i\delta} \equiv A\lambda^3(\rho - i\eta), \quad (2.35)$$

we arrive at

$$V_{\text{CKM}} = \begin{pmatrix} 1 - \frac{1}{2}\lambda^2 & \lambda & A\lambda^3(\rho - i\eta) \\ -\lambda & 1 - \frac{1}{2}\lambda^2 & A\lambda^2 \\ A\lambda^3(1 - \rho - i\eta) & -A\lambda^2 & 1 \end{pmatrix} + \dots \quad (2.36)$$

This is the "Wolfenstein parametrization" of the CKM matrix [33], and is valid to order λ^4 .

Concerning the test of the CKM picture of CP violation, the central targets are the unitarity of the CKM matrix, which is described by

$$V_{\text{CKM}}^\dagger \cdot V_{\text{CKM}} = V_{\text{CKM}} \cdot V_{\text{CKM}}^\dagger = \hat{1}, \quad (2.37)$$

imposes the following conditions on the matrix elements:

$$\sum_{j=1}^3 |V_{ij}|^2 = 1, \quad \sum_{i=1}^3 |V_{ij}|^2 = 1, \quad \sum_{k=1}^3 V_{ik}^* V_{kj} = 0. \quad (2.38)$$

It is very convenient to discuss the predictions of the unitarity by using the unitarity triangle, which is just a geometrical representation of the relation in Eq.(2.38) which equals zero in the complex plane. The most commonly used unitarity triangle is obtained from the constraint

$$V_{ub}V_{ud}^* + V_{cb}V_{cd}^* + V_{tb}V_{td}^* = 0.$$

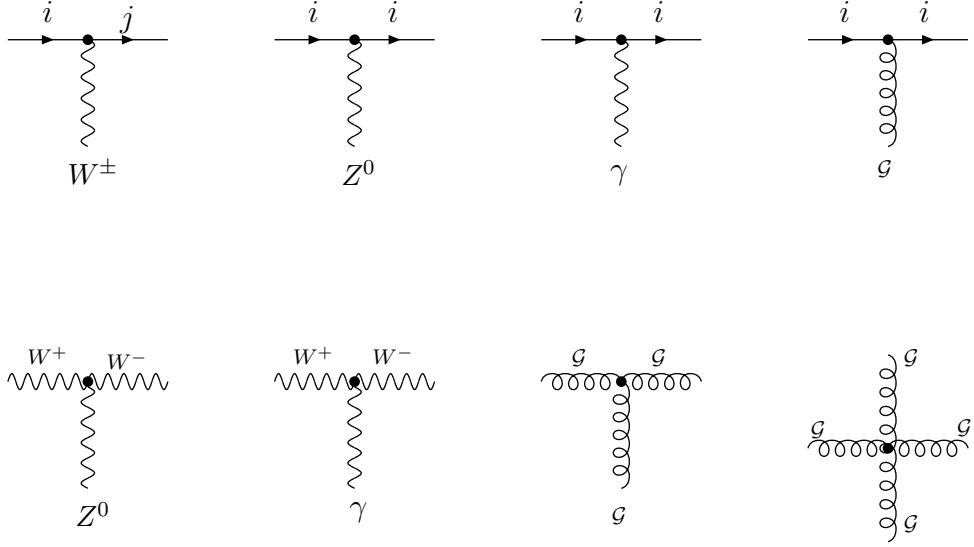


Figure 2.1: The basic vertices representing the interactions of the quarks with the gauge bosons. The labels i and j represent the flavour quantum number ($i, j = u, d, c, s, t, b$).

The B- system provides an excellent ground for measuring many aspects of this triangle. The present situation about the knowledge of the element of the CKM matrix can be summarized by [34]

$$|V_{us}| = \lambda = 0.2196 \pm 0.0026, \quad |V_{cb}| = (41.2 \pm 2.0) \times 10^{-3},$$

$$\frac{|V_{ub}|}{\lambda|V_{cb}|} = 0.40 \pm 0.08, \quad |V_{ub}| = (35.7 \pm 3.1) \times 10^{-4},$$

implying

$$A = 0.85 \pm 0.04.$$

2.1.2 Neutral Current and Flavor Changing Neutral Current

In addition to charged-current interactions, $SU(2)_L \times U(1)_Y$ model also predicts neutral current weak interactions. The relevant Lagrangian is

$$\mathcal{L}_{NC} = -\frac{\sqrt{g^2 + g'^2}}{2} J_Z^\mu \left(-\sin \theta_W B_\mu + \cos \theta_W W_\mu^3 \right), \quad (2.39)$$

where the weak neutral current is given by

$$J_Z^\mu = \sum_j \left[\bar{u}_{Lj} \gamma^\mu u_{Lj} - \bar{d}_{Lj} \gamma^\mu d_{Lj} + \bar{\nu}_{Lj} \gamma^\mu \nu_{Lj} - \bar{e}_{Lj} \gamma^\mu e_{Lj} \right] - 2 \sin^2 \theta_W J_Q^\mu. \quad (2.40)$$

Here j is for the various flavors of quarks and leptons, and J_Q^μ is the electromagnetic current. Like the electromagnetic current J_Z^μ is flavor-diagonal in the SM, so the form is not affected by the unitary transformations that relate the mass and weak bases. It was for this reason that the GIM mechanism [25] was introduced into the model, along with its prediction of the charm quark and the orthogonality of the quark-mixing matrix V_{CKM} . Without it the d and s quarks would not have had the same $SU(2)_L \times U(1)_Y$ assignments, and flavor-changing neutral currents (FCNC) would have resulted. Thus, it follows from the \mathcal{L}_{CC} , \mathcal{L}_{NC} and \mathcal{L}_{QCD} parts of the \mathcal{L}_{SM} that interactions in the SM can be represented by the elementary vertices in Fig. (2.1).

FCNC transitions only occur in the loop level in the SM and they are represented by the penguin and the box diagrams with virtual electroweak bosons and quarks in the loop. Examples of penguin and box diagrams contributing to the FCNC process $b \rightarrow s$ are given by Figs (2.2) and (2.3). For example, if all

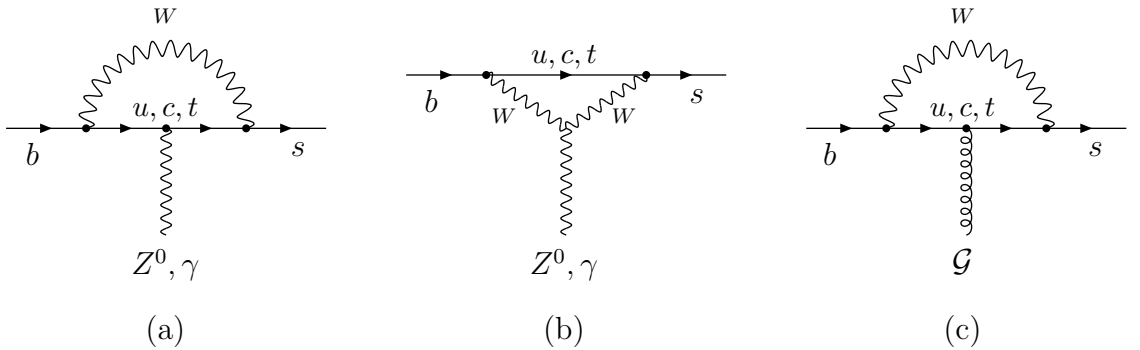


Figure 2.2: Examples of penguin diagrams which contribute to the FCNC process $b \rightarrow s$. Diagrams (a) and (b) are electroweak penguins graphs, and diagram (c) is a gluonic penguin graph.

up-type quarks had identical masses, $m_u = m_c = m_t$, the only difference between graphs with different up type quarks would be the coupling to the W boson via

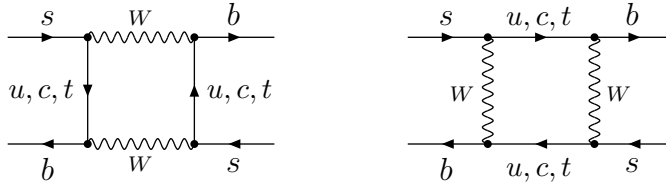


Figure 2.3: Examples of box diagrams.

the CKM matrix elements. The sum of the three possible diagrams would then be proportional to

$$V_{ub}V_{us}^* + V_{cb}V_{cs}^* + V_{tb}V_{ts}^*,$$

which vanishes because of the unitarity of the CKM matrix. This vanishing of the sum of the three graphs is known as the GIM mechanism. In reality, the masses of the quarks are not equal and the result of these graphs is therefore proportional to the mass difference of the up-type quarks. Since the top quark is so much heavier than the up and the charm quark, the graphs with the top quark in the loop dominate the process.

2.1.3 Unsatisfactory Features of the SM

Despite the fact that the SM is a mathematically consistent renormalizable field theory that has been very successful in describing most of the elementary particles phenomenology, there are several unsatisfactory features. Let us enumerate some of them:

- **Number of free parameters:** There are at least 19 physical parameters that can not be computed in the context of the SM: 3 gauge couplings, 6 quark and 3 charged-lepton masses with 3 charged weak mixing angles and 1 CP-violating phase and 2 parameters to characterize the Higgs sector and 1 CP-violating non-perturbative vacuum angle.
- **The Higgs sector of the theory:** It remains unknown so far, and there is not any fundamental reason to assume that this sector must be minimal

i.e. only one Higgs doublet.

- **The "Hierarchy" Problem:** From some theoretical arguments discussed briefly in previous subsection we have an upper limit for the Higgs mass, $m_H < 1$ TeV. Within the SM, there are quantum corrections to this tree-level Higgs mass, $\delta m_H^2 \sim \Lambda^2$, where Λ is a higher scale in the theory. If there were no higher scale, one would simply interpret Λ as an ultraviolet cutoff and take the view that m_H is a measured parameter and its bare mass is not an observable. However, since gravity is not included in the SM, there is for sure another relevant scale, a scale $\Lambda \simeq M_{Planck} \simeq 10^{19}$ GeV . Hence the natural scale for m_H is $\mathcal{O}(\Lambda)$, which is much larger than the expected value.

One solution to this problem is to replace elementary Higgs fields by bound states of fermions. Technicolor and composite Higgs models are in this category [35]. Another possibility is supersymmetry [36], in which there is postulated a superpartner fermion and a superpartner boson for every fermion and boson in the theory. This solves the hierarchy problem, since the SM diagrams generating the divergences in the Higgs mass are cancelled by the new diagrams in which superpartners propagate in the loop.

- **Gravity is not included in the SM:** General relativity can be formulated as a classical field theory, but attempts to quantize it yield a non-renormalizable theory. The hope is to unify gravity with other forces in such a way that the infinities arising in different sectors cancel among themselves, yielding a combined renormalizable theory.
- **Origin of CP violation:** In the SM the only source of CP violation is the complex Cabibbo-Kobayashi-Maskawa (CKM) matrix elements which appears too weak to drive the observed asymmetry in nature.
- **Masses of neutrinos:** Experiments operated in underground sites suggest a solid evidence for neutrino oscillations [37], which imply nonzero masses

for neutrinos. However, it is not possible to introduce masses of neutrinos in the SM, since there is no RH neutrino.

These and many other unsatisfactory features of the SM lead the physicists to search for new models beyond it.

2.2 Rare B Meson Decays

The weak decays concern with all the unanswered questions of the SM summarized above and their phenomenology is very rich. Among the weak decays, the rare decays have a special place for providing the essential information about the higher structure of the SM, and also poorly studied aspects of it, particularly CKM matrix elements, the leptonic decay constants, etc.

By "rare" decays, it is generally meant two classes of transitions: 1) Decays due to the $b \rightarrow u$, which are suppressed relative to $b \rightarrow c$ modes by the CKM factor $|V_{ub}/V_{cb}| \approx 0.006$. An example is the exclusive mode $B \rightarrow \rho \ell \nu$, with a branching ratio of 2.5×10^{-4} .

2) A second class of rare decay modes is transitions that do not arise at the tree level in the SM, but may originate through loop effects. Consequently, rare B decays, for example, are mediated by FCNC processes of the kind $b \rightarrow s$ or $b \rightarrow d$, whereas rare K decays originate from their $s \rightarrow d$ counterparts.

In comparison with kaons, the B meson system has several features which make it well-suited to study flavor physics and CP violation. Because the top quark in loop diagrams is neither GIM nor CKM suppressed, large CP violating effects and large mixing are possible in the natural B systems. For the same reason, a variety of rare decays have large enough branching fractions to allow for detailed studies. Finally, since the b quark mass is much larger than the typical scale of the strong interaction, long-distance strong interactions are generally less important and are under better control than in kaon physics.

Rare B-meson decays are also sensitive to new physics beyond the SM, since in these additional contributions to the decay rate, SM particles are replaced

by new particles such as the supersymmetric charginos or gluinos in SUSY theories, that can give contributions comparable to those of the SM. This makes it possible to observe new physics indirectly - a strategy complementary to the direct production of new (e.g., supersymmetric) particles and is reserved for the planned hadronic machines such as the LHC at CERN. For the indirect search of the particles, there are several B physics experiments successfully running : the CLEO experiment (Cornell, USA) [38], the BaBar experiment at SLAC (Stanford, USA) [39] and the BELLE experiment at KEK (Tsukuba, Japan) [40], hadronic B physics program at FERMILAB (Batavia, USA) [41]. There are also independent B physics experiments planned at the hadronic colliders: the LHC- B experiment at CERN in Geneva [42] and the B TeV experiment at FERMILAB [43].

2.3 The Effective Hamiltonian Theory

In order to deal with rare decays theoretically, one must first calculate the transition amplitude \mathcal{M} for $B \rightarrow f$, which can get many contributions represented by different Feynman diagrams such as the one in Fig.(2.2) and (2.3). However, these weak decays are mediated through weak interactions of quarks, whose strong interactions bind the quarks into hadrons. Hence QCD effects must be considered too. At short distances much smaller than $\hbar c/\Lambda_{QCD}$ these effects can be described perturbatively by the exchanges of gluons. When travelling over a distance of order $\hbar c/\Lambda_{QCD}$, however, quarks and gluons hadronize and QCD becomes nonperturbative. Therefore the physics from different length scales, or equivalently, from different energy scales must be treated separately. The theoretical tool for this is the operator product expansion (OPE). In OPE, the transition amplitude \mathcal{M} for $B \rightarrow f$ decay may be expressed as

$$\mathcal{M} = \frac{G_F}{\sqrt{2}} \sum_i V_{CKM}^i C_i(\mu, m_{heavy}) \langle f | O_i(\mu) | B \rangle \left[1 + \mathcal{O}\left(\frac{m_b^2}{m_W^2}\right) \right], \quad (2.41)$$

where O_i are local operators and C_i are the Wilson coefficients. Both O_i and C_i depend on the QCD renormalization scale μ , and C_i depends on mass of

the W boson and other heavy particles such as the top quark as well. The expansion in Eq. (2.41) is very convenient. The non-perturbative QCD effects are contained in the matrix elements of the operators O_i , which are independent of the large momentum scale of heavy particles. The Wilson coefficient functions C_i are independent of the states f and B and can be calculated in perturbation theory. Thus, OPE allows for a separation of an amplitude of the B-meson decay process into two distinct parts; the long distance contributions contained in the operator matrix elements and the short-distance physics described by the Wilson coefficients. The renormalization scale μ separating these two regimes is chosen by requiring that the strong coupling constant is low enough to make meaningful the perturbative calculations. For the decays of D and B mesons, a common choice is usually $\mu = \mathcal{O}(m_c)$ and $\mu = \mathcal{O}(m_b)$, respectively. Since physical amplitudes can not depend on μ , the μ -dependence in the operators $O_i(\mu)$ is cancelled by that in the Wilson coefficients $C_i(\mu)$.

The $\langle f|O_i(\mu)|B\rangle$ includes long-distance effects and can not be evaluated from perturbation theory. In principle such quantities can be evaluated using sophisticated non-perturbative methods such as lattice calculation or QCD sum rules. In case of certain B-meson decays, the Heavy Quark Effective Theory (HQET) [44] is also a useful tool. However, all these non-perturbative methods have some limitations and consequently in weak decays of mesons, hadronic matrix elements constitute the dominant theoretical uncertainties.

In contrast to the long-distance contributions, due to the asymptotic freedom of QCD the strong interaction effects at short distances are calculable in perturbation theory in the strong coupling $\alpha_s(\mu)$. Wilson coefficients are determined by matching the full theory onto a five quark effective theory. In this process W^\pm , Z^0 , the top-quark and generally all heavy particles with masses higher than m_W are integrated out. The matching in question is achieved using the following procedure:

- Calculation of the amplitude in the full theory, \mathcal{M}_{full} , from all relevant Feynman diagrams with quarks and gluons,

- Calculation of the operator matrix elements,
- Extraction of $C_i(\mu)$ from $\mathcal{M}_{full} = \mathcal{M}_{eff}$.

The resulting $C_i(\mu)$ s depend generally on the masses of the heavy particles which have been integrated out and are in the form of an expansion in $\alpha_s(\mu)$:

$$C_i = \sum_n a_n \alpha_s^n(\mu). \quad (2.42)$$

Although $\alpha_s(\mu)$ is small enough in the full range of relevant short-distance scales of $\mathcal{O}(1\text{GeV})$ to serve as a reasonable expansion parameter, the expansion in Eq. (2.42) typically shows the appearance of large logarithms of the kind $\alpha_s(\mu) \ln(m_W/\mu)$, where $\mu = \mathcal{O}(1\text{GeV})$, so that even when $\alpha_s(\mu)$ is a good expansion parameter, this product in the calculation of the coefficients $C_i(\mu)$ spoils the validity of the usual perturbation series. It is therefore necessary to replace the usual perturbation theory by a renormalized-group improved perturbation theory that allows an efficient summation of logarithmic terms to all orders in perturbation theory. The leading term in this case comes from the resummation of the terms $[\alpha_s(\mu) \ln(m_W/\mu)]^n$, the so-called leading log approximation. Generally speaking, it is often insufficient to stop at the leading log approximation, and the next-to-leading order corrections should be included, which may exhibit some interesting features absent in leading log approximation.

An important feature of the OPE in Eq. (2.41) is the universality of the coefficients C_i : they are independent of the external states; that is, their numerical value is the same for all final states f . Therefore one can view the C_i 's as effective coupling constants and the O_i 's as the corresponding interaction vertices. Thus one can set up the effective Hamiltonian as

$$\mathcal{H}_{eff} = \frac{G_F}{\sqrt{2}} \sum_i V_{CKM}^i C_i(\mu, m_{heavy}) O_i(\mu) + h.c. \quad (2.43)$$

Typical penguin and box diagrams for $b \rightarrow s$ transitions are displaced in Figs. (2.4). The amplitude \mathcal{M} is the sum over all internal up-quarks

$$\mathcal{M} = \sum_{i=u,c,t} V_{ib} V_{is}^* \mathcal{M}_i. \quad (2.44)$$

Using the unitarity of CKM matrix, which implies that

$$\sum_{i=u,c,t} V_{ib}V_{is}^* = 0 \quad (2.45)$$

together with the smallness of V_{ub} implying $V_{ub}V_{us}^* \ll V_{tb}V_{ts}^*$, we arrive at

$$\mathcal{M} = V_{tb}V_{ts}^*(\mathcal{M}_t - \mathcal{M}_c) + V_{ub}V_{us}^*(\mathcal{M}_u - \mathcal{M}_c) \simeq V_{tb}V_{ts}^*(\mathcal{M}_t - \mathcal{M}_c). \quad (2.46)$$

Keeping in mind this and the general steps necessary to build an effective Hamiltonian summarized above, let us write explicitly the effective Hamiltonian describing semileptonic weak decays of B mesons in the quark level in the SM:

$$\mathcal{H}_{eff}(b \rightarrow s\ell^+\ell^-) = -\frac{4 G_F}{\sqrt{2}} V_{tb}V_{ts}^* \sum_{i=1}^{10} C_i(\mu) \mathcal{O}_i(\mu), \quad (2.47)$$

where the operator basis is given as follows [9]-[11]

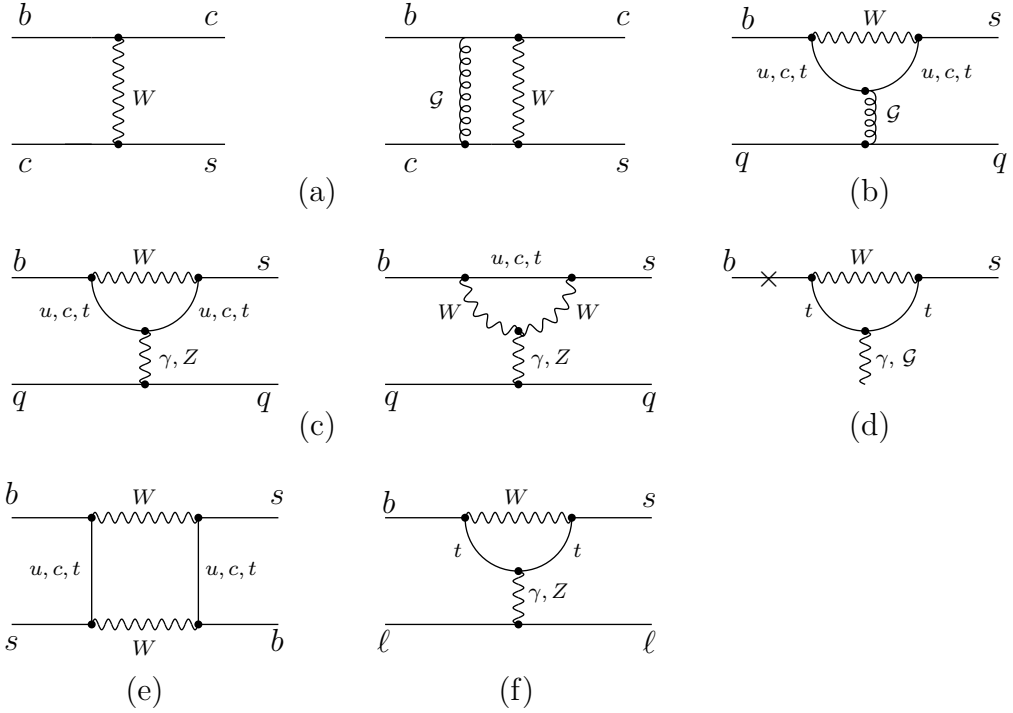


Figure 2.4: Typical leading logarithmic order penguin and box diagrams in the SM.

Current-current operators (Fig. 2.4(a)):

$$\begin{aligned} O_1 &= (\bar{s}_{L\alpha}\gamma_\mu c_{L\beta})(\bar{c}_{L\beta}\gamma^\mu b_{L\alpha}) \\ O_2 &= (\bar{s}_{L\alpha}\gamma_\mu c_{L\alpha})(\bar{c}_{L\beta}\gamma^\mu b_{L\beta}), \end{aligned} \quad (2.48)$$

QCD-penguin operators (Fig. 2.4(b)):

$$\begin{aligned}
O_3 &= (\bar{s}_{L\alpha}\gamma_\mu b_{L\alpha}) \sum_{q=u,d,s,c,b} (\bar{q}_{L\beta}\gamma^\mu q_{L\beta}) \\
O_4 &= (\bar{s}_{L\alpha}\gamma_\mu b_{L\beta}) \sum_{q=u,d,s,c,b} (\bar{q}_{L\beta}\gamma^\mu q_{L\alpha}), \\
O_5 &= (\bar{s}_{L\alpha}\gamma_\mu b_{L\alpha}) \sum_{q=u,d,s,c,b} (\bar{q}_{R\beta}\gamma^\mu q_{R\beta}) \\
O_6 &= (\bar{s}_{L\alpha}\gamma_\mu b_{L\beta}) \sum_{q=u,d,s,c,b} (\bar{q}_{R\beta}\gamma^\mu q_{R\alpha}), \tag{2.49}
\end{aligned}$$

Electroweak-penguin operators (Fig. 2.4(c)):

$$\begin{aligned}
O_7 &= \frac{3}{2}(\bar{s}_{L\alpha}\gamma_\mu b_{L\alpha}) \sum_{q=u,d,s,c,b} e_q (\bar{q}_{R\beta}\gamma^\mu q_{R\beta}), \\
O_8 &= \frac{3}{2}(\bar{s}_{L\alpha}\gamma_\mu b_{L\beta}) \sum_{q=u,d,s,c,b} e_q (\bar{q}_{R\beta}\gamma^\mu q_{R\alpha}), \\
O_9 &= \frac{3}{2}(\bar{s}_{L\alpha}\gamma_\mu b_{L\alpha}) \sum_{q=u,d,s,c,b} e_q (\bar{q}_{L\beta}\gamma^\mu q_{L\beta}), \\
O_{10} &= \frac{3}{2}(\bar{s}_{L\alpha}\gamma_\mu b_{L\beta}) \sum_{q=u,d,s,c,b} e_q (\bar{q}_{L\beta}\gamma^\mu q_{L\alpha}). \tag{2.50}
\end{aligned}$$

Magnetic-penguin operators (Fig. 2.4(d)):

$$\begin{aligned}
\mathcal{O}_{7\gamma} &= \frac{e}{16\pi^2} \bar{s} \sigma^{\mu\nu} (m_b R + m_s L) b F_{\mu\nu}, \\
\mathcal{O}_{8G} &= \frac{g_s}{16\pi^2} \bar{s}_\alpha T_{\alpha\beta}^a b_\beta \sigma^{\mu\nu} (m_b R + m_s L) G_{\mu\nu}^a, \tag{2.51}
\end{aligned}$$

$\Delta S = 2$ and $\Delta B = 2$ operators (Fig. 2.4(e)):

$$O(\Delta S = 2, \Delta B = 2) = (\bar{s}_{L\alpha}\gamma_\mu b_{L\alpha})(\bar{s}_{L\beta}\gamma^\mu b_{L\beta}). \tag{2.52}$$

Semi-leptonic operators (Fig. 2.4(f)):

$$\begin{aligned}
O_9 &= \frac{e}{16\pi^2} (\bar{s}_L\gamma_\mu b_L)(\bar{\ell}\gamma_\mu \ell), \\
O_{10} &= \frac{e}{16\pi^2} (\bar{s}_L\gamma_\mu b_L)(\bar{\ell}\gamma_\mu \gamma_5 \ell) \tag{2.53}
\end{aligned}$$

where $L(R) = (1 \mp \gamma_5)/2$, $\sigma_{\mu\nu} = \frac{i}{2}[\gamma_\mu, \gamma_\nu]$, α, β are $SU(3)$ colour indices and T^a , $a = 1 \dots 8$ are the generators of QCD. Here $F_{\mu\nu}$ and $G_{\mu\nu}^a$ are the field strength tensors of the electromagnetic and strong interactions, respectively.

The coupling strength of the introduced effective vertices \mathcal{O}_i is given by the Wilson coefficients $C_i(\mu)$. Their values at a large scale $\mu = m_W$ are obtained from a “matching” of the effective with the full theory. In the SM, the $C_i(m_W)$ s read as follows [10, 12, 13]

$$\begin{aligned}
C_{1,3\dots 6}(m_W) &= 0 , \\
C_2(m_W) &= 1 , \\
C_7(m_W) &= \frac{3x_t^3 - 2x_t^2}{4(x_t - 1)^4} \ln x_t + \frac{-8x_t^3 - 5x_t^2 + 7x_t}{24(x_t - 1)^3} , \\
C_8(m_W) &= \frac{-3x_t^2}{4(x_t - 1)^4} \ln x_t + \frac{-x_t^3 + 5x_t^2 + 2x_t}{8(x_t - 1)^3} , \\
C_9(m_W) &= \frac{4}{9} + \frac{1}{\sin^2 \theta_W} \left(-B(x_t) + (1 - 4 \sin^2 \theta_W)(C(x_t) - D(x_t)) \right), \\
C_{10}(m_W) &= \frac{1}{\sin^2 \theta_W} \left(B(x_t) - C(x_t) \right), \tag{2.54}
\end{aligned}$$

with $x = m_t^2/m_W^2$ and

$$\begin{aligned}
B(x_t) &= \frac{x_t}{4(x_t - 1)^2} \ln x_t + \frac{x_t}{4(x_t - 1)} , \\
C(x_t) &= \frac{x_t(3x_t + 2)}{8(x_t - 1)^2} \ln x_t + \frac{x_t(x_t - 6)}{8(x_t - 1)} , \\
D(x_t) &= \frac{x_t^2(5x_t^2 - 2x_t - 6)}{18(x_t - 1)^4} \ln x_t - \frac{4}{9} \ln x_t + \frac{-19x_t^3 + 25x_t^2}{36(x_t - 1)^3} . \tag{2.55}
\end{aligned}$$

The leading logarithmic (LL) order diagrams in the SM are subject to QCD corrections, which are proportional to the powers of $\alpha_s(m_W) \ln(m_W^2/m_b^2)$ and too large to be an expansion parameter. Therefore, to calculate them, one applies the renormalization group equation (RGE) for the Wilson coefficients, which looks like

$$\mu \frac{d}{d\mu} C_i(\mu) = \sum_j \gamma_{ji} C_j(\mu) , \tag{2.56}$$

where γ , called the anomalous dimension matrix, indicates that in general the operators mix under renormalization. Eq. (2.56) can be solved in perturbation theory and this solution gives the running of the Wilson coefficients under QCD from $\mu = m_W$ (a larger scale) down to the low scale $\mu \approx m_b$, which is a relevant scale for B-decays. After these matching and the RGE evaluation steps, the $C_i(\mu)$ s

can be decomposed into a leading logarithmic (LL), next-to-leading logarithmic (NLL) and next-next-to-leading logarithmic (NNLL), etc., parts according to

$$C_i(\mu) = C_i^{(0)}(\mu) + \frac{\alpha_s}{4\pi} C_i^{(1)}(\mu) + \frac{\alpha_s^2}{(4\pi)^2} C_i^{(2)}(\mu) + \mathcal{O}(\alpha_s^3). \quad (2.57)$$

The initial values of the above RGE are the $C_i^{(0)}(m_W)$, which in the lowest order in the SM are given by Eq. (2.54). In the LL approximation, the Wilson coefficients for the operators O_1, \dots, O_8 are given by [13]-[17]

$$\begin{aligned} C_i^{(0)}(\mu) &= \sum_{j=1}^8 k_{ij} \eta^{a_j} \quad (i = 1, \dots, 6), \\ C_7^{(0)eff}(\mu) &= \eta^{\frac{16}{23}} C_7^{(0)}(m_W) + \frac{8}{3} \left(\eta^{\frac{14}{23}} - \eta^{\frac{16}{23}} \right) C_8^{(0)}(m_W) + \sum_{j=1}^8 h_j \eta^{a_j}, \end{aligned} \quad (2.58)$$

with

$$\eta = \frac{\alpha_s(m_W)}{\alpha_s(\mu)}, \quad (2.59)$$

where

$$\alpha_s(\mu) = \frac{4\pi}{\beta_0 \ln(\mu^2/\Lambda_{QCD}^2)} \left[1 - \frac{\beta_1 \ln \ln(\mu^2/\Lambda_{QCD}^2)}{\beta_0^2 \ln(\mu^2/\Lambda_{QCD}^2)} \right], \quad (2.60)$$

with $\beta_0 = 23/3$ and $\beta_1 = 116/3$ when number of flavors are five. The numbers a_j , k_{ij} and h_j are given as

$$\begin{aligned} a_j &= \left(\frac{14}{23}, \frac{16}{23}, \frac{6}{23}, -\frac{12}{23}, 0.4086, -0.8994, 0.1456 \right), \\ k_{1j} &= \left(0, 0, \frac{1}{2}, -\frac{1}{2}, 0, 0, 0, 0 \right), \\ k_{2j} &= \left(0, 0, \frac{1}{2}, \frac{1}{2}, 0, 0, 0, 0 \right), \\ k_{3j} &= \left(0, 0, -\frac{1}{14}, \frac{1}{6}, 0.0510, -0.1403, -0.0113, 0.0054 \right), \\ k_{4j} &= \left(0, 0, -\frac{1}{14}, -\frac{1}{6}, 0.0984, 0.1214, 0.0156, 0.0026 \right), \\ k_{5j} &= \left(0, 0, 0, 0, -0.0397, 0.0117, -0.0025, 0.0304 \right), \\ k_{6j} &= \left(0, 0, 0, 0, 0.0335, 0.0239, -0.0462, -0.0112 \right), \\ h_j &= \left(2.2996, -1.088, -\frac{3}{7}, -\frac{1}{14}, -0.6494, -0.038, -0.0186, -0.0057 \right). \end{aligned} \quad (2.61)$$

Table 2.4: Values of the SM Wilson coefficients at $\mu \sim m_b$ scale.

C_1	C_2	C_3	C_4	C_5	C_6	C_7^{eff}	C_9	C_{10}
-0.248	1.107	0.011	-0.026	0.007	-0.031	-0.313	4.344	-4.624

The coefficient $C_8(\mu)$ does not enter the formula for $b \rightarrow s\ell^+\ell^-$, and its analytic expression can be found in ref.[14]. Since O_{10} does not renormalize under QCD its coefficient C_{10} does not depend on μ .

Using the parameters listed in Appendix A, the numerical values of the Wilson coefficients in the LL approximation is given in Table (2.4).

Finally, including LL as well as NLL we have

$$\begin{aligned}
C_9^{\text{eff}} &= C_9 \\
&+ h(u, s) \left(3C_1(\mu) + C_2(\mu) + 3C_3(\mu) + C_4(\mu) + 3C_5(\mu) + C_6(\mu) \right) \\
&- \frac{1}{2} h(1, s) \left(4C_3(\mu) + 4C_4(\mu) + 3C_5(\mu) + C_6(\mu) \right) \\
&- \frac{1}{2} h(0, s) \left(C_3(\mu) + 3C_4(\mu) \right) + \frac{2}{9} \left(3C_3(\mu) + C_4(\mu) + 3C_5(\mu) + C_6(\mu) \right),
\end{aligned} \tag{2.62}$$

where

$$h(u, s) = -\frac{8}{9} \ln \frac{m_b}{\mu} - \frac{8}{9} \ln u + \frac{8}{27} + \frac{4}{9} x \tag{2.63}$$

$$-\frac{2}{9} (2+x) |1-x|^{1/2} \begin{cases} \left(\ln \left| \frac{\sqrt{1-x}+1}{\sqrt{1-x}-1} \right| - i\pi \right), & \text{for } x \equiv \frac{4u^2}{s} < 1 \\ 2 \arctan \frac{1}{\sqrt{x-1}}, & \text{for } x \equiv \frac{4u^2}{s} > 1, \end{cases}$$

$$h(0, s) = \frac{8}{27} - \frac{8}{9} \ln \frac{m_b}{\mu} - \frac{4}{9} \ln s + \frac{4}{9} i\pi, \tag{2.64}$$

with $s = (p_{\ell^+} + p_{\ell^-})^2/m_b^2$ and $u = \frac{m_c}{m_b}$. In addition, several groups has recently evaluated the NNLL level contributions to the Wilson coefficients [45]-[52]. For a detailed discussion of the present status of the $b \rightarrow s\ell^+\ell^-$ transition one can look at ref. [53].

It should be noted here that the value of the Wilson coefficient C_9^{eff} above corresponds only to the short-distance (SD) contributions. C_9^{eff} also receives long-distance (LD) contributions due to conversion of the real $\bar{c}c$ into lepton pair $\ell^+\ell^-$ i.e., with the reaction chain $B \rightarrow \gamma + V(c\bar{c}) \rightarrow \gamma\ell^+\ell^-$. This additional

Table 2.5: Charmonium ($\bar{c}c$) masses and widths [32].

Meson	Mass (GeV)	BR($V \rightarrow \ell^+\ell^-$)	Γ (MeV)
$J/\Psi(1s)$	3.097	6.0×10^{-2}	0.088
$\Psi(2s)$	3.686	8.3×10^{-3}	0.277
$\Psi(3770)$	3.770	1.1×10^{-5}	23.6
$\Psi(4040)$	4.040	1.4×10^{-5}	52
$\Psi(4160)$	4.159	1.0×10^{-5}	78
$\Psi(4415)$	4.415	1.1×10^{-5}	43

contributions appear as exclusive modes for which the momentum scale of the intermediate quarks is a strong interaction scale and not the short distance scale m_W . This forces us to view the intermediate states as hadrons rather than quarks. To calculate this LD contributions, an effective Lagrangian \mathcal{L}_{res} corresponding to these kind of $\bar{c}c$ resonances is added to the original effective Lagrangian for the process $B \rightarrow \gamma\ell^+\ell^-$. The resulting structure of \mathcal{L}_{res} is the same as that of the operator O_9 in (2.53). It is then convenient to include the resonance contribution by simply making the replacement

$$C_9^{eff}(\mu) \rightarrow C_9^{eff}(\mu) + Y_{res} . \quad (2.65)$$

It is possible to parametrize the resonance $\bar{c}c$ contribution Y_{reson} in Eq.(2.65) using a Breit-Wigner shape with normalizations fixed by data given by [54]

$$Y_{res}(s) = -\frac{3}{\alpha_{em}^2} \kappa \sum_{V_i=J/\psi,\psi',\dots} \frac{\pi\Gamma(V_i \rightarrow \ell^+\ell^-)m_{V_i}}{sm_B^2 - m_{V_i} + im_{V_i}\Gamma_{V_i}} \times [(3C_1(\mu) + C_2(\mu) + 3C_3(\mu) + C_4(\mu) + 3C_5(\mu) + C_6(\mu))] . \quad (2.66)$$

There are six known resonances in the $\bar{c}c$ system that can contribute to the decay modes $B_s \rightarrow \gamma\ell^+\ell^-$. Their properties are summarized in Table (2.5).

The phenomenological parameter κ in Eq. (2.66) is usually taken as ~ 2.3 .

CHAPTER 3

MODEL INDEPENDENT ANALYSIS OF $B_s \rightarrow \gamma \ell^+ \ell^-$ DECAYS

It is well known that the rare B meson decays, as being FCNC processes, are sensitive to the structure of the standard model (SM), and its possible extensions. Therefore, these decays may serve as an important tool to investigate the new physics prior to any possible experimental clue about it. The experimental situation concerning B physics is promising too. In addition to several experiments running successfully, like the BELLE experiment at KEK and the BaBar at SLAC, new facilities will also start to explore B physics in a near future, like the LHC-B experiment at CERN and BTeV at FERMILAB.

Among the rare B-meson decays, the semileptonic $B_s \rightarrow \gamma \ell^+ \ell^-$ ($\ell = e, \mu, \tau$) decays are especially interesting due to their relative cleanliness and sensitivity to new physics. $B_s \rightarrow \gamma \ell^+ \ell^-$ decay is induced by $B \rightarrow \ell^+ \ell^-$ one, which can in principle serve as a useful process to determine the fundamental parameters of the SM since the only non-perturbative quantity in its theoretical calculation is the decay constant f_{B_s} , which is reliably known. However, in the SM, matrix element of $B \rightarrow \ell^+ \ell^-$ decay is proportional to the lepton mass and therefore corresponding branching ratio will be suppressed. Although $\ell = \tau$ channel is free from this suppression, its experimental observation is quite difficult due to low efficiency. In this connection, it has been pointed out [55]-[62] that the radiative leptonic $B^+ \rightarrow \ell^+ \nu_\ell \gamma$ ($\ell = e, \mu$) decays have larger branching ratios than purely leptonic modes. It has been shown [19, 63] that similar enhancements take place also in the radiative decay $B_s \rightarrow \gamma \ell^+ \ell^-$ in which the photon emitted from any of the charged lines in addition to the lepton pair makes it possible to overcome the helicity suppression. For that reason, the investigation of the $B_s \rightarrow \gamma \ell^+ \ell^-$ decays becomes interesting.

As an exclusive process, the theoretical calculation of $B_s \rightarrow \gamma \ell^+ \ell^-$ decay requires the additional knowledge about the decay form factors. These are the matrix elements of the effective Hamiltonian between the initial B and final photon states, when a photon is released from the initial quark lines, which give rise to the so called "structure dependent" (SD) contributions to the amplitude, and between the B and the vacuum states for the "internal Bremsstrahlung" (IB) part, which arises when a photon is radiated from final leptons. Finding these hadronic transition matrix elements is related to the nonperturbative sector of the QCD and should be calculated by means of a nonperturbative approach. Thus, their theoretical calculation yields the main uncertainty in the prediction of the exclusive rare decays. The form factors for B decays into γ and a vacuum state have been calculated in the framework of light-cone QCD sum rules in [18, 19] and in the framework of the light front quark model in [20]. In addition, it has been proposed a model in [21] for the $B \rightarrow \gamma$ form factors which obeys all the restrictions obtained from the gauge invariance combined with the large energy effective theory.

Various kinematical distributions of the $B_s \rightarrow \gamma \ell^+ \ell^-$ decays have been studied in many earlier works. The analysis in the framework of the SM can be found in [19, 20, 59, 63]. The new physics effects in these decays have been studied in some models, like minimal supersymmetric Standard model (MSSM) [22],[64]-[66] and the two Higgs doublet model (2HDM) [67]-[70], and shown that different observables, like branching ratio, forward-backward asymmetry, etc., are very sensitive to the physics beyond the SM. In $B_s \rightarrow \gamma \ell^+ \ell^-$ decay, in addition to the branching ratio and lepton pair forward-backward asymmetry, it is possible to study some other experimentally observable quantities associated with the final state leptons and photon, such as the photon and lepton polarization asymmetries. Along this line, the polarization asymmetries of the final state lepton in $B_s \rightarrow \gamma \ell^+ \ell^-$ decays have been studied in MSSM in [22] and concluded that they can be very useful for accurate determination of various Wilson coefficients.

In this work, we will investigate the new physics effects in the photon and

lepton polarization asymmetries in the $B_s \rightarrow \gamma \ell^+ \ell^-$ decay. In rare B meson decays, the new physics effects can appear in two different ways: one way is through new contributions to the Wilson coefficients that is already present in the SM, and the other is through the new operators in the effective Hamiltonian which is absent in the SM. In this work we use a most general model independent effective Hamiltonian that combines both these approaches and contains the scalar and tensor type interactions as well as the vector types (see Eq.(3.2) below).

This chapter is organized as follows: In Sec. 3.1, we give the most general effective Hamiltonian for the quark level process $b \rightarrow s \ell^+ \ell^-$. In Sec. 3.2, we first give the definitions of the form factors, and then introduce the corresponding matrix element. Finally, we calculate the decay rate of the process $B_s \rightarrow \gamma \ell^+ \ell^-$.

3.1 Effective Hamiltonian

The effective Hamiltonian for $b \rightarrow s \ell^+ \ell^-$ transition in the SM can be written as

$$\begin{aligned} \mathcal{H}_{eff} = & \frac{\alpha G_F}{\sqrt{2}\pi} V_{ts} V_{tb}^* \left\{ (C_9^{eff} - C_{10}) (\bar{s} \gamma_\mu L b \bar{\ell} \gamma^\mu L \ell) \right. \\ & \left. + (C_9^{eff} + C_{10}) \bar{s} \gamma_\mu L b \bar{\ell} \gamma^\mu R \ell - 2C_7 \frac{m_b}{q^2} \bar{s} i \sigma_{\mu\nu} q^\nu R b \bar{\ell} \gamma^\mu \ell \right\}, \quad (3.1) \end{aligned}$$

where q is the momentum transfer. It is seen from Eq. (3.1) that it is not included the right handed components of the related wave function into the effective Hamiltonian. This follows from the fact that in the SM only left handed parts of the wave functions enter into the weak interactions. However, to construct a more general effective Hamiltonian going beyond the SM, one must take into account the right handed components of the leptons and quarks together with the left handed ones. In this way the effective Hamiltonian for $b \rightarrow s \ell^+ \ell^-$ transition can be written in terms of twelve model independent four-Fermi interactions as follows [71]:

$$\begin{aligned} \mathcal{H}_{eff} = & \frac{G\alpha}{\sqrt{2}\pi} V_{ts} V_{tb}^* \left\{ C_{SL} \bar{s} i \sigma_{\mu\nu} \frac{q^\nu}{q^2} L b \bar{\ell} \gamma^\mu \ell + C_{BR} \bar{s} i \sigma_{\mu\nu} \frac{q^\nu}{q^2} R b \bar{\ell} \gamma^\mu \ell \right. \\ & \left. + C_{LL}^{tot} \bar{s}_L \gamma_\mu b_L \bar{\ell}_L \gamma^\mu \ell_L + C_{LR}^{tot} \bar{s}_L \gamma_\mu b_L \bar{\ell}_R \gamma^\mu \ell_R + C_{RL} \bar{s}_R \gamma_\mu b_R \bar{\ell}_L \gamma^\mu \ell_L \right\} \end{aligned}$$

$$\begin{aligned}
& +C_{RR} \bar{s}_R \gamma_\mu b_R \bar{\ell}_R \gamma^\mu \ell_R + C_{LRLR} \bar{s}_L b_R \bar{\ell}_L \ell_R + C_{RLLR} \bar{s}_R b_L \bar{\ell}_L \ell_R \\
& +C_{LRRL} \bar{s}_L b_R \bar{\ell}_R \ell_L + C_{RLRL} \bar{s}_R b_L \bar{\ell}_R \ell_L + C_T \bar{s} \sigma_{\mu\nu} b \bar{\ell} \sigma^{\mu\nu} \ell \\
& +iC_{TE} \epsilon^{\mu\nu\alpha\beta} \bar{s} \sigma_{\mu\nu} b \bar{\ell} \sigma_{\alpha\beta} \ell \Big\} .
\end{aligned} \tag{3.2}$$

In the equation above, C_X are the coefficients of the four-Fermi interactions with $X = LL, LR, RL, RR$ describing vector, $X = LRLR, RLLR, LRRL, RLRL$ scalar and $X = T, TE$ tensor type interactions. We note that several of the Wilson coefficients in Eq. (3.2) do already exist in the SM: C_{LL} and C_{LR} are in the form $C_9^{eff} - C_{10}$ and $C_9^{eff} + C_{10}$ for the $b \rightarrow s \ell^+ \ell^-$ decay in the SM, while the coefficients C_{SL} and C_{BR} correspond to $-2m_s C_7^{eff}$ and $-2m_b C_7^{eff}$, respectively. Therefore, writing

$$\begin{aligned}
C_{LL}^{tot} &= C_9^{eff} - C_{10} + C_{LL} , \\
C_{LR}^{tot} &= C_9^{eff} + C_{10} + C_{LR} ,
\end{aligned}$$

we see that C_{LL}^{tot} and C_{LR}^{tot} contain the contributions from the SM and also from the new physics.

3.2 Matrix Elements and the Decay Rate

Having established the general form of the effective Hamiltonian, next step is calculation of the matrix element of the $B_s \rightarrow \gamma \ell^+ \ell^-$ decay, which can be obtained as a sum of the structure-dependent, \mathcal{M}_{SD} , and internal Bremsstrahlung, \mathcal{M}_{IB} , parts ,

$$\mathcal{M} = \mathcal{M}_{SD} + \mathcal{M}_{IB}. \tag{3.3}$$

This exclusive decay can receive short-distance contributions from the box, Z, and photon penguin diagrams for $b \rightarrow s$ transition by attaching an additional photon line to any internal or external lines. As pointed out before [19, 58], contributions coming from the release of the free photon from any charged internal line are strongly suppressed by a factor of m_b^2/m_W^2 and neglected in the following analysis. Moreover, from helicity arguments, the contributions of the diagrams where photon is emitted from the final charged lepton lines must be proportional

to the lepton mass m_ℓ ($\ell = e, \mu, \tau$). Hence, the main contributions to this decay come from diagrams, when photon is attached to the initial and final fermions.

When a photon is released from the initial quark lines it contributes to the so-called "structure dependent" (SD) part of the amplitude, \mathcal{M}_{SD} . Then, it follows from Eq. (3.2) that, in order to calculate \mathcal{M}_{SD} , the matrix elements needed and their definitions in term of the various form factors are as follows [58, 63]:

$$\begin{aligned} \langle \gamma(k) | \bar{s} \gamma_\mu (1 \mp \gamma_5) b | B(p_B) \rangle &= \frac{e}{m_B^2} \left\{ \epsilon_{\mu\nu\lambda\sigma} \varepsilon^{*\nu} q^\lambda k^\sigma g(q^2) \right. \\ &\quad \left. \pm i \left[\varepsilon^{*\mu}(kq) - (\varepsilon^* q) k^\mu \right] f(q^2) \right\}, \end{aligned} \quad (3.4)$$

$$\langle \gamma(k) | \bar{s} \sigma_{\mu\nu} b | B(p_B) \rangle = \frac{e}{m_B^2} \epsilon_{\mu\nu\lambda\sigma} \left[G \varepsilon^{*\lambda} k^\sigma + H \varepsilon^{*\lambda} q^\sigma + N (\varepsilon^* q) q^\lambda k^\sigma \right], \quad (3.5)$$

$$\langle \gamma(k) | \bar{s} (1 \mp \gamma_5) b | B(p_B) \rangle = 0, \quad (3.6)$$

$$\langle \gamma(k) | \bar{s} i \sigma_{\mu\nu} q^\nu b | B(p_B) \rangle = \frac{e}{m_B^2} i \epsilon_{\mu\nu\alpha\beta} q^\nu \varepsilon^{\alpha*} k^\beta G, \quad (3.7)$$

and

$$\begin{aligned} \langle \gamma(k) | \bar{s} i \sigma_{\mu\nu} q^\nu (1 + \gamma_5) b | B(p_B) \rangle &= \frac{e}{m_B^2} \left\{ \epsilon_{\mu\alpha\beta\sigma} \varepsilon^{\alpha*} q^\beta k^\sigma g_1(q^2) \right. \\ &\quad \left. + i \left[\varepsilon_\mu^*(qk) - (\varepsilon^* q) k_\mu \right] f_1(q^2) \right\}, \end{aligned} \quad (3.8)$$

where ε_μ^* and k_μ are the four-vector polarization and four-momentum of the photon, respectively, p_B is the momentum of the B meson, and G , H and N can be expressed in terms of the form factors g_1 and f_1 by using Eqs. (3.5), (3.7) and (3.8). To make some numerical predictions, we need the explicit forms of the form factors g , f , g_1 and f_1 . They are calculated in framework of light-cone QCD sum rules in [63, 58], and also in [21] in terms of two parameters $F(0)$ and m_F . In our work, we have used the results of [58] in which q^2 dependencies of the form factors are given by

$$g(q^2) = \frac{1 \text{ GeV}}{\left(1 - \frac{q^2}{5.6^2}\right)^2}, \quad f(q^2) = \frac{0.8 \text{ GeV}}{\left(1 - \frac{q^2}{6.5^2}\right)^2}$$

$$g_1(q^2) = \frac{3.74 \text{ GeV}^2}{\left(1 - \frac{q^2}{40.5}\right)^2}, \quad f_1(q^2) = \frac{0.68 \text{ GeV}^2}{\left(1 - \frac{q^2}{30}\right)^2}.$$

The matrix element describing the structure-dependent part can be obtained from Eqs. (3.4)–(3.8) as

$$\begin{aligned} \mathcal{M}_{SD} = & \frac{\alpha G_F}{4\sqrt{2}\pi} V_{tb} V_{ts}^* \frac{e}{m_B^2} \\ & \left\{ \bar{\ell} \gamma^\mu (1 - \gamma_5) \ell \left[A_1 \epsilon_{\mu\nu\alpha\beta} \varepsilon^{*\nu} q^\alpha k^\beta + i A_2 \left(\varepsilon_\mu^*(kq) - (\varepsilon^* q) k_\mu \right) \right] \right. \\ & + \bar{\ell} \gamma^\mu (1 + \gamma_5) \ell \left[B_1 \epsilon_{\mu\nu\alpha\beta} \varepsilon^{*\nu} q^\alpha k^\beta + i B_2 \left(\varepsilon_\mu^*(kq) - (\varepsilon^* q) k_\mu \right) \right] \\ & + i \epsilon_{\mu\nu\alpha\beta} \bar{\ell} \sigma^{\mu\nu} \ell \left[G \varepsilon^{*\alpha} k^\beta + H \varepsilon^{*\alpha} q^\beta + N (\varepsilon^* q) q^\alpha k^\beta \right] \\ & \left. + i \bar{\ell} \sigma_{\mu\nu} \ell \left[G_1 (\varepsilon^{*\mu} k^\nu - \varepsilon^{*\nu} k^\mu) + H_1 (\varepsilon^{*\mu} q^\nu - \varepsilon^{*\nu} q^\mu) + N_1 (\varepsilon^* q) (q^\mu k^\nu - q^\nu k^\mu) \right] \right\}, \end{aligned} \quad (3.9)$$

where

$$\begin{aligned} A_1 &= \frac{1}{q^2} (C_{BR} + C_{SL}) g_1 + (C_{LL}^{tot} + C_{RL}) g, \\ A_2 &= \frac{1}{q^2} (C_{BR} - C_{SL}) f_1 + (C_{LL}^{tot} - C_{RL}) f, \\ B_1 &= \frac{1}{q^2} (C_{BR} + C_{SL}) g_1 + (C_{LR}^{tot} + C_{RR}) g, \\ B_2 &= \frac{1}{q^2} (C_{BR} - C_{SL}) f_1 + (C_{LR}^{tot} - C_{RR}) f, \\ G &= 4C_T g_1, & N &= -4C_T \frac{1}{q^2} (f_1 + g_1), \\ H &= N(qk), & G_1 &= -8C_{TE} g_1, \\ N_1 &= 8C_{TE} \frac{1}{q^2} (f_1 + g_1), & H_1 &= N_1(qk). \end{aligned}$$

When photon is radiated from the lepton line we get the so-called "internal Bremsstrahlung" (IB) contribution, \mathcal{M}_{IB} . Using the expressions

$$\begin{aligned} \langle 0 | \bar{s} \gamma_\mu \gamma_5 b | B(p_B) \rangle &= -i f_B p_{B\mu}, \\ \langle 0 | \bar{s} \sigma_{\mu\nu} (1 + \gamma_5) b | B(p_B) \rangle &= 0, \end{aligned}$$

and conservation of the vector current, we get

$$\begin{aligned} \mathcal{M}_{IB} &= \frac{\alpha G_F}{4\sqrt{2}\pi} V_{tb} V_{ts}^* e f_B i \left\{ F \bar{\ell} \left(\frac{\not{\varepsilon}^* \not{p}_B}{2p_1 k} - \frac{\not{p}_B \not{\varepsilon}^*}{2p_2 k} \right) \gamma_5 \ell \right. \\ & \left. + F_1 \bar{\ell} \left[\frac{\not{\varepsilon}^* \not{p}_B}{2p_1 k} - \frac{\not{p}_B \not{\varepsilon}^*}{2p_2 k} + 2m_\ell \left(\frac{1}{2p_1 k} + \frac{1}{2p_2 k} \right) \not{\varepsilon}^* \right] \ell \right\}, \end{aligned} \quad (3.10)$$

where

$$\begin{aligned}
F &= 2m_\ell \left(C_{LR}^{tot} - C_{LL}^{tot} + C_{RL} - C_{RR} \right) + \frac{m_B^2}{m_b} \left(C_{LRLR} - C_{RLLR} - C_{LRRL} + C_{RLRL} \right), \\
F_1 &= \frac{m_B^2}{m_b} \left(C_{LRLR} - C_{RLLR} + C_{LRRL} - C_{RLRL} \right).
\end{aligned} \tag{3.11}$$

The next task is the calculation of the decay rate of $B_s \rightarrow \gamma \ell^+ \ell^-$ decay, which is determined from the following expression:

$$\Gamma = \frac{(2\pi)^4}{2E_B} \int \frac{d^3\vec{p}_1}{(2\pi)^3 2E_1} \frac{d^3\vec{p}_2}{(2\pi)^3 2E_2} \frac{d^3\vec{k}}{(2\pi)^3 2E_\gamma} |\mathcal{M}|^2 \delta^4(q - p_1 - p_2) \tag{3.12}$$

where \mathcal{M} is the matrix element of the decay. When the final state polarizations are not measured, we must sum over their spin states by making use of the following projection operators

$$\begin{aligned}
\sum_{spin} \ell(p_1) \bar{\ell}(p_1) &= \not{p}_1 - m_\ell, \\
\sum_{spin} \ell(p_2) \bar{\ell}(p_2) &= \not{p}_2 + m_\ell, \\
\sum_{spin} \varepsilon_\mu \varepsilon_\nu^* &= -g_{\mu\nu}
\end{aligned} \tag{3.13}$$

In the center of mass (c.m.) frame of the dileptons $\ell^+ \ell^-$, where we take $z = \cos \theta$ and θ is the angle between the momentum of the B_s -meson and that of ℓ^- , double differential decay width is found to be

$$\frac{d\Gamma}{dx dz} = \frac{1}{(2\pi)^3 64} x v m_B |\mathcal{M}|^2, \tag{3.14}$$

where $x = 2E_\gamma/m_B$, $v = \sqrt{1 - \frac{4r}{1-x}}$, $r = m_\ell^2/m_B^2$ and

$$|\mathcal{M}|^2 = C \left(|\mathcal{M}_{SD}|^2 + |\mathcal{M}_{IB}|^2 + 2Re(\mathcal{M}_{SD} \mathcal{M}_{IB}^*) \right) \tag{3.15}$$

with $C = \left| \frac{\alpha G_F}{4\sqrt{2}\pi} V_{tb} V_{ts}^* e \right|^2$ and

$$\begin{aligned}
|\mathcal{M}_{SD}|^2 &= \frac{16}{m_B^4} \left\{ 8 \left(|G_1|^2 + |G|^2 \right) (p_1 \cdot k) (p_2 \cdot k) + 2m_\ell \left[(Im[A_1 G_1^*] - Im[B_1 G_1^*]) \right. \right. \\
&\quad \left. \left. \left((p_1 \cdot k) - (p_2 \cdot k) \right) + (Re[A_2 G^*] - Re[B_2 G^*]) \left((p_1 \cdot k) - (p_2 \cdot k) \right) \right. \right. \\
&\quad \left. \left. - \left(Im[A_2 G_1^*] + Im[B_2 G_1^*] \right) \left((p_1 \cdot k) + (p_2 \cdot k) \right) - \left(Re[A G_1^*] + Re[B G_1^*] \right) \right. \right.
\end{aligned}$$

$$\begin{aligned}
& \left. \left((p_1 \cdot k)(p_2 \cdot k) \right) \right] (k \cdot q) + 2 \left(\text{Re}[A_1 A_2^*] - \text{Re}[B_1 B_2^*] \right) \left((p_1 \cdot q)(p_2 \cdot k) \right. \\
& - (p_1 \cdot k)(p_2 \cdot q) \left. \right) (k \cdot q) + 3 m_\ell \left[\left(\text{Re}[A_2 H^*] - \text{Re}[B_2 H^*] \right) \left((p_1 \cdot q) - (p_2 \cdot q) \right) \right. \\
& - \left. \left(\text{Im}[A_2 H_1^*] + \text{Im}[B_2 H_1^*] \right) \left((p_1 \cdot q) + (p_2 \cdot q) \right) \right] (k \cdot q) + m_\ell \left(- \text{Re}[A_2 N^*] \right. \\
& + \left. \text{Re}[B_2 N^*] \right) \left[\left((p_1 \cdot q) - (p_2 \cdot q) \right) (k \cdot q)^2 + m_\ell \left[2 m_\ell \text{Re}[A_1 B_1^*] \right. \right. \\
& + \left. 2 m_\ell \text{Re}[A_2 B_2^*] + \left(\text{Im}[A_2 N_1^*] + \text{Im}[B_2 N_1^*] \right) \left((p_1 \cdot q) + (p_2 \cdot q) \right) \right] (k \cdot q)^2 \\
& + \left. 2 \text{Re}[G_1 H_1^*] \left[2 (p_1 \cdot q)(p_2 \cdot k) + 2 (p_1 \cdot k)(p_2 \cdot q) + \left(3 m_\ell^2 - (p_1 \cdot p_2) \right) (k \cdot q) \right] \right. \\
& + \left. 2 \text{Re}[G H^*] \left[2 (p_1 \cdot q)(p_2 \cdot k) + 2 (p_1 \cdot k)(p_2 \cdot q) - \left(3 m_\ell^2 + (p_1 \cdot p_2) \right) (k \cdot q) \right] \right. \\
& + \left. |H_1|^2 \left[4 (p_1 \cdot q)(p_2 \cdot q) + \left(3 m_\ell^2 - (p_1 \cdot p_2) \right) q^2 \right] + |H|^2 \left[4 (p_1 \cdot q)(p_2 \cdot q) \right. \right. \\
& - \left. \left. \left(3 m_\ell^2 + (p_1 \cdot p_2) \right) q^2 \right] + \left(- 2 \text{Re}[G_1 N_1^*] - |N_1|^2 q^2 \right) \left[(k \cdot q) \left(2 (p_1 \cdot q)(p_2 \cdot k) \right. \right. \right. \\
& + \left. \left. 2 (p_1 \cdot k)(p_2 \cdot q) + \left(m_\ell^2 - (p_1 \cdot p_2) \right) (k \cdot q) \right) - 2 (p_1 \cdot k)(p_2 \cdot k) q^2 \right] \\
& + \left(|A_1|^2 + |A_2|^2 + |B_1|^2 + |B_2|^2 \right) \left[(p_1 \cdot q)(p_2 \cdot k)(k \cdot q) + (p_1 \cdot k) \right. \\
& \left. \left((p_2 \cdot q)(k \cdot q) - (p_2 \cdot k) q^2 \right) \right] + \left(G^* N + G N^* + |N|^2 q^2 \right) \\
& \left[- 2 (p_1 \cdot q)(p_2 \cdot k)(k \cdot q) + \left(m_\ell^2 + (p_1 \cdot p_2) \right) (k \cdot q)^2 + (p_1 \cdot k) \right. \\
& \left. \left(- 2 (p_2 \cdot q)(k \cdot q) + 2 (p_2 \cdot k) q^2 \right) \right] + 2 m_\ell \left[\left(- \text{Im}[A_1 H_1^*] + \text{Im}[B_1 H_1^*] \right) \right. \\
& \left. \left[\left((p_1 \cdot q) - (p_2 \cdot q) \right) (k \cdot q) + \left(- (p_1 \cdot k) + (p_2 \cdot k) \right) q^2 \right] \right. \\
& + \left. \left(- \text{Re}[A_1 H^*] + \text{Re}[B_1 H^*] \right) \right. \\
& \left. \left. \left. \left[\left((p_1 \cdot q) + (p_2 \cdot q) \right) (k \cdot q) - \left((p_1 \cdot k) + (p_2 \cdot k) \right) q^2 \right] \right] \right\} , \tag{3.16}
\end{aligned}$$

$$\begin{aligned}
|\mathcal{M}_{IB}|^2 &= \frac{4}{(p_1 \cdot k)^2 (p_2 \cdot k)^2} f_B^2 \left\{ (|F_1|^2 - |F|^2) m_\ell^2 \left[m_\ell^2 (p_1 \cdot k)^2 - 2 (p_1 \cdot p_2) \right. \right. \\
& \left. \left. (p_1 \cdot k)(p_2 \cdot k) + m_\ell^2 (p_2 \cdot k)^2 \right] + (|F_1|^2 + |F|^2) \left[- m_\ell^2 (p_1 \cdot k)^2 \left((p_1 \cdot p_2) \right. \right. \right. \\
& + \left. \left. (p_1 \cdot k) \right) + (p_1 \cdot k) \left[2 (p_1 \cdot p_2)^2 - \left(m_\ell^2 - 2 (p_1 \cdot p_2) \right) (p_1 \cdot k) \right. \right. \\
& + \left. \left. (p_1 \cdot k)^2 \right] (p_2 \cdot k) - \left(m_\ell^2 - 2 (p_1 \cdot k) \right) \left[(p_1 \cdot p_2) + (p_1 \cdot k)(p_2 \cdot k) \right]^2 \right. \\
& \left. \left. - \left(m_\ell^2 - (p_1 \cdot k) \right) (p_2 \cdot k)^3 \right] \right\} , \tag{3.17}
\end{aligned}$$

and

$$2 \text{Re}|\mathcal{M}_{IB} \mathcal{M}_{SD}^*| = \frac{-8}{(p_1 \cdot k)(p_2 \cdot k) m_B^2} f_B \left\{ - \left[3 (p_1 \cdot k)^2 (p_2 \cdot q) \right. \right.$$

$$\begin{aligned}
& + (p_2 \cdot k) \left[3(p_1 \cdot q)(p_2 \cdot k) + (p_1 \cdot p_2) \left(2(p_1 \cdot q) - (k \cdot q) \right) + \left(-2(p_2 \cdot q) \right. \right. \\
& + \left. \left. 3(k \cdot q) \right) m_\ell^2 \right] + (p_1 \cdot k) \left[2(p_1 \cdot p_2)(p_2 \cdot q) + (p_2 \cdot k)(p_2 \cdot q) - (p_1 \cdot p_2)(k \cdot q) \right. \\
& + \left. 3(k \cdot q) m_\ell^2 + (p_1 \cdot q) \left((p_2 \cdot k) - 2m_\ell^2 \right) \right] \text{Im}[F_1 H_1^*] \Big] + \left[2(p_1 \cdot q)^2 (p_2 \cdot k)^2 \right. \\
& + (p_1 \cdot q)(p_2 \cdot k) \left[3(p_2 \cdot k)(k \cdot q) + (p_1 \cdot k) \left(-4(p_2 \cdot q) + (k \cdot q) \right) \right] \\
& + (p_1 \cdot k)^2 \left(2(p_2 \cdot q)^2 + 3(p_2 \cdot q)(k \cdot q) - 2(p_2 \cdot k)q^2 \right) \\
& + (p_2 \cdot k)(k \cdot q)^2 \left((-p_1 \cdot p_2) + m_\ell^2 \right) + (p_1 \cdot k) \left[(p_2 \cdot k)(p_2 \cdot q)(k \cdot q) \right. \\
& - \left. 2(p_2 \cdot k)^2(q \cdot q) + (k \cdot q)^2 \left((-p_1 \cdot p_2) + m_\ell^2 \right) \right] \text{Im}[F_1 N_1^*] \\
& - \left((p_1 \cdot k) + (p_2 \cdot k) \right) (k \cdot q) m_\ell \left[\left((p_1 \cdot k) + (p_2 \cdot k) \right) \text{Re}[A_1^* F] \right. \\
& + \left. \left((p_1 \cdot k) + (p_2 \cdot k) \right) \text{Re}[B_1^* F] + \left((p_1 \cdot k) - (p_2 \cdot k) \right) \left(\text{Re}[A_1^* F_1] - \text{Re}[B_1^* F_1] \right) \right] \\
& + m_\ell \left[\left[- \left[\left((p_1 \cdot k) + (p_2 \cdot k) \right) \left[- \left((p_1 \cdot q)(p_2 \cdot k) \right) + (p_1 \cdot k)(p_2 \cdot q) \right] \right] \right. \right. \\
& + \left. \left((p_1 \cdot k) - (p_2 \cdot k) \right) (k \cdot q) \left((p_1 \cdot p_2) + (p_1 \cdot k) + (p_2 \cdot k) + m_\ell^2 \right) \right] \\
& \left(\text{Re}[A_2^* F] - \text{Re}[B_2^* F] \right) + \left[\left((-p_1 \cdot k) + (p_2 \cdot k) \right) \right. \\
& \left. \left[- \left((p_1 \cdot q)(p_2 \cdot k) \right) + (p_1 \cdot k)(p_2 \cdot q) \right] \right] \\
& + \left. \left((p_1 \cdot k) + (p_2 \cdot k) \right) (k \cdot q) \left((p_1 \cdot p_2) + (p_1 \cdot k) + (p_2 \cdot k) - m_\ell^2 \right) \right] \left(\text{Re}[A_2^* F_1] \right. \\
& + \left. \left. \text{Re}[B_2^* F_1] \right) \right] + 2 \left[-2(p_1 \cdot k)(p_2 \cdot k) \left((p_1 \cdot p_2) + (p_2 \cdot k) \right) + (p_2 \cdot k)^2 m_\ell^2 \right. \\
& + (p_1 \cdot k)^2 \left(-2(p_2 \cdot k) + m_\ell^2 \right) \left(\text{Im}[F_1 G_1^*] - \text{Re}[F^* G] \right) \\
& - \left[-3(p_1 \cdot k)^2 (p_2 \cdot q) + (p_1 \cdot k) \left[- \left((p_1 \cdot q)(p_2 \cdot k) \right) - 2(p_1 \cdot p_2)(p_2 \cdot q) \right. \right. \\
& - \left. \left. (p_2 \cdot k)(p_2 \cdot q) + (p_1 \cdot p_2)(k \cdot q) + 2(p_1 \cdot q) m_\ell^2 + 3(k \cdot q) m_\ell^2 \right] \right. \\
& + (p_2 \cdot k) \left[-3(p_1 \cdot q)(p_2 \cdot k) + (p_1 \cdot p_2) \left(-2(p_1 \cdot q) + (k \cdot q) \right) \right. \\
& + \left. \left. \left(2(p_2 \cdot q) + 3(k \cdot q) \right) m_\ell^2 \right] \right] \text{Re}[F^* H] + \left[-2(p_1 \cdot q)^2 (p_2 \cdot k)^2 \right. \\
& + (p_1 \cdot q)(p_2 \cdot k) \left[4(p_1 \cdot k)(p_2 \cdot q) - \left((p_1 \cdot k) + 3(p_2 \cdot k) \right) (k \cdot q) \right] \\
& + (p_1 \cdot k)^2 \left(-2(p_2 \cdot q)^2 - 3(p_2 \cdot q)(k \cdot q) + 2(p_2 \cdot k)q^2 \right) \\
& + (p_2 \cdot k)(k \cdot q)^2 \left((p_1 \cdot p_2) + m_\ell^2 \right) + (p_1 \cdot k) \left[- \left((p_2 \cdot k)(p_2 \cdot q)(k \cdot q) \right) \right.
\end{aligned}$$

$$+ 2(p_2 \cdot k)^2 q^2 + (k \cdot q)^2 ((p_1 \cdot p_2) + m_\ell^2) \Big] \text{Re}[F N^*] \Big\} . \quad (3.18)$$

We note that $|\mathcal{M}_{IB}|^2$ term has infrared singularity due to the emission of soft photon. In order to obtain a finite result, we follow the approach described in [19] and impose a cut on the photon energy, i.e., we require $E_\gamma \geq 25$ MeV, which corresponds to detect only hard photons experimentally. This cut requires that $E_\gamma \geq \delta m_B/2$ with $\delta = 0.01$. So, we have calculated the necessary formulae for the study of the polarization properties of the final state photon and leptons in $B_s \rightarrow \gamma \ell^+ \ell^-$ decay to which our next two chapters are devoted.

CHAPTER 4

PHOTON POLARIZATIONS IN $B_s \rightarrow \gamma \ell^+ \ell^-$ DECAY

In a radiative decay mode, like ours, the final state photon can emerge with a definite polarization and provide another kinematical variable to study the new physics effects [66]. Here, the rare $B_s \rightarrow \gamma \ell^+ \ell^-$ decay will be studied by taking into account the photon polarization. Although experimental measurement of this variable would be much more difficult than that of e.g., the polarization of the final leptons in $B_s \rightarrow \gamma \ell^+ \ell^-$ decay, this is still another kinematical variable for studying radiative decays. Therefore, it is important to investigate the sensitivity of such "photon polarization asymmetry" in $B_s \rightarrow \gamma \ell^+ \ell^-$ decay to the new Wilson coefficients in addition to studying the total and differential branching ratios with polarized final state photon.

We note that in a recent work [72] it has been considered the related mode $B_s \rightarrow \gamma \nu \bar{\nu}$ with a polarized photon in a similar way and showed that the spectrum is sensitive to the types of the interactions so that it is useful to discriminate the various new physics effects.

In Sec.1 of this chapter, we calculate the differential decay width and the photon polarization asymmetry for the $B_s \rightarrow \gamma \ell^+ \ell^-$ decay when the photon is in positive and negative helicity states. Sec. 2 is devoted to the numerical analysis and discussion of our results.

4.1 Photon Polarization

In a radiative decay, when the final state photon emerges with a definite polarization there follows the question of how sensitive the branching ratio is to the new Wilson coefficients when the photon is in the positive or negative helicity

states. To find an answer to this question for $B_s \rightarrow \gamma \ell^+ \ell^-$ decay, we evaluate $\frac{d\Gamma(\varepsilon^*=\varepsilon_1)}{dx}$ and $\frac{d\Gamma(\varepsilon^*=\varepsilon_2)}{dx}$ in the c.m. frame of $\ell^+ \ell^-$, in which four-momenta and polarization vectors, ε_1 and ε_2 , are as follows:

$$\begin{aligned} P_B &= (E_B, 0, 0, E_k), & k &= (E_k, 0, 0, E_k), \\ p_1 &= (p, 0, p\sqrt{1-z^2}, -pz), & p_2 &= (p, 0, -p\sqrt{1-z^2}, pz), \\ \varepsilon_1 &= (0, 1, i, 0)/\sqrt{2}, & \varepsilon_2 &= (0, 1, -i, 0)/\sqrt{2}, \end{aligned} \quad (4.1)$$

where $E_B = m_B(2-x)/2\sqrt{1-x}$, $E_k = m_B x/2\sqrt{1-x}$, and $p = m_B\sqrt{1-x}/2$. Using the above forms, we obtain

$$\frac{d\Gamma(\varepsilon^* = \varepsilon_i)}{dx} = \left| \frac{\alpha G_F}{4\sqrt{2}\pi} V_{tb} V_{ts}^* \right|^2 \frac{\alpha}{(2\pi)^3} \frac{\pi}{4} m_B \Delta(\varepsilon_i), \quad (4.2)$$

where

$$\begin{aligned} \Delta(\varepsilon_1) &= \frac{vx}{3} \left\{ 4x \left((8r+x) |H_1|^2 - (4r-x) |H|^2 \right) \right. \\ &\quad - 6m_\ell (1-x)^2 \text{Im}[(A_2 + A_1 + B_2 + B_1)G_1^*] \\ &\quad + \frac{2}{x} (1-x)^2 (2r+x) \left(|G_1|^2 + |G|^2 + 2\text{Im}[-G_1 G^*] \right) \\ &\quad - 12m_\ell (1-x)x \text{Im}[(A_2 + A_1 + B_2 + B_1)H_1^*] + 4(1-x) \left((8r+x) \text{Im}[GH_1^*] \right. \\ &\quad + (4r-x) \text{Im}[G_1 H^*] \left. \right) + 6m_\ell^2 (1-x)^2 \text{Re}[(A_1 + A_2)(B_1 + B_2)] \\ &\quad + m_B^2 (1-x)^2 (x-r) \left(|A_1|^2 + |A_2|^2 + |B_1|^2 + |B_2|^2 + 2 + \text{Re}[A_1 A_2^* + B_1 B_2^*] \right) \\ &\quad - 6m_\ell (1-x)^2 \text{Re}[(A_2 + A_1 + B_2 + B_1)G^*] \\ &\quad + 4(1-x) \left((8r+x) \text{Re}[G_1 H_1^*] - (4r-x) \text{Re}[GH^*] \right) \left. \right\} \\ &\quad + \frac{2x}{(1-x)^2} f_B^2 \left\{ \left(-2vx + (1-4r+x^2) \ln[u] \right) |F|^2 \right. \\ &\quad + 2(1-x) \left(2vx - (1-4r+x) \ln[u] \right) \text{Re}[FF_1^*] \\ &\quad + \left[2vx(4r-1) + (1+16r^2+x^2-4r(1+2x)) \ln[u] |F_1|^2 \right] \left. \right\} \\ &\quad + 2x f_B \left\{ \left(vx + 2r \ln[u] \right) \text{Im}[-FH_1^*] \right. \\ &\quad + m_\ell (1-x) \ln[u] \text{Re}[(A_2 + A_1 + B_2 + B_1)F^*] \\ &\quad - m_\ell \left(2vx + (1-4r-x) \ln[u] \right) \text{Re}[(A_2 + A_1 + B_2 + B_1)F_1^*] \left. \right\} \end{aligned}$$

$$\begin{aligned}
& - 2(v - 2r\ln[u]) \operatorname{Im}[(-F_1 + F)(G_1^* + G^*)] + 2(vx - 2r\ln[u])\operatorname{Re}[F_1 H^*] \\
& + \frac{2}{(1-x)} \left[(vx(1+x) + 2r(1-3x)\ln[u])\operatorname{Im}[F_1 H_1^*] \right. \\
& \left. - (1+x)(vx - 2r\ln[u])\operatorname{Re}[F_1 H^*] \right] \Big\}, \tag{4.3}
\end{aligned}$$

and

$$\begin{aligned}
\Delta(\varepsilon_2) = & \frac{vx}{3} \left\{ 4x \left((8r+x)|H_1|^2 - (4r-x)|H|^2 \right) \right. \\
& - 6m_\ell(1-x)^2 \operatorname{Im}[(A_2 - A_1 + B_2 - B_1)G_1^*] \\
& + \frac{2}{x}(1-x)^2(2r+x) \left(|G_1|^2 + |G|^2 - 2\operatorname{Im}[-G_1 G^*] \right) \\
& - 12m_\ell(1-x)x \operatorname{Im}[(A_2 - A_1 + B_2 - B_1)H_1^*] - 4(1-x) \left((8r+x)\operatorname{Im}[GH_1^*] \right. \\
& + (4r-x)\operatorname{Im}[G_1 H^*] \Big) + 6m_\ell^2(1-x)^2 \operatorname{Re}[(A_1 - A_2)(B_1 - B_2)] \\
& + m_B^2(1-x)^2(x-r) \left(|A_1|^2 + |A_2|^2 + |B_1|^2 + |B_2|^2 - 2\operatorname{Re}[A_1 A_2^* + B_1 B_2^*] \right) \\
& - 6m_\ell(1-x)^2 \operatorname{Re}[(A_2 - A_1 + B_2 - B_1)G^*] \\
& + 4(1-x) \left((8r+x)\operatorname{Re}[G_1 H_1^*] - (4r-x)\operatorname{Re}[GH^*] \right) \Big\} \\
& + \frac{2x}{(1-x)^2} f_B^2 \left\{ (-2vx + (1-4r+x^2)\ln[u])|F|^2 \right. \\
& - 2(1-x)(2vx - (1-4r+x) + \ln[u])\operatorname{Re}[FF_1^*] \\
& + \left(2vx(4r-1) + (1+16r^2+x^2-4r(1+2x))\ln[u]|F_1|^2 \right) \Big\} \\
& + 2x f_B \left\{ - (vx + 2r\ln[u])\operatorname{Im}[-FH_1^*] \right. \\
& - m_\ell(1-x)\ln[u] + \operatorname{Re}[(A_2 - A_1 + B_2 \pm B_1)F^*] \\
& - m_\ell \left(2vx + (1-4r-x)\ln[u] \right) + \operatorname{Re}[(A_2 - A_1 + B_2 - B_1)F_1^*] \\
& - 2(v - 2r\ln[u])\operatorname{Im}[(-F_1 - F)(G_1^* - G^*)] - 2(vx - 2r\ln[u])\operatorname{Re}[F_1 H^*] \\
& + \frac{2}{(1-x)} \left((vx(1+x) + 2r(1-3x)\ln[u])\operatorname{Im}[F_1 H_1^*] \right. \\
& \left. - (1+x)(vx - 2r\ln[u])\operatorname{Re}[F_1 H^*] \right) \Big\}, \tag{4.4}
\end{aligned}$$

where $u = 1 + v/1 - v$.

The effects of polarized photon can also be studied through a variable "photon

polarization asymmetry" [66]:

$$H(x) = \frac{\frac{d\Gamma(\varepsilon^*=\varepsilon_1)}{dx} - \frac{d\Gamma(\varepsilon^*=\varepsilon_2)}{dx}}{\frac{d\Gamma(\varepsilon^*=\varepsilon_1)}{dx} + \frac{d\Gamma(\varepsilon^*=\varepsilon_2)}{dx}} = \frac{\Delta(\varepsilon_1) - \Delta(\varepsilon_2)}{\Delta_0}, \quad (4.5)$$

where

$$\begin{aligned} \Delta(\varepsilon_1) - \Delta(\varepsilon_2) = & \frac{4}{3}x^2v \left\{ \frac{2x(1+2r-x)}{(-1+x)} \text{Im}[G_1G^*] - 3m_\ell x \left(\text{Im}[(A_1+B_1)G_1^*] \right. \right. \\ & + \left. \text{Re}[(A_2+B_2)G^*] \right) - 6m_\ell(1-x) \left(\text{Im}[(A_1+B_1)H_1^*] \right) + 2 \left((1+8r-x) \right. \\ & \left. \text{Im}[GH_1^*] - (1-4r-x) \text{Im}[G_1H^*] \right) + m_B^2 x \left(3r \text{Re}[A_2B_1^* + A_1B_2^*] \right. \\ & \left. + (1-r-x) \text{Re}[B_1B_2^* + A_1A_2^*] \right) \left. \right\} + 8f_B^2 \left(2v(1-x) - (2-4r-x) \ln[u] \right) \\ & + 4f_B x \left\{ 2(v(x-1) - 2r \ln[u]) \text{Im}[FH_1^*] + m_\ell x \ln[u] \text{Re}[(A_2+B_2)F^*] \right. \\ & + m_\ell \left(2v(x-1) + (4r-x) \ln[u] \right) \text{Re}[(A_1+B_1)F_1^*] + 2(v-2r \ln[u]) \text{Re}[F_1G^*] \\ & \left. - \text{Im}[FG_1^*] + 2(v(1-x) - 2r \ln[u]) \text{Re}[F_1H^*] \right\}, \quad (4.6) \end{aligned}$$

and

$$\begin{aligned} \Delta_0 = & x^3v \left\{ 4m_\ell \text{Re}[(A_1+B_1)G^*] - 4m_B^2 r \text{Re}[A_1B_1^* + A_2B_2^*] - 4 \left(|H_1|^2 (1-x) \right. \right. \\ & + \left. \left. \text{Re}[G_1H_1^*]x \right) \frac{(1+8r-x)}{x^2} - 4 \left(|H|^2 (1-x) + \text{Re}[GH^*]x \right) \frac{(1-4r-x)}{x^2} \right. \\ & + \frac{1}{3}m_B^2 \left(2 \text{Re}[GN^*] + m_B^2 |N|^2 (1-x) \right) (1-4r-x) \\ & + \frac{1}{3}m_B^2 \left(2 \text{Re}[G_1N_1^*] + m_B^2 |N_1|^2 (1-x) \right) (1+8r-x) \\ & - \frac{2}{3}m_B^2 \left(|A_1|^2 + |A_2|^2 + |B_1|^2 + |B_2|^2 \right) (1-r-x) \\ & - \frac{4}{3} \left(|G|^2 + |G_1|^2 \right) \frac{(1+2r-x)}{(1-x)} + 2m_\ell \text{Im} \left([A_2+B_2][6H_1^*(1-x) \right. \\ & + \left. 2G_1^*x - m_B^2 N_1^*x(1-x)] \frac{1}{x} \right) + 4f_B \left\{ 2v \left[\text{Re}[FG^*] \frac{1}{(1-x)} - \text{Re}[FH^*] \right. \right. \\ & + \left. m_B^2 \text{Re}[FN^*] + m_\ell \text{Re}[(A_2+B_2)F_1^*] \right] x(1-x) \\ & + \left. \ln[u] \left[m_\ell \text{Re}[(A_2+B_2)F_1^*] x(x-4r) + 2 \text{Re}[FH^*] (1-x+2r(x-2)) \right. \right. \\ & \left. \left. - 4rx \text{Re}[FG^*] + m_B^2 \text{Re}[FN^*] x(x-1) - m_\ell \text{Re}[(A_1+B_1)F^*] x^2 \right] \right\} \\ & + 2 \left[m_B^2 \text{Im}[F_1N_1^*] \left(v(1-x) + (x-1-2rx) \ln[u] \right) + \text{Im}[F_1H_1^*] \left[v(x-1) \right. \right. \end{aligned}$$

$$\begin{aligned}
& + \frac{1 - x - 4r(2x - 1)\ln[u]}{x} + \text{Im}[F_1 G_1^*](v - 2r\ln[u]) \\
& + 4f_B^2 \left\{ 2v \left(|F|^2 + (1 - 4r)|F_1|^2 \right) \frac{(1 - x)}{x} + \ln[u] \left[|F|^2 \left(2 + \frac{4r}{x} - \frac{2}{x} - x \right) \right. \right. \\
& \left. \left. + |F_1|^2 \left[2(1 - 4r) - \frac{2(1 - 6r + 8r^2)}{x} - x \right] \right] \right\}. \tag{4.7}
\end{aligned}$$

The expression in Eq. (4.6) agrees with [66] for the SM case with neutral Higgs contributions.

4.2 Numerical Analysis and Discussion

We present here our numerical analysis of the branching ratio (BR) and photon polarization asymmetries (H) for $B_s \rightarrow \gamma \ell^+ \ell^-$ decays with $\ell = \tau, \mu$. We use the input parameters given in Appendix A.

As for the values of the new Wilson coefficients, which are responsible for the new physics beyond the SM, they are the free parameters in this work. However, it is possible to establish ranges out of experimentally measured branching ratios of the semileptonic rare B-meson decays $B \rightarrow K \ell^+ \ell^-$ and $B \rightarrow K^* \ell^+ \ell^-$, recently announced by BaBar and BELLE Collaboration (See Eq. (1.2)). In addition, it is now available an upper bound of pure leptonic rare B-decays in the $B^0 \rightarrow \mu^+ \mu^-$ mode [73]:

$$BR(B^0 \rightarrow \mu^+ \mu^-) \leq 2.0 \times 10^{-7} .$$

Using these available experimental data we find that the right order of magnitude for the new Wilson coefficients is in the range $-4 \leq C_X \leq 4$, assuming that they are real. We further note that some of the new Wilson coefficients in Eq. (3.2) appear in some well known models beyond the SM, like some MSSM scenarios, and in literature there exists studies to establish ranges out of constraints under various precision measurements for these coefficients (see, e.g., [74]). Our choice for the range of the new Wilson coefficients above are also in agreement with these calculations.

We present the results of our analysis in a series of figures. Before their discussion we give our SM predictions for the unpolarized BRs without LD effects for reference:

$$\begin{aligned} BR(B_s \rightarrow \gamma\mu^+\mu^-) &= 1.52 \times 10^{-8}, \\ BR(B_s \rightarrow \gamma\tau^+\tau^-) &= 1.19 \times 10^{-8}, \end{aligned}$$

which are in good agreement with the results of ref. [59].

In Figs. (4.1) and (4.2), we present the dependence of the $BR^{(1)}$ and $BR^{(2)}$ for $B_s \rightarrow \gamma\mu^+\mu^-$ decay on the new Wilson coefficients, where the superscripts (1) and (2) correspond to the positive and negative helicity states of photon, respectively. From these figures we see that $BR^{(1)}$ and $BR^{(2)}$ are more sensitive to all type of the scalar interactions as compared to the vector and tensor types; receiving the maximum contribution from the one with coefficient C_{RLRL} and C_{LRLR} , respectively. From Fig. (4.2), we also observe that dependence of $BR^{(2)}$ on all the new Wilson coefficients is symmetric with respect to the zero point, while for $BR^{(1)}$, this symmetry is slightly lifted for the vector type interactions (Fig.(4.1)). It follows that $BR^{(2)}$ decreases in the region $-4 \leq C_X \leq 0$ and tends to increase in between $0 \leq C_X \leq +4$. $BR^{(1)}$ exhibits a similar behavior, except for the vector interactions with coefficients C_{LL} , C_{RL} and C_{LR} : it is almost insensitive to the existence of vector C_{LR} type interactions and slightly increases with the increasing values of C_{LL} and C_{RL} , receiving a value lower than the SM one between -4 and 0 .

Differential branching ratio can also give useful information about new physics effects. Therefore, in Figs. (4.3)-(4.8) we present the dependence of the differential branching ratio with a polarized photon for the $B_s \rightarrow \gamma\mu^+\mu^-$ decay on the dimensionless variable $x = 2E_\gamma/m_B$ at different values of vector, tensor and scalar interactions with coefficients C_{LL} , C_{TE} and C_{RLRL} . We observe that tensor (scalar) type interactions change the spectrum near the large (small)-recoil limit, $x \rightarrow 1$ ($x \rightarrow 0$), as seen from Figs.(4.5)-(4.6) (Figs.(4.7)-(4.8)). However, the vector type interactions increase the spectrum in the center of the phase space

and do not change it at the large or small-recoil limit (Figs.(4.3), (4.4)). We also see from Figs. (4.3) and (4.4) that when $C_{LL} > 0$, the related vector interaction gives constructive contribution to the SM result, but for the negative values of C_{LL} the contribution is destructive. Therefore, it is possible to get the information about the sign of new Wilson coefficients from measurement of the differential branching ratio.

From Figs. (4.1)-(4.8), we also see that the branching ratios with a positive helicity photon are greater than those with a negative helicity one. To see this we rewrite Eq. (4.3)-(4.4) for the SM in the limit $m_\ell \rightarrow 0$,

$$\begin{aligned} \Delta(\varepsilon_i) &= \frac{m_B^2}{3} x^2 (-1+x)^2 \left\{ \left| (C_9^{eff} - C_{10})(g \pm f) - \frac{2C_7}{(1-x)m_B^2} m_b (g_1 \pm f_1) \right|^2 \right. \\ &\quad \left. + \left| (C_9^{eff} + C_{10})(g \pm f) - \frac{2C_7}{(1-x)m_B^2} m_b (g_1 \pm f_1) \right|^2 \right\}, \end{aligned} \quad (4.8)$$

where $+(-)$ is for $i = 1(2)$. It obviously follows that $BR^{(1)} > BR^{(2)}$. We note that this fact can be seen more clearly from the comparison of the differential BRs for (1) and (2) cases for the vector interactions with the coefficient C_{LL} , given in Figs. (4.3) and (4.4), where $dBR^{(1)}/dx$ is larger about four times compared to $dBR^{(2)}/dx$.

In addition to the total and differential branching ratios, for radiative decays like ours, studying the effects of polarized photon may provide useful information about new Wilson coefficients. For this purpose, we present the dependence of the integrated photon polarization asymmetry H for $B_s \rightarrow \gamma \mu^+ \mu^-$ decay on the new Wilson coefficients in Figs. (4.9) and (4.10). We see from Fig. (4.9) that spectrum of H is almost symmetrical with respect to the zero point for all the new Wilson coefficients, except the C_{RL} . The coefficient C_{RL} , when it is between -2 and 0 , is also the only one which gives the constructive contribution to the SM prediction of H , which we find $H(B_s \rightarrow \gamma \mu^+ \mu^-) = 0.74$. This behavior is also seen from Fig. (4.10), in which we plot the differential photon polarization asymmetry $H(x)$ for the same decay as a function of x for the different values of the vector interaction with coefficients C_{RL} . From these two figures, we can conclude that performing measurement of H at different photon energies can

give information about the signs of the new Wilson coefficients, as well as their magnitudes.

Note that the results presented in this work can easily be applied to the $B_s \rightarrow \gamma \tau^+ \tau^-$ decay. For example, in Figs. (4.11) and (4.12), we present the dependence of the $BR^{(1)}$ and $BR^{(2)}$ for $B_s \rightarrow \gamma \tau^+ \tau^-$ decay on the new Wilson coefficients. We observe that in contrary to the $\mu^+ \mu^-$ final state, spectrum of $BR^{(1)}$ and $BR^{(2)}$ for $\tau^+ \tau^-$ final state is not symmetrical with respect to zero point, except for the coefficient C_{TE} . Otherwise, we observe three types of behavior for $BR^{(2)}$ from Fig. (4.12): as the new Wilson coefficients C_{LRRL} , C_{RLLR} , C_{LL} and C_{RR} increase, $BR^{(2)}$ also increases. This behavior is reversed for coefficients C_{LRLR} , C_{RLRL} , C_{LR} and C_{RL} , i.e., $BR^{(2)}$ decreases with the increasing values of these coefficients. However, situation is different for the tensor type interactions: $BR^{(2)}$ decreases when C_T and C_{TE} increase from -4 to 0 and then increases in the positive half of the range. We also observe from Fig. (4.11) that spectrum of $BR^{(1)}$ is identical to that of $BR^{(2)}$ for the coefficients C_{LRLR} , C_{LRRL} , C_{RLLR} , C_{LL} , C_{RR} and C_{TE} in between $-4 \leq C_X \leq +4$. For the rest of the coefficients, namely C_{RLRL} , C_{LR} , C_T , it stands slightly below and almost parallel to the SM prediction in the positive half of the range, although its behavior is the same as $BR^{(2)}$ when $-4 \leq C_X \leq 0$.

Finally, we present two more figures related to the photon polarization asymmetry H for $B_s \rightarrow \gamma \tau^+ \tau^-$ decay. Fig. (4.13) shows the dependence of the integrated photon polarization asymmetry H on the new Wilson coefficients. We present the differential photon polarization asymmetry $H(x)$ for the same decay as a function of x for the different values of the scalar interactions with coefficients C_{LRRL} in Fig. 5(4.14). We see from Fig. (4.13) that in contrary to the $\mu^+ \mu^-$ final state, spectrum of H for $\tau^+ \tau^-$ final state is not symmetrical with respect to zero point. It also follows that when $0 \leq C_X \leq 4$ the dominant contribution to H for $B_s \rightarrow \gamma \tau^+ \tau^-$ decay comes from C_{RLRL} and C_{LR} . However, for the negative part of the range H receives constructive contributions mostly from C_{LRRL} , as clearly seen also from Fig. (4.14).

In summary, by using a most general model independent effective Hamiltonian, which contains both scalar and tensor type interactions as well as the vector types, the total and the differential branching ratios of the rare $B_s \rightarrow \gamma \ell^+ \ell^-$ decay have been studied by taking into account the polarization effects of the photon. In addition, the sensitivity of "photon polarization asymmetry" in this radiative decay to the new Wilson coefficients has been investigated. It has been shown that all these physical observables are very sensitive to the existence of new physics beyond SM and their experimental measurements can give valuable information about it.

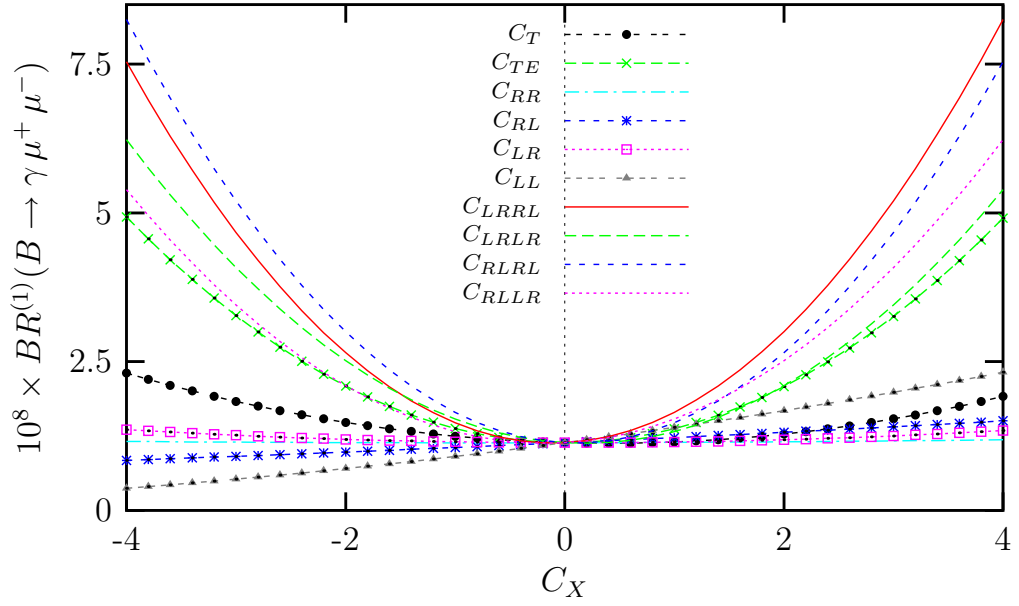


Figure 4.1: The dependence of the integrated branching ratio for the $B_s \rightarrow \gamma \mu^+ \mu^-$ decay with photon in positive helicity state on the new Wilson coefficients with LD effects .

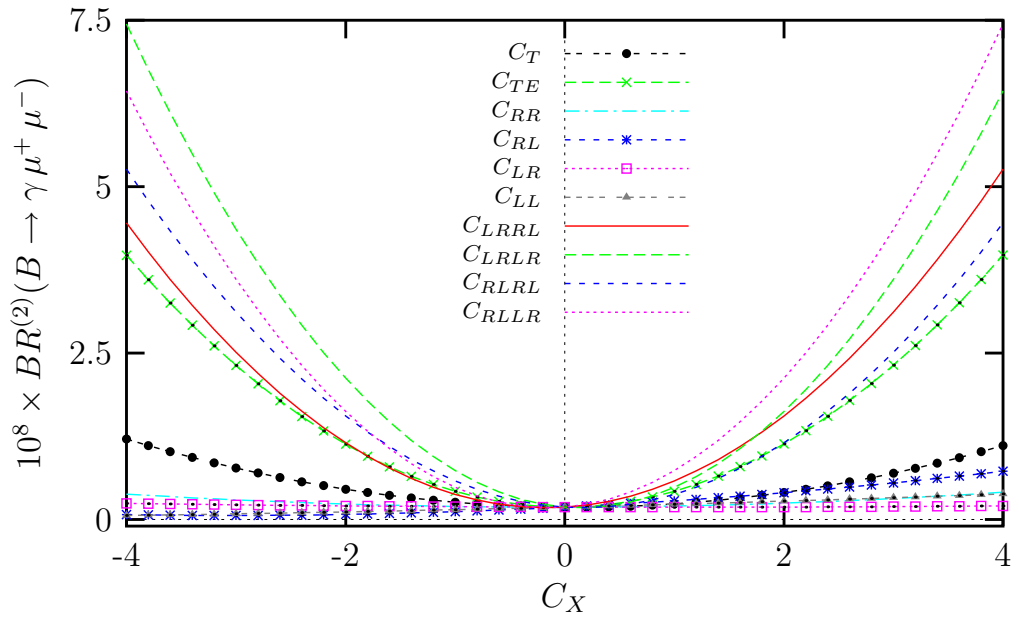


Figure 4.2: The dependence of the integrated branching ratio for the $B_s \rightarrow \gamma \mu^+ \mu^-$ decay with photon in negative helicity state on the new Wilson coefficients with LD effects .

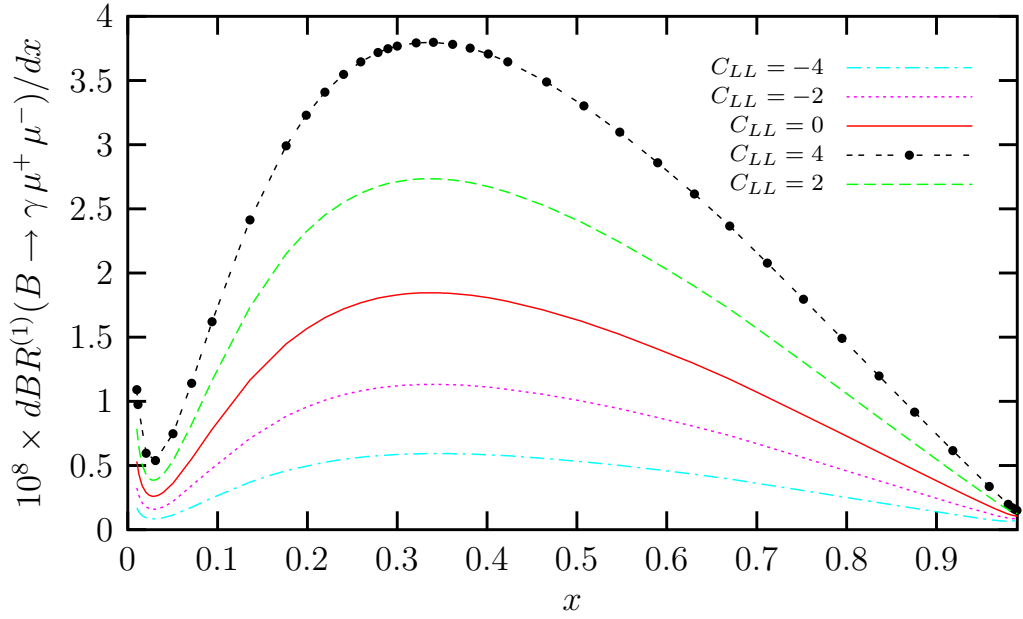


Figure 4.3: The dependence of the differential branching ratio for the $B_s \rightarrow \gamma \mu^+ \mu^-$ decay with photon in the positive helicity state on the dimensionless variable $x = 2E_\gamma/m_B$ at different values of vector interaction with coefficient C_{LL} without LD effects.

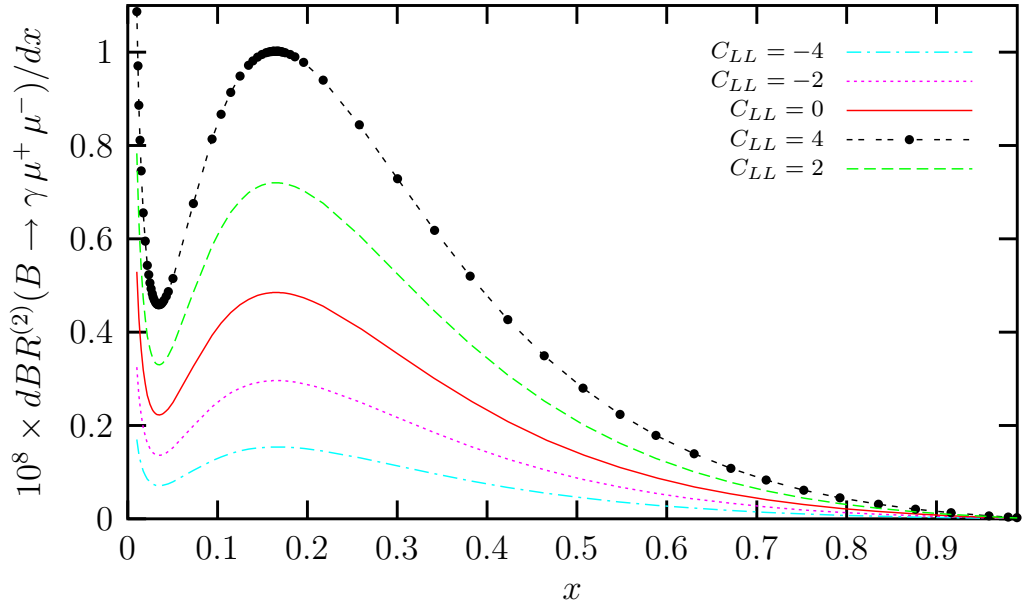


Figure 4.4: The same as Fig.(4.3), but with photon in the negative helicity state.

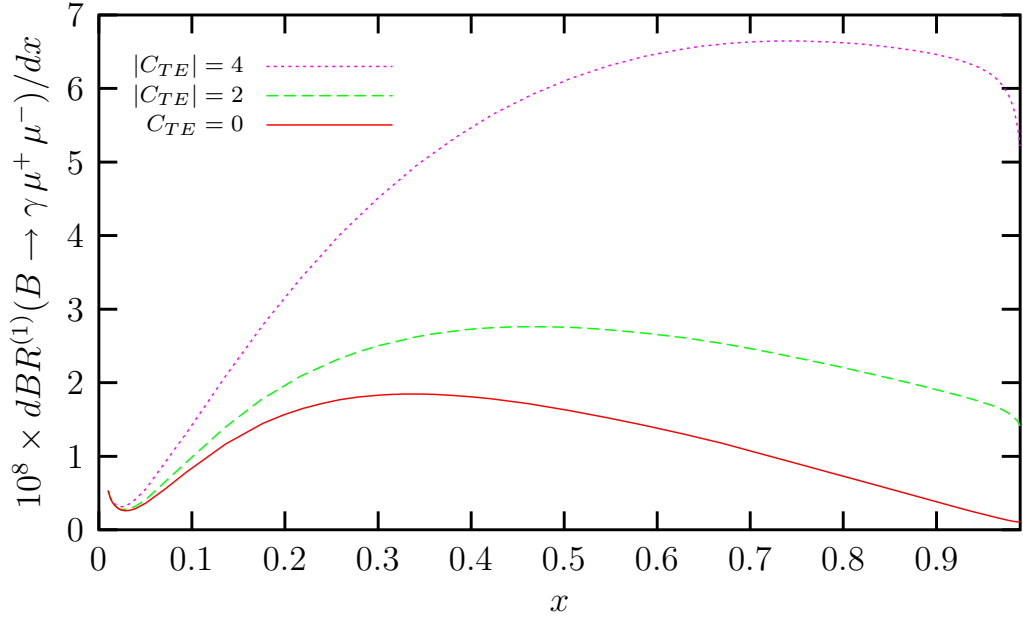


Figure 4.5: The dependence of the differential branching ratio for the $B_s \rightarrow \gamma \mu^+ \mu^-$ decay with photon in the positive helicity state on the dimensionless variable $x = 2E_\gamma/m_B$ at different values of tensor interaction with coefficient C_{TE} without LD effects.

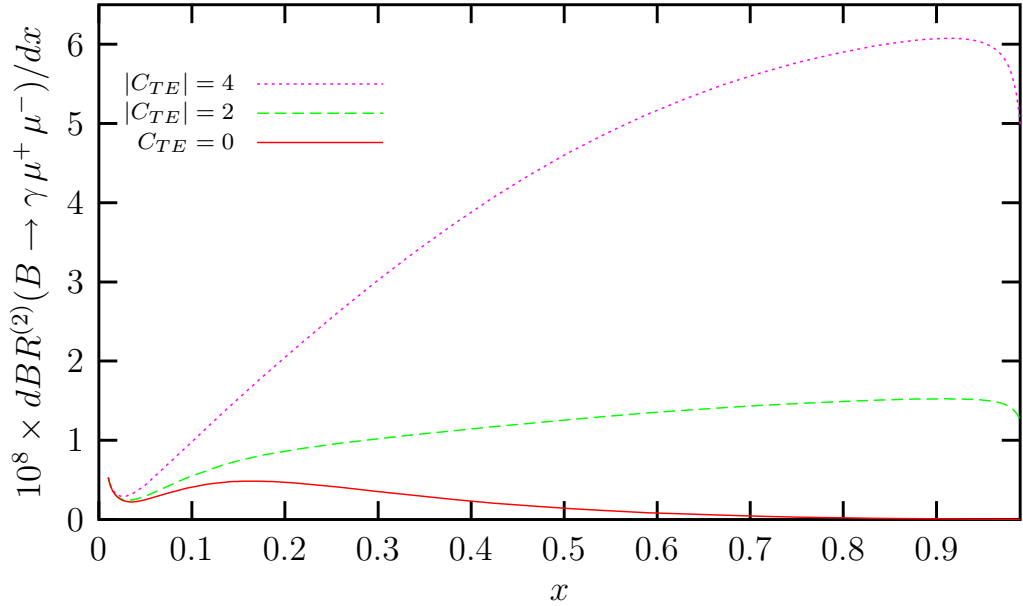


Figure 4.6: The same as Fig.(4.5), but with photon in the negative helicity state.

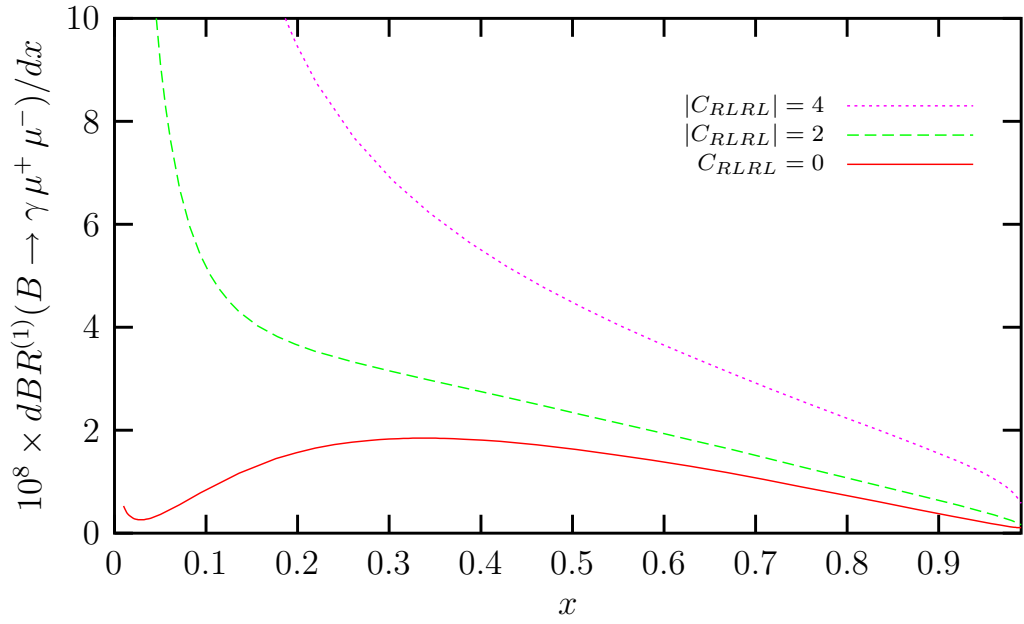


Figure 4.7: The dependence of the differential branching ratio for the $B_s \rightarrow \gamma \mu^+ \mu^-$ decay with photon in the positive helicity state on the dimensionless variable $x = 2E_\gamma/m_B$ at different values of scalar interaction with coefficient C_{RLRL} without LD effects.

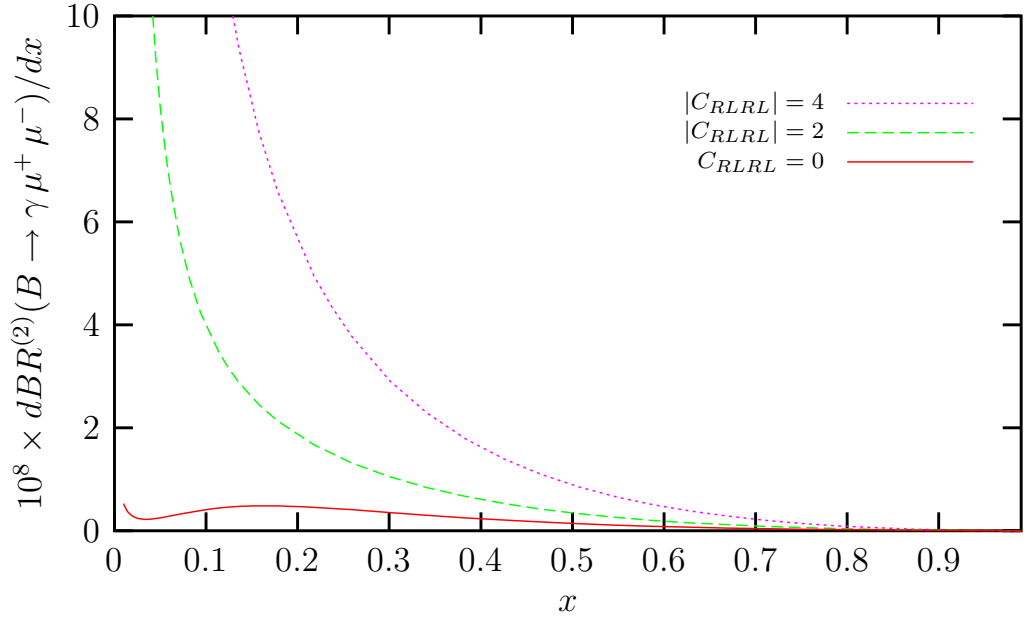


Figure 4.8: The same as Fig.(4.7), but with photon in the negative helicity state.

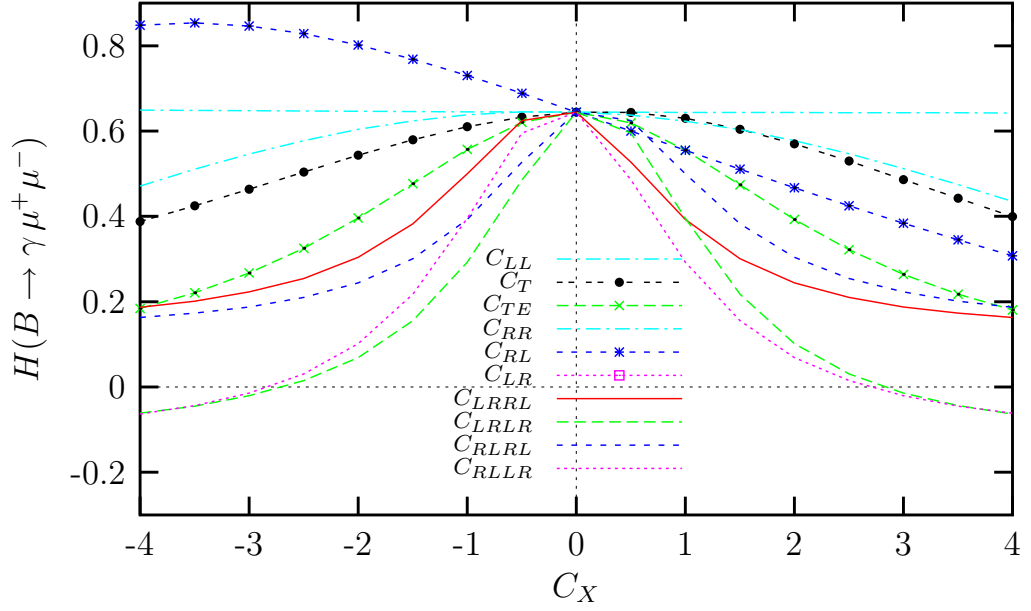


Figure 4.9: The dependence of the integrated photon polarization asymmetry for the $B_s \rightarrow \gamma \mu^+ \mu^-$ decay on the new Wilson coefficients with LD effects.

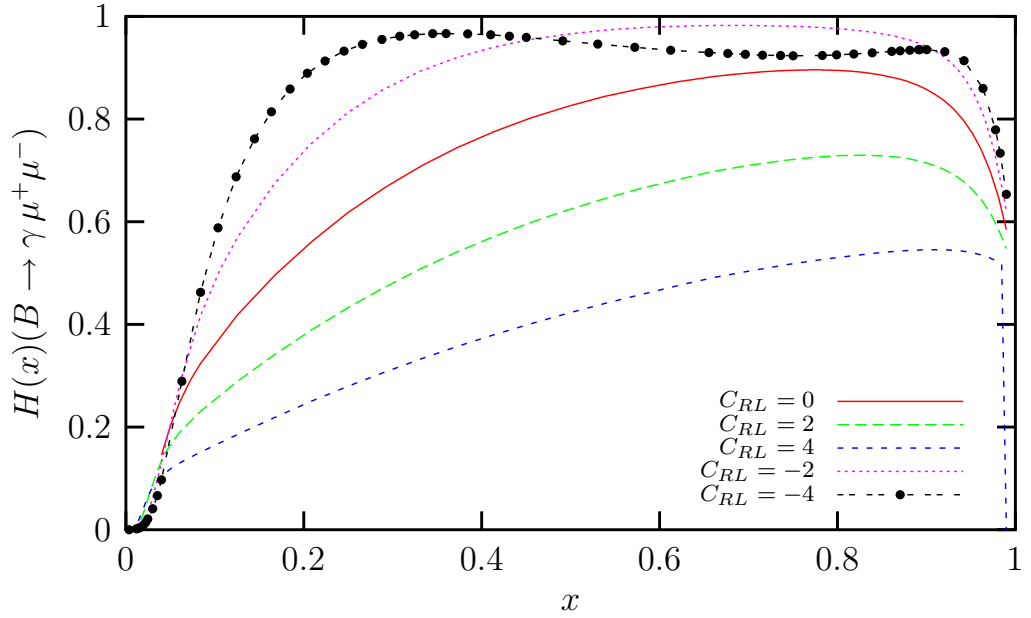


Figure 4.10: The dependence of the differential photon polarization asymmetry for the $B_s \rightarrow \gamma \mu^+ \mu^-$ decay on the dimensionless variable $x = 2E_\gamma/m_B$ for different values of C_{RL} without LD effects.

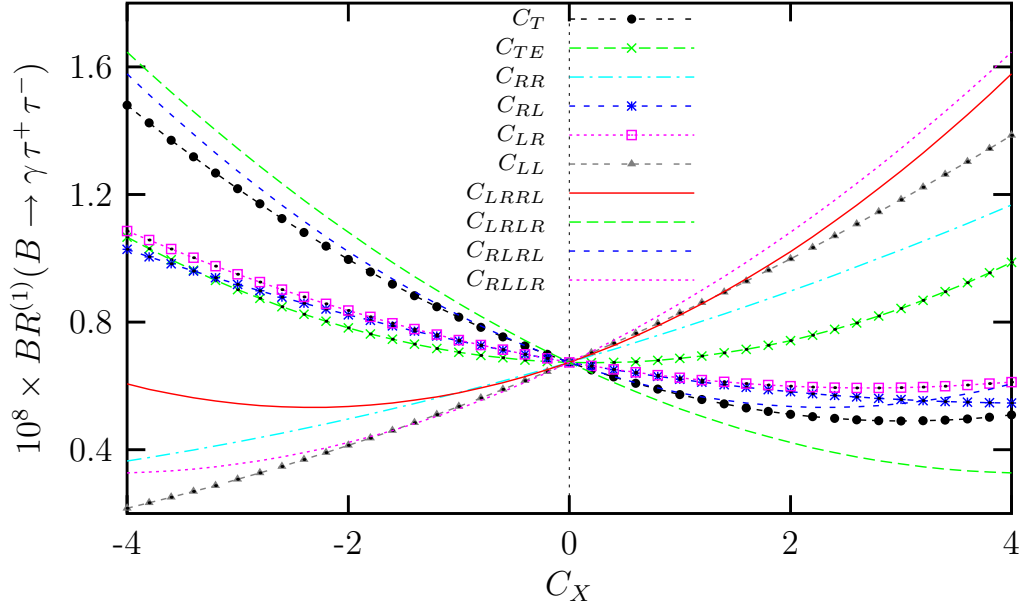


Figure 4.11: The dependence of the integrated branching ratio for the $B_s \rightarrow \gamma \tau^+ \tau^-$ decay with photon in the positive helicity state on the new Wilson coefficients with LD effects.

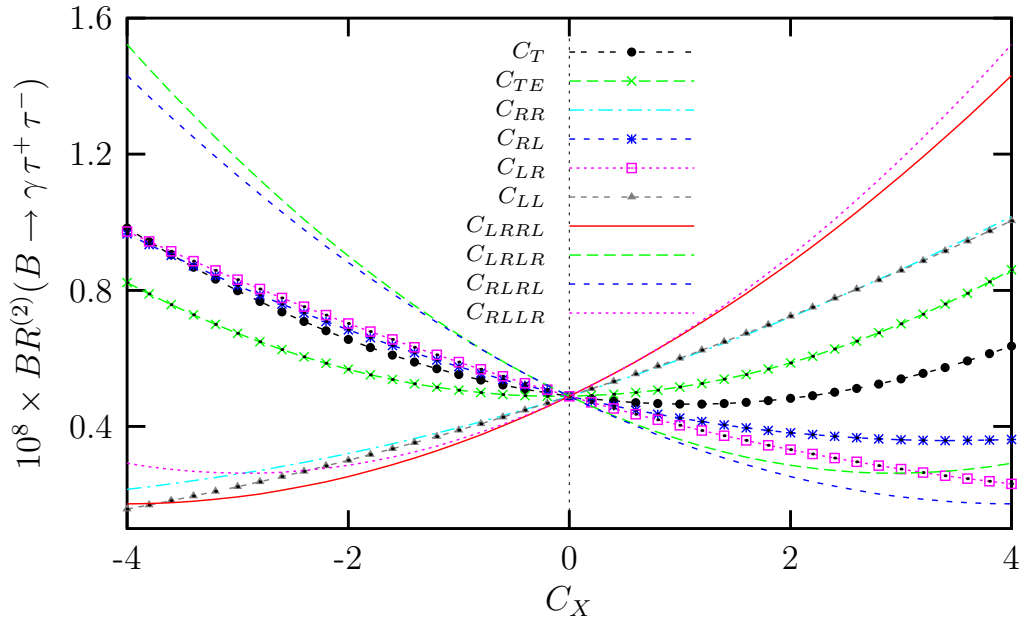


Figure 4.12: The same as Fig.(4.11), but with photon in negative helicity state.

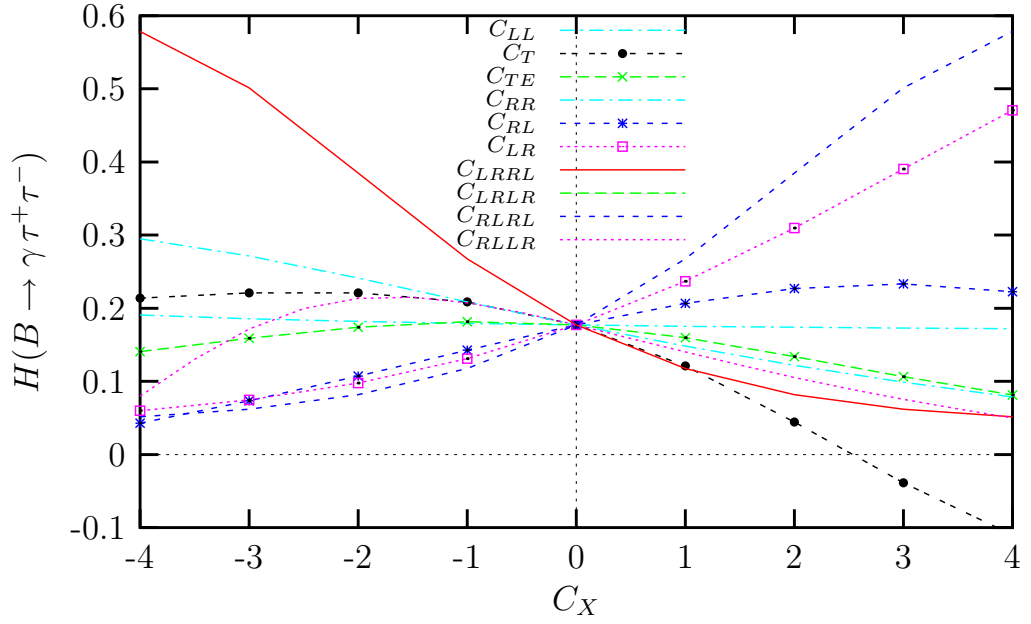


Figure 4.13: The dependence of the integrated photon polarization asymmetry for the $B_s \rightarrow \gamma \tau^+ \tau^-$ decay on the new Wilson coefficients with LD effects.

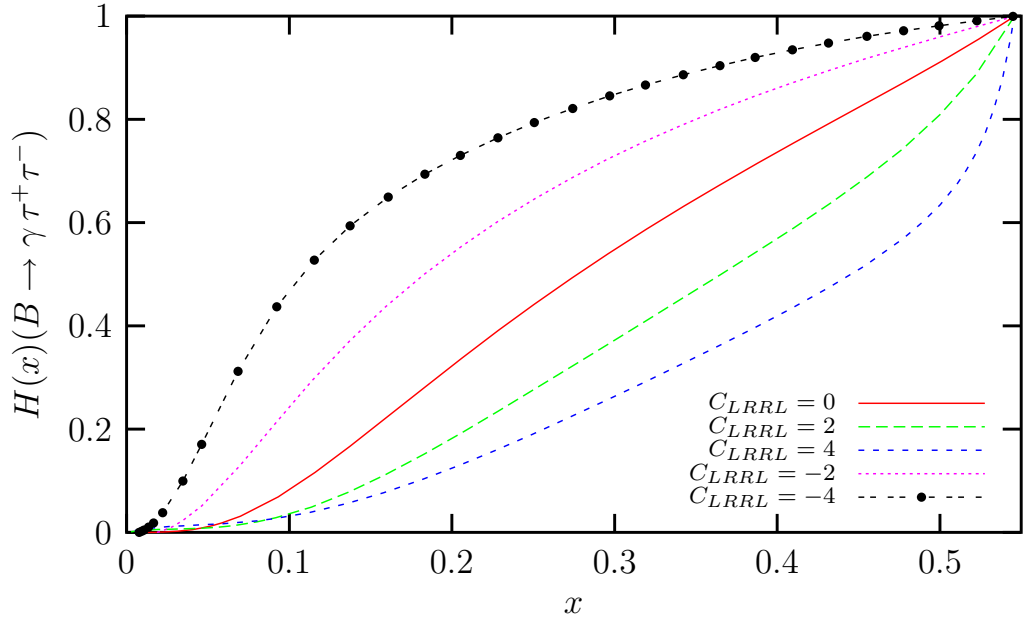


Figure 4.14: The dependence of the differential photon polarization asymmetry for the $B_s \rightarrow \gamma \tau^+ \tau^-$ decay on the dimensionless variable $x = 2E_\gamma/m_B$ for different values of C_{LRRL} without LD effects.

CHAPTER 5

LEPTON POLARIZATIONS IN $B_s \rightarrow \gamma \ell^+ \ell^-$ DECAY

In the $B_s \rightarrow \gamma \ell^+ \ell^-$ decay, like the effects of polarized photon, effects of the polarization asymmetries of the final state leptons can also be very useful for accurate determination of various Wilson coefficients. The final state leptons in this decay can have longitudinal P_L , transverse P_T and normal P_N polarizations. Here, P_T is the component of the polarization lying in the decay plane and P_N is the one that is normal to the decay plane. Since these three components contain different combinations of Wilson coefficients they may provide independent information about the further investigations of the SM and its possible extensions.

In this chapter, starting again with the most general model independent form of the effective Hamiltonian given by (3.2), we calculate the analytical expressions of the various lepton polarization asymmetries and lepton-antilepton combined asymmetries in the next two sections. The last section is devoted to the numerical analysis and discussion of results.

5.1 Lepton Polarization Asymmetry

We first introduce the spin projection operators given by

$$\begin{aligned} P^- &= \frac{1}{2}(1 + \gamma_5 \not{S}_j^-) , \\ P^+ &= \frac{1}{2}(1 - \gamma_5 \not{S}_j^+) , \end{aligned} \tag{5.1}$$

for ℓ^- and ℓ^+ , respectively. Here, $j = L, T, N$ denotes the longitudinal, transverse and normal components of the polarizations, respectively. The four vectors $S_{\mu j}^{\pm}$, which satisfy

$$S^- \cdot p_1 = S^+ \cdot p_2 = 0 \quad \text{and} \quad S^- \cdot S^- = S^+ \cdot S^+ = -1, \tag{5.2}$$

are defined in the rest frame of ℓ^- and ℓ^+ , respectively as

$$\begin{aligned}
S_L^{-\mu} &\equiv (0, \vec{e}_L^-) = \left(0, \frac{\vec{p}_1}{|\vec{p}_1|}\right), \\
S_N^{-\mu} &\equiv (0, \vec{e}_N^-) = \left(0, \frac{\vec{k} \times \vec{p}_1}{|\vec{k} \times \vec{p}_1|}\right), \\
S_T^{-\mu} &\equiv (0, \vec{e}_T^-) = \left(0, \vec{e}_N^- \times \vec{e}_L^-\right), \\
S_L^{+\mu} &\equiv (0, \vec{e}_L^+) = \left(0, \frac{\vec{p}_2}{|\vec{p}_2|}\right), \\
S_N^{+\mu} &\equiv (0, \vec{e}_N^+) = \left(0, \frac{\vec{k} \times \vec{p}_2}{|\vec{k} \times \vec{p}_2|}\right), \\
S_T^{+\mu} &\equiv (0, \vec{e}_T^+) = \left(0, \vec{e}_N^+ \times \vec{e}_L^+\right).
\end{aligned} \tag{5.3}$$

The longitudinal unit vector S_L is boosted to the CM frame of $\ell^+\ell^-$ by Lorentz transformation:

$$\begin{aligned}
S_{L,CM}^{-\mu} &= \left(\frac{|\vec{p}_1|}{m_\ell}, \frac{E_\ell \vec{p}_1}{m_\ell |\vec{p}_1|}\right), \\
S_{L,CM}^{+\mu} &= \left(\frac{|\vec{p}_1|}{m_\ell}, -\frac{E_\ell \vec{p}_1}{m_\ell |\vec{p}_1|}\right),
\end{aligned} \tag{5.4}$$

while P_T and P_N are not changed by the boost since they lie in the perpendicular directions.

P_L , P_T and P_N in the $B_s \rightarrow \gamma\ell^+\ell^-$ decay are defined as

$$P_i^\mp(x) = \frac{\frac{d\Gamma}{dx}(\vec{n}^\mp = \vec{e}_i^\mp) - \frac{d\Gamma}{dx}(\vec{n}^\mp = -\vec{e}_i^\mp)}{\frac{d\Gamma}{dx}(\vec{n}^\mp = \vec{e}_i^\mp) + \frac{d\Gamma}{dx}(\vec{n}^\mp = -\vec{e}_i^\mp)}, \tag{5.5}$$

where P^\mp represents the charged lepton ℓ^\mp polarization asymmetry for $i = L, T, N$. For any spin direction \vec{n}^\mp of ℓ^\mp , the differential decay rate of the $B_s \rightarrow \gamma\ell^+\ell^-$ decays can be written as

$$\frac{d\Gamma}{dx}(\vec{n}^\mp) = \frac{1}{2} \left(\frac{d\Gamma}{dx}\right)_0 \left[1 + \left(P_L^\mp \vec{e}_L^\mp + P_T^\mp \vec{e}_T^\mp + P_N^\mp \vec{e}_N^\mp\right) \cdot \vec{n}^\mp\right], \tag{5.6}$$

where $\left(\frac{d\Gamma}{dx}\right)_0$ is the decay rate when the final state polarizations are not measured and it is equivalent to Δ_0 in Eq. (4.7).

After some lengthy algebra, we obtain the following expressions for the polarization components of the ℓ^\pm leptons in $B_s \rightarrow \gamma \ell^+ \ell^-$ decays:

$$\begin{aligned}
P_L^+ = & \frac{1}{6v \Delta_0} \left\{ x v^3 \left[\frac{m_B^3 x^2 (1-x) (12r + (1-x)(v^2 - 1)) \text{Im}[(A_2 - B_2) N_1^*]}{\sqrt{r}} \right. \right. \\
& + 4m_B^2 x^2 (1-x) ((|A_1|^2 + |A_2|^2 - |B_1|^2 - |B_2|^2) - \text{Im}[GN_1^*] + \text{Im}[G_1 N^*]) \\
& - 24x(1-x) (\text{Im}[G_1 H^*] - \text{Im}[GH_1^*]) + 4(1-x)^2 (-12\text{Im}[H_1 H^*] \\
& + m_B^4 x^2 \text{Im}[N_1 N^*]) + 16x^2 \text{Im}[(-G - m_B \sqrt{r} A_2) G_1^*] \\
& + \frac{m_B x^2 (-12r + (1-x)(v^2 - 1)) (\text{Im}[B_2 G_1^*] - \text{Re}[(-A_1 + B_1) G^*])}{\sqrt{r}} \\
& - \frac{m_B x^2 (12r + (1-x)(v^2 - 1)) (\text{Im}[(A_1 + B_1) G_1^*] + \text{Re}[(A_2 + B_2) G^*])}{\sqrt{r}} \\
& + 24m_B \sqrt{r} (1-x) (-x) (-2\text{Im}[(B_2 - A_2) H_1^*] + \text{Re}[(A_2 + B_2) H^*]) \\
& \left. - \frac{m_B^3 x^2 (1-x)^2 (v^2 - 1) \text{Re}[(A_2 + B_2) N^*]}{\sqrt{r}} \right] \\
& - \frac{48f_B^2 (1 + (1-x)^2 - 4r(2-x)) ((1-x)v + (2r-1+x) \ln[u]) \text{Re}[F_1 F^*]}{(-x)(1-x)} \\
& + 24f_B \ln[u] \left[2 (-1 + x + 2r(2-x)) \text{Im}[FH_1^*] - \frac{m_l}{(1-x)} (2r-1+x)x^2 \right. \\
& \quad \left(\text{Re}[(A_1 - B_1) F^*] - \text{Re}[(A_2 - B_2) F_1^*] \right) + \frac{2m_l r}{(1-x)} x (-x \text{Re}[(A_1 + B_1) F_1^*] \\
& + (2-x) \text{Re}[(A_2 + B_2) F^*]) + \frac{4r}{(1-x)} x (\text{Im}[FG_1^*] + (4r-1) \text{Re}[F_1 G^*]) \\
& - 2(4r-1)(1-x)v^2 \text{Re}[F_1 H^*] - m_B^2 x ((-1+x) \text{Im}[FN_1^*] \\
& + (1-x-2r(2-x)) \text{Re}[F_1 N^*]) \left. \right] + 24f_B v \left[-2x \text{Im}[F(G_1 \right. \\
& + m_B^2 N_1 - (1-x) H_1)^*] - m_l x^2 \text{Re}[(A_1 - A_2 + B_1) F_1^*] \\
& - m_l x^2 \text{Re}[A_1 F^* + B_2 F_1^*] - x \left(-2(1-4r) \text{Re}[F_1 G^*] \right. \\
& + m_l \text{Re}[(- (2-x) A_2 - x B_1) F^*]) + x \left(m_l (2-x) \text{Re}[B_2 F^*] \right. \\
& \left. \left. - 2(1-x)v^2 \text{Re}[F_1 H^*] + 2m_B^2 ((1-x) - 2r(2-x)) \text{Re}[F_1 N^*] \right) \right] \left. \right\}, \quad (5.7)
\end{aligned}$$

$$P_L^- = \frac{1}{6v \Delta_0} \left\{ x v^3 \left[- \frac{m_B^3 x^2 (1-x) (12r + (1-x)(v^2 - 1)) \text{Im}[(A_2 - B_2) N_1^*]}{\sqrt{r}} \right. \right.$$

$$\begin{aligned}
& + 4m_B^2x^2(1-x)\left(-(|A_1|^2 + |A_2|^2 - |B_1|^2 - |B_2|^2) - \text{Im}[GN_1^*]\right. \\
& + \text{Im}[G_1N^*]) - 24x(1-x)\left(\text{Im}[G_1H^*] - \text{Im}[GH_1^*]\right) + 4(1-x)^2 \\
& \left(-12\text{Im}[H_1H^*] + m_B^4(-x)^2\text{Im}[N_1N^*]\right) + 16(-x)^2\text{Im}[(-G + m_B\sqrt{r}A_2)G_1^*] \\
& - \frac{m_B(-x)^2\left(-12r + (1-x)(v^2 - 1)\right)\left(\text{Im}[B_2G_1^*] - \text{Re}[(-A_1 + B_1)G^*]\right)}{\sqrt{r}} \\
& - \frac{m_Bx^2\left(12r + (1-x)(v^2 - 1)\right)\left(\text{Im}[(A_1 + B_1)G_1^*] + \text{Re}[(A_2 + B_2)G^*]\right)}{\sqrt{r}} \\
& - 24m_B\sqrt{r}x(1-x)\left(2\text{Im}[(B_2 - A_2)H_1^*] + \text{Re}[(A_2 + B_2)H^*]\right) \\
& - \left.\frac{m_B^3x^2(1-x)^2(v^2 - 1)\text{Re}[(A_2 + B_2)N^*]}{\sqrt{r}}\right] \\
& - \frac{48f_B^2\left(1 + (1-x)^2 - 4r(2-x)\right)\left((1-x)v + (2r-1+x)\ln[u]\right)\text{Re}[F_1F^*]}{(-x)(1-x)} \\
& + 24f_B\ln[u]\left[2\left(-1+x+2r(2-x)\right)\text{Im}[FH_1^*] + \frac{m_l}{(1-x)}(2r-1+x)x^2\right. \\
& \left.\left(\text{Re}[(A_1 - B_1)F^*] - \text{Re}[(A_2 - B_2)F_1^*]\right) + \frac{2m_lr}{(1-x)}x\left(-x\text{Re}[(A_1 + B_1)F_1^*]\right.\right. \\
& + (2-x)\text{Re}[(A_2 + B_2)F^*]) + \frac{4r}{(1-x)}x\left(\text{Im}[FG_1^*] + (4r-1)\text{Re}[F_1G^*]\right) \\
& - 2(4r-1)(1-x)v^2\text{Re}[F_1H^*] - m_B^2x\left(\left(-1+x\right)\text{Im}[FN_1^*]\right. \\
& + \left.\left.\left((1-x) - 2r(2-x)\right)\text{Re}[F_1N^*]\right)\right] + 24f_Bv\left[-2x\text{Im}[F(G_1 + m_B^2N_1\right. \\
& - (1-x)H_1)^*] - m_lx^2\text{Re}[(A_1 - A_2 + B_1)F_1^*] \\
& + m_lx^2\text{Re}[A_1F^* + B_2F_1^*] - x\left(-2(1-4r)\text{Re}[F_1G^*]\right. \\
& + m_l\text{Re}\left(\left.-(2-x)A_2 + xB_1\right)F^*\right) + x\left(m_l(2-x)\text{Re}[B_2F^*]\right. \\
& \left.\left.- 2(1-x)v^2\text{Re}[F_1H^*] + 2m_B^2\left((1-x) - 2r(2-x)\right)\text{Re}[F_1N^*]\right)\right]\left.\right\}, \quad (5.8)
\end{aligned}$$

$$\begin{aligned}
P_T^+ &= \frac{1}{\Delta_0}\left\{\frac{\left(2\sqrt{r} - \sqrt{(1-x)}\right)}{(1-x)v}xf_Bm_B\pi\left[(1-x)v^2(2-x)\text{Re}[(A_1 - B_1)F^*]\right.\right. \\
& - x\left(4r + (1-x)\right)\text{Re}[(A_2 + B_2)F^*] + \left.4r(-2 + 3x)\right) \\
& + (1-x)(2-x)\text{Re}[(A_1 + B_1)F_1^*] - (1-x)v^2x\text{Re}[(A_2 - B_2)F_1^*] \\
& \left.- 8\sqrt{r}\left[\text{Im}[F(-G_1x - 2(1-x)H_1)^*] - (1-4r)\text{Re}[F_1G^*]\right]/m_B\right\}
\end{aligned}$$

$$\begin{aligned}
& + \frac{\pi v}{4\sqrt{(1-x)}} x^2 \left[8\sqrt{r} \operatorname{Im}[(-G_1 x + 2sH_1)G^*] + 2m_B(1-x) \left(-(4r+1-x) \right. \right. \\
& \operatorname{Im}[(A_1 + B_1)H_1^*] - (4r-1+x) \operatorname{Re}[(A_1 - B_1)H^*]) - 2m_B^2 \sqrt{r}(-x)(1-x) \\
& \operatorname{Re}[(A_1 + B_1)(A_2 + B_2)^*] + m_B(-x) \left(-(1-x-4r) (\operatorname{Im}[(A_2 - B_2)G_1^*] \right. \\
& \left. \left. + \operatorname{Re}[(A_1 - B_1)G^*]) + (4r+1-x) (\operatorname{Im}[(A_1 + B_1)G_1^*] + \operatorname{Re}[(A_2 + B_2)G^*]) \right) \right] \\
& + 4\pi v f_B^2 (4r-1) \operatorname{Re}[F_1 F^*] \left. \right\}, \tag{5.9}
\end{aligned}$$

$$\begin{aligned}
P_T^- & = \frac{1}{\Delta_0} \left\{ \frac{(2\sqrt{r} - \sqrt{(1-x)})}{(1-x)v} x f_B m_B \pi \left[(x-1)v^2(2-x) \operatorname{Re}[(A_1 - B_1)F^*] \right. \right. \\
& - x(4r + (1-x)) \operatorname{Re}[(A_2 + B_2)F^*] + (4r(-2+3x)) + (1-x)(2-x) \\
& \operatorname{Re}[(A_1 + B_1)F_1^*] + (1-x)v^2 x \operatorname{Re}[(A_2 - B_2)F_1^*] \\
& \left. - 8\sqrt{r} \left[\operatorname{Im}[F(-G_1 x - 2(1-x)H_1)^*] - (1-4r) \operatorname{Re}[F_1 G^*] \right] / m_B \right] \\
& + \frac{\pi v}{4\sqrt{(1-x)}} x^2 \left[8\sqrt{r} \operatorname{Im}[(-G_1 x + 2sH_1)G^*] + 2m_B(1-x) \right. \\
& \left((-4r-1+x) \operatorname{Im}[(A_1 + B_1)H_1^*] + (4r-1+x) \operatorname{Re}[(A_1 - B_1)H^*] \right) \\
& + 2m_B^2 \sqrt{r} x(1-x) \operatorname{Re}[(A_1 + B_1)(A_2 + B_2)^*] \\
& - m_B x \left[1-x-4r \left(\operatorname{Im}[(A_2 - B_2)G_1^*] \right. \right. \\
& \left. \left. + \operatorname{Re}[(A_1 - B_1)G^*] \right) + (4r+1-x) \left(\operatorname{Im}[(A_1 + B_1)G_1^*] \right. \right. \\
& \left. \left. + \operatorname{Re}[(A_2 + B_2)G^*] \right) \right] + 4\pi v f_B^2 (4r-1) \operatorname{Re}[F_1 F^*] \left. \right\}, \tag{5.10}
\end{aligned}$$

$$\begin{aligned}
P_N^+ & = \frac{\pi}{4\Delta_0} x \left\{ x \sqrt{(1-x)} v^2 \left[-2m_B^2 \sqrt{r} x \left(\operatorname{Im}[A_1 B_2^*] + \operatorname{Im}[A_2 B_1^*] \right) + 8\sqrt{r} \left(\operatorname{Im}[GH^*] \right. \right. \right. \\
& - \operatorname{Im}[G_1 H_1^*]) - 2m_B(1-x) \left(\operatorname{Im}[(A_1 + B_1)H^*] + \operatorname{Re}[(A_1 - B_1)H_1^*] \right) \\
& \left. \left. - m_B x \left(\operatorname{Im}[(A_1 - A_2 + B_1 + B_2)G^*] - \operatorname{Re}[(-A_1 + A_2 + B_1 + B_2)G_1^*] \right) \right] \right. \\
& - 4(2\sqrt{r} - \sqrt{(1-x)}) m_B f_B \left[(2-x) \operatorname{Im}[(A_1 + B_1)F^*] \right. \\
& + (2-x-8r) \operatorname{Im}[(A_1 - B_1)F_1^*] - x \operatorname{Im}[(A_2 - B_2)F^*] - x \operatorname{Im}[(A_2 + B_2)F_1^*] \\
& \left. \left. + 8\sqrt{r} \left(\operatorname{Im}[F(G-H)^*] + \operatorname{Re}[F_1 H_1^*] \right) / m_B \right] \right\}, \tag{5.11}
\end{aligned}$$

and

$$\begin{aligned}
P_N^- = & \frac{\pi}{4\Delta_0} x \left\{ x \sqrt{(1-x)} v^2 \left[2m_B^2 \sqrt{r} x \left(\text{Im}[A_1 B_2^*] + \text{Im}[A_2 B_1^*] \right) + 8\sqrt{r} \left(\text{Im}[GH^*] \right. \right. \right. \\
& - \left. \left. \text{Im}[G_1 H_1^*] \right) - 2m_B (1-x) \left(\text{Im}[(A_1 + B_1) H^*] \right. \right. \\
& - \left. \left. \text{Re}[(A_1 - B_1) H_1^*] \right) - m_B x \left(\text{Im}[(A_1 + A_2 + B_1 - B_2) G^*] \right. \right. \\
& - \left. \left. \text{Re}[(A_1 + A_2 - B_1 + B_2) G_1^*] \right) \right] - 4 \left(2\sqrt{r} - \sqrt{(1-x)} \right) m_B f_B \left[(2-x) \right. \\
& \left. \text{Im}[(A_1 + B_1) F^*] - (2-x-8r) \text{Im}[(A_1 - B_1) F_1^*] \right. \\
& + \left. x \text{Im}[(A_2 - B_2) F^*] - x \text{Im}[(A_2 + B_2) F_1^*] \right. \\
& \left. + 8\sqrt{r} \left(\text{Im}[F(G-H)^*] + \text{Re}[F_1 H_1^*] \right) / m_B \right] \left. \right\}, \tag{5.12}
\end{aligned}$$

where $u = 1 + v/1 - v$.

From Eqs. (5.7)-(5.12), we see that in the limit $m_\ell \rightarrow 0$, longitudinal polarization asymmetry for the $B_s \rightarrow \gamma \ell^+ \ell^-$ decay is only determined by the scalar and tensor interactions, while transverse and normal components receive contributions mainly from the tensor and scalar interactions, respectively. Therefore, experimental measurement of these observables may provide important hints for the new physics beyond the SM.

5.2 Lepton Anti-lepton Combined Asymmetries

One can also obtain useful information about new physics by performing a combined analysis of the lepton and antilepton polarizations. In an earlier work along this line, the combinations $P_L^- + P_L^+$, $P_T^- - P_T^+$ and $P_N^- + P_N^+$ were considered for the inclusive $B \rightarrow X_s \tau^+ \tau^-$ decay [75], because it was argued that within the SM $P_L^- + P_L^+ = 0$, $P_T^- - P_T^+ \approx 0$ and $P_N^- + P_N^+ = 0$ so that any deviation from these results would be a definite indication of new physics. Later same discussion was done in connection with the exclusive processes $B \rightarrow K^{(*)} \ell^+ \ell^-$ and shown that within the SM the above-mentioned combinations of the ℓ^+ and ℓ^- polarizations vanish only at zero lepton mass limit [76]. In [65], the same combinations of the lepton and antilepton polarizations were analyzed in for $B_s \rightarrow \gamma \ell^+ \ell^-$ decay within

the MSSM model and concluded that the results quoted in earlier works that these quantities identically vanish in the SM was a process dependent statement.

Now, we would like to analyze the same combinations of the various polarization asymmetries in a model independent way and discuss the possible new physics effects through these observables.

For $P_L^- + P_L^+$, we find from Eq. (5.7) and (5.8) that

$$\begin{aligned}
P_L^- + P_L^+ &= \frac{1}{3v\Delta_0} \left\{ xv^3 \left(4m_B^2 x^2 (1-x) (\text{Im}[G_1 N^*] - \text{Im}[GN_1^*]) \right. \right. \\
&- 24x(1-x) (\text{Im}[G_1 H^*] - \text{Im}[GH_1^*]) + 4(1-x)^2 (-12\text{Im}[H_1 H^*]) \\
&+ m_B^4 x^2 \text{Im}[N_1 N^*] + 16x^2 \text{Im}[-GG_1^*] \\
&- \frac{m_B x^2 (12r + (1-x)(v^2 - 1)) (\text{Im}[(A_1 + B_1)G_1^*] + \text{Re}[(A_2 + B_2)G^*])}{\sqrt{r}} \\
&+ \frac{24m_B \sqrt{r} (-x)(1-x) \text{Re}[(A_2 + B_2)H^*]}{\sqrt{r}} \\
&+ \left. \frac{m_B^3 x^2 (1-x)^2 (v^2 - 1) \text{Re}[(A_2 + B_2)N^*]}{\sqrt{r}} \right) \\
&- \frac{48f_B^2 (1 + (1-x)^2 - 4r(2-x)) ((1-x)v + (2r-1+x)\ln[u]) \text{Re}[F_1 F^*]}{-x(1-x)} \\
&+ 24f_B \ln[u] \left(2(-1+x+2r(2-x)) \text{Im}[FH_1^*] + \frac{4r}{(1-x)} x (\text{Im}[FG_1^*] \right. \\
&+ (4r-1) \text{Re}[F_1 G^*]) + \frac{2m_l r}{(1-x)} x \left(-x \text{Re}[(A_1 + B_1)F_1^*] \right. \\
&+ (2-x) \text{Re}[(A_2 + B_2)F^*]) - 2(4r-1)(1-x)v^2 \text{Re}[F_1 H^*] \\
&- \left. m_B^2 x (-(1-x) \text{Im}[FN_1^*] + ((1-x) - 2r(2-x)) \text{Re}[F_1 N^*]) \right) \\
&+ 24f_B v ((1-x) - 1) \left(2 \text{Im}[F(G_1 + (1-x)(m_B^2 N_1 - H_1))^*] \right. \\
&+ m_l x \text{Re}[(A_1 + B_1)F_1^*] - 2((1-4r) \text{Re}[F_1 G^*] - (1-x)v^2 \text{Re}[F_1 H^*]) \\
&- \left. m_l (2-x) \text{Re}[(A_2 + B_2)F^*] - 2((1-x) - 2r(2-x))m_B^2 \text{Re}[F_1 N^*] \right) \Big\} \quad (5.13)
\end{aligned}$$

We now consider $P_T^- - P_T^+$. It reads from Eq. (5.9) and (5.10) as

$$\begin{aligned}
P_T^- - P_T^+ &= -\frac{2\pi v}{\Delta_0} m_B x \left\{ (2\sqrt{r} - \sqrt{(1-x)}) f_B [(2-x) \right. \\
&\quad \text{Re}[(A_1 - B_1)F^*] - x \text{Re}[(A_2 - B_2)F_1^*]] \\
&- \frac{1}{4\sqrt{(1-x)}} x \left[2(1-x)(4r-1+x) \text{Re}[(A_1 - B_1)H^*] \right.
\end{aligned}$$

$$- x \left[(1-x-4r) \left(\text{Im}[(A_2 - B_2)G_1^*] + \text{Re}[(A_1 - B_1)G^*] \right) \right] \Bigg\}. \quad (5.14)$$

Finally, for $P_N^- + P_N^+$, we get from Eq. (5.11) and (5.12)

$$\begin{aligned} P_N^- + P_N^+ = & -\frac{\pi}{2\Delta_0} x m_B \left\{ -x \sqrt{(1-x)v^2} \left[8\sqrt{r} \left(\text{Im}[GH^*] \right. \right. \right. \\ & - \text{Im}[G_1 H_1^*] \Big) / m_B - 2(1-x) \left(\text{Im}[(A_1 + B_1)H^*] \right) \\ & - x \left(\text{Im}[(A_1 + B_1)G^*] - \text{Re}[(A_2 + B_2)G_1^*] \right) \Big] - 4 \left(2\sqrt{r} - \sqrt{(1-x)} \right) f_B \\ & \left[(2-x) \text{Im}[(A_1 + B_1)F^*] - x \text{Im}[(A_2 + B_2)F_1^*] \right. \\ & \left. + 8\sqrt{r} \left(\text{Im}[F(G-H)^*] + \text{Re}[F_1 H_1^*] \right) / m_B \right] \Bigg\}. \end{aligned} \quad (5.15)$$

We can now easily obtain from Eq. (5.13)-(5.15) that sum of the longitudinal and normal polarization asymmetries of ℓ^+ and ℓ^- and the difference of transverse polarization asymmetry for $B_s \rightarrow \gamma \ell^+ \ell^-$ decay do not vanish in the SM, but given by

$$\begin{aligned} (P_L^- + P_L^+)_{SM} &= \frac{64f_B}{(1-x)v} m_\ell^2 (2-x)x \left((1-x)v \right. \\ & \left. - 2r \ln[u] \right) \text{Re} \left[C_{10} \left(C_9^{eff} f - \frac{2C_7^{eff} m_b}{q^2} f_1 \right)^* \right], \\ (P_T^- - P_T^+)_{SM} &= 16f_B \pi m_\ell v \left(1 - (1-x)^2 \right) \left(2\sqrt{r} - \sqrt{(1-x)} \right) |C_{10}|^2 g, \\ (P_N^- + P_N^+)_{SM} &= 16f_B \pi m_B m_\ell (2-x)(-x) \left(2\sqrt{r} - \sqrt{(1-x)} \right) \\ & \text{Im} \left[C_{10} \left(C_9^{eff} g - \frac{2C_7^{eff} m_b}{q^2} g_1 \right)^* \right], \end{aligned} \quad (5.16)$$

which do not coincide with those given in [65], although our conclusion that within the SM, $P_L^- + P_L^+ = 0$, $P_T^- - P_T^+ \approx 0$ and $P_N^- + P_N^+ = 0$ at only zero lepton mass limit, does.

Before giving our numerical results and their discussion, we like to note a final point about their calculations. As seen from the expressions of the lepton polarizations given by Eqs. (5.13)-(5.15), they are functions of x as well as the new Wilson coefficients. Thus, in order to investigate the dependencies of these observables on the new Wilson coefficients, we eliminate the parameter x by performing its integration over the allowed kinematical region. In this way we

obtain the average values of the lepton polarizations, which are defined by

$$\langle P_i \rangle = \frac{\int_{1-(2m_\ell/m_B)^2}^{\delta} P_i(x) \frac{d\Gamma}{dx} dx}{\int_{1-(2m_\ell/m_B)^2}^{\delta} \frac{d\Gamma}{dx} dx}. \quad (5.17)$$

As we noted in Sec. 3.2, the part of $d\Gamma/dx$ in Eqn. (5.17) which receives contribution from the $|\mathcal{M}_{IB}|^2$ term has infrared singularity due to the emission of soft photon. To obtain a finite result from these integrations, we follow the approach described in [19] and impose a cut on the photon energy, i.e., we require $E_\gamma \geq 25$ MeV, which corresponds to detect only hard photons experimentally. This cut implies that $E_\gamma \geq \delta m_B/2$ with $\delta = 0.01$.

5.3 Numerical Analysis

We present the results of our analysis in a series of figures. We use the input parameters given in Appendix A. Before the discussion of these figures, we give our SM predictions for the longitudinal, transverse and the normal components of the lepton polarizations for $B_s \rightarrow \gamma \ell^+ \ell^-$ decay for μ (τ) channel for reference:

$$\begin{aligned} \langle P_L^- \rangle &= -0.850 (-0.227), \\ \langle P_T^- \rangle &= -0.065 (-0.190), \\ \langle P_N^- \rangle &= -0.014 (-0.061). \end{aligned}$$

In Figs. (5.1) and (5.2), we present the dependence of the averaged longitudinal polarization $\langle P_L^- \rangle$ of ℓ^- and the combination $\langle P_L^- + P_L^+ \rangle$ for $B_s \rightarrow \gamma \mu^+ \mu^-$ decay on the new Wilson coefficients. From these figures we see that $\langle P_L^- \rangle$ is strongly dependent on scalar type interactions with coefficient C_{RLRL} and C_{LRRL} , and quite sensitive to the tensor type interactions, while the combined average $\langle P_L^- + P_L^+ \rangle$ is mainly determined by scalar interactions only. The fact that values of $\langle P_L^- \rangle$ becomes substantially different from the SM value (at $C_X = 0$) as C_X becomes different from zero indicates that measurement of the longitudinal lepton polarization in $B_s \rightarrow \gamma \mu^+ \mu^-$ decay can be very useful to investigate new physics beyond the SM. We note that in Fig. (5.2), we have

not explicitly exhibit the dependence on vector type interactions since we have found that $\langle P_L^- + P_L^+ \rangle$ is not sensitive to them at all. This is what is already expected since vector type interactions are cancelled when the longitudinal polarization asymmetry of the lepton and antilepton is considered together. We also observe from Fig. (5.2) that $\langle P_L^- + P_L^+ \rangle$ becomes almost zero at $C_X = 0$, which confirms the SM result, and its dependence on C_X is symmetric with respect to this zero point. It is interesting to note also that $\langle P_L^- + P_L^+ \rangle$ is positive for all values of C_{RLRL} and C_{LRRL} , while it is negative for remaining scalar type interactions.

Figs. (5.3) and (5.4) are the same as Figs. (5.1) and (5.2), but for the $B_s \rightarrow \gamma\tau^+\tau^-$ decay. Similar to the muon case, $\langle P_L^- \rangle$ is sensitive to scalar type interactions, but all type. It is an decreasing (increasing) function of C_{RLRL} and C_{RLLR} (C_{LRRL} and C_{LRLR}). The value of $\langle P_L^- \rangle$ is positive when $C_{RLRL} \lesssim -1$, $C_{RLLR} \lesssim -2$, $C_{LRRL} \gtrsim 1$ and $C_{LRLR} \gtrsim 2$. As seen from Fig. (5.4) that the behavior of the combined average $\langle P_L^- + P_L^+ \rangle$ for $B_s \rightarrow \gamma\tau^+\tau^-$ decay is different from the muon case in that it changes sign for a given scalar type interaction: e.g., $\langle P_L^- + P_L^+ \rangle > 0$ when $C_{RLRL}, C_{RLLR} \lesssim 0$, while $\langle P_L^- + P_L^+ \rangle < 0$ when $C_{RLRL}, C_{RLLR} \gtrsim 0$. Therefore, it can provide valuable information about the new physics to determine the sign and the magnitude of $\langle P_L^- \rangle$ and $\langle P_L^- + P_L^+ \rangle$.

In Figs. (5.5) and (5.6), the dependence of the averaged transverse polarization $\langle P_T^- \rangle$ of ℓ^- and the combination $\langle P_T^- - P_T^+ \rangle$ for $B_s \rightarrow \gamma\mu^+\mu^-$ decay on the new Wilson coefficients are presented. We see from Fig. (5.5) that $\langle P_T^- \rangle$ strongly depends on the scalar interactions with coefficient C_{RLRL} and C_{LRRL} and quite weakly on the all other Wilson coefficients. It is also interesting to note that $\langle P_T^- \rangle$ is positive (negative) for the negative (positive) values of C_{LRRL} , except a small region about the zero values of the coefficient, while its behavior with respect to C_{RLRL} is opposite. As being different from $\langle P_T^- \rangle$ case, in the combination $\langle P_T^- - P_T^+ \rangle$ there appears strong dependence on scalar interaction with coefficients C_{RLLR} and C_{LRLR} too, as well as on C_{RLRL} and C_{LRRL} . It is also quite sensitive to the tensor interaction with coefficient C_T .

Figs. (5.7) and (5.8) are the same as Figs. (5.5) and (5.6), but for the $B_s \rightarrow \gamma\tau^+\tau^-$ decay. As in the muon case, for τ channel too, the dominant contribution to the transverse polarization comes from the scalar interactions, but it exhibits a more sensitive dependence to the remaining types of interactions as well than the muon case. As seen from Fig. (5.8) that $\langle P_T^- - P_T^+ \rangle$ is negative for all values of the new Wilson coefficients, while $\langle P_T^- \rangle$ again changes sign depending on the change in the new Wilson coefficients: e.g., $\langle P_T^- \rangle > 0$ only when $C_{LRRL} \lesssim -2$ and $C_{RLRL}, C_{LR} \gtrsim 2$. Remembering that in SM in massless lepton case, $\langle P_T^- \rangle \approx 0$ and $\langle P_T^- - P_T^+ \rangle \approx 0$, determination of the sign of these observables can give useful information about the existence of new physics.

In Figs. (5.9) and (5.10), we present the dependence of the averaged normal polarization $\langle P_N^- \rangle$ of ℓ^- and the combination $\langle P_N^- + P_N^+ \rangle$ for $B_s \rightarrow \gamma\mu^+\mu^-$ decay on the new Wilson coefficients. We observe from these figures that behavior of both $\langle P_N^- \rangle$ and $\langle P_N^- + P_N^+ \rangle$ are determined by tensor type interactions with coefficient C_{TE} . They are both positive (negative) when $C_{TE} \lesssim 0$ ($C_{TE} \gtrsim 0$).

Figs. (5.11) and (5.12) are the same as Figs. (5.9) and (5.10), but for the $B_s \rightarrow \gamma\tau^+\tau^-$ decay. As being different from the muon case, $\langle P_N^- \rangle$ for τ channel is also sensitive to the vector type interaction with coefficient C_{LL} , as well as the tensor types and it is negative for all values of the new Wilson coefficients. As for the combination $\langle P_N^- + P_N^+ \rangle$ for τ channel, it is negative too for all values of C_X , except for $C_{TE} \lesssim -2$.

In summary, by using the general model independent form of the effective Hamiltonian, the sensitivity of the longitudinal, transverse and normal polarizations of ℓ^\pm , as well as lepton-antilepton combined asymmetries, on the new Wilson coefficients have been investigated. It has been shown that all physical observables discussed are very sensitive to the existence of new physics beyond SM and their experimental measurements can give valuable information about it, as in the photon case given in Chapter 4.

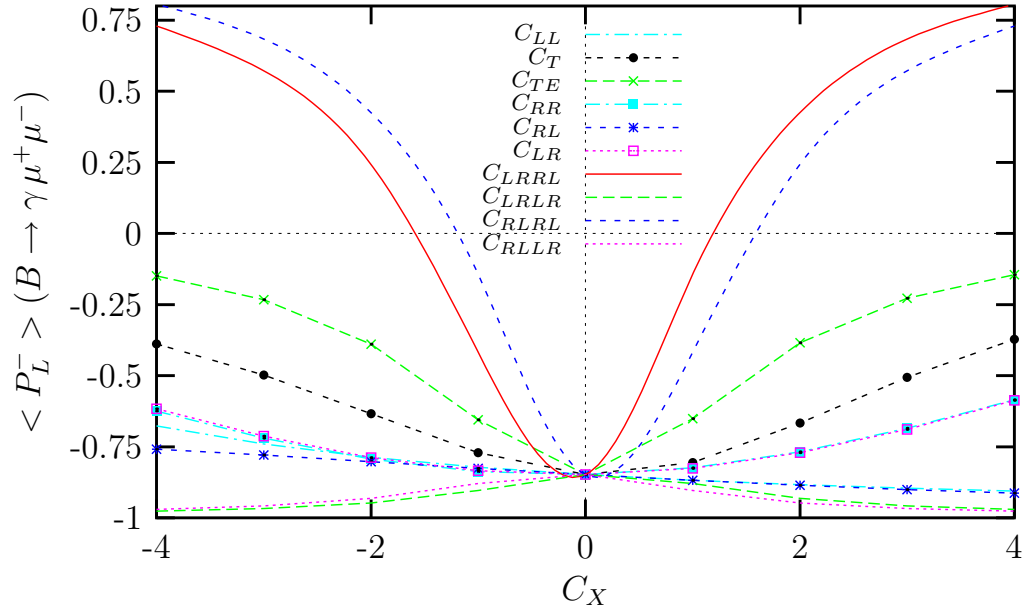


Figure 5.1: The dependence of the averaged longitudinal polarization $\langle P_L^- \rangle$ of ℓ^- for the $B_s \rightarrow \gamma \mu^+ \mu^-$ decay on the new Wilson coefficients .

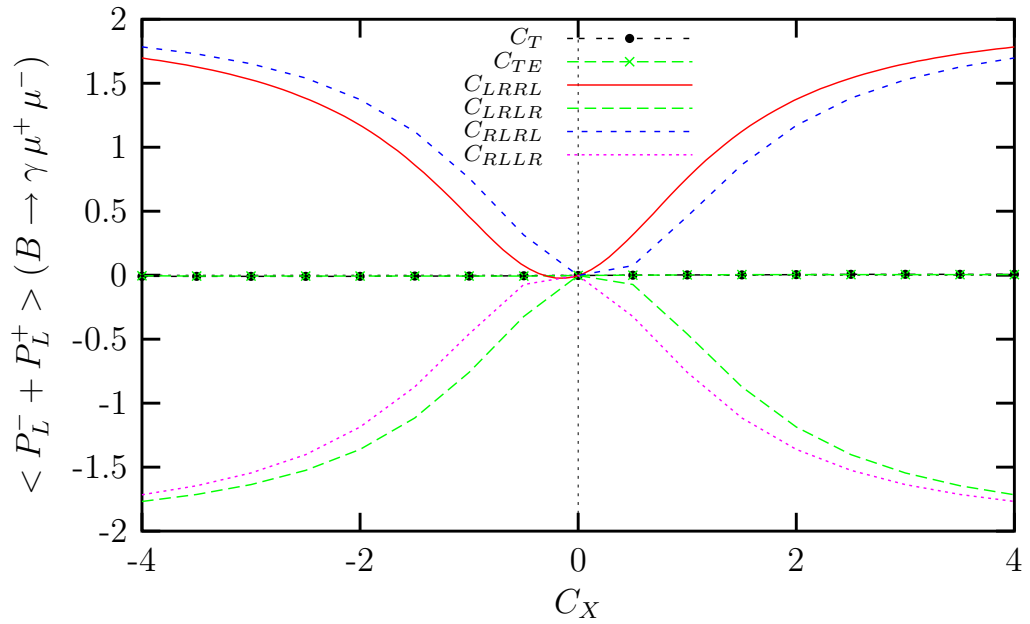


Figure 5.2: The dependence of the combined averaged longitudinal lepton polarization $\langle P_L^- + P_L^+ \rangle$ for the $B_s \rightarrow \gamma \mu^+ \mu^-$ decay on the new Wilson coefficients .

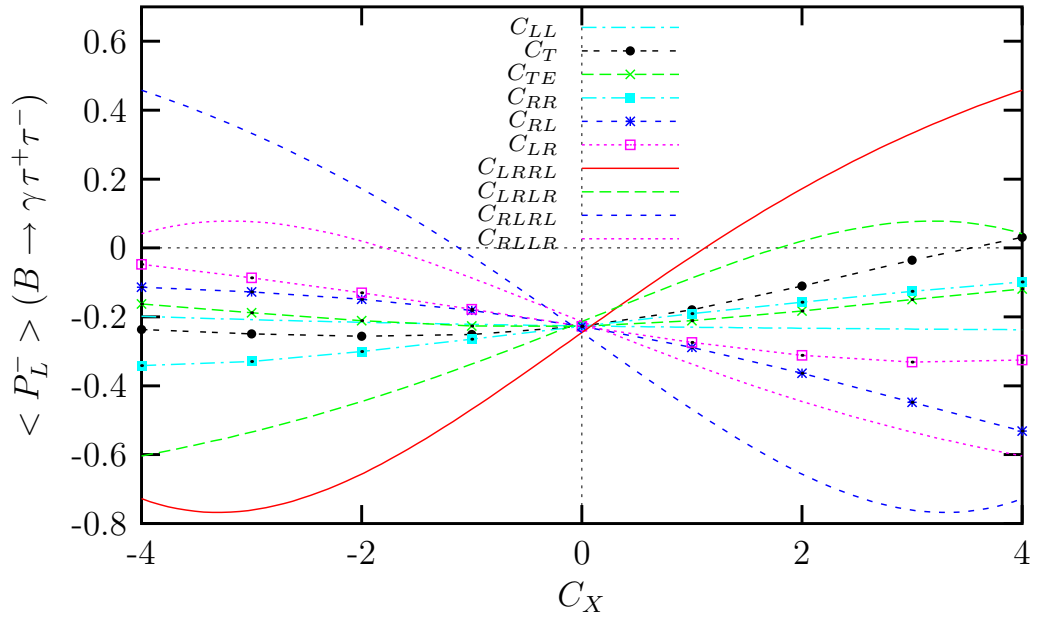


Figure 5.3: The same as Fig.(5.1), but for the $B_s \rightarrow \gamma \tau^+ \tau^-$ decay .

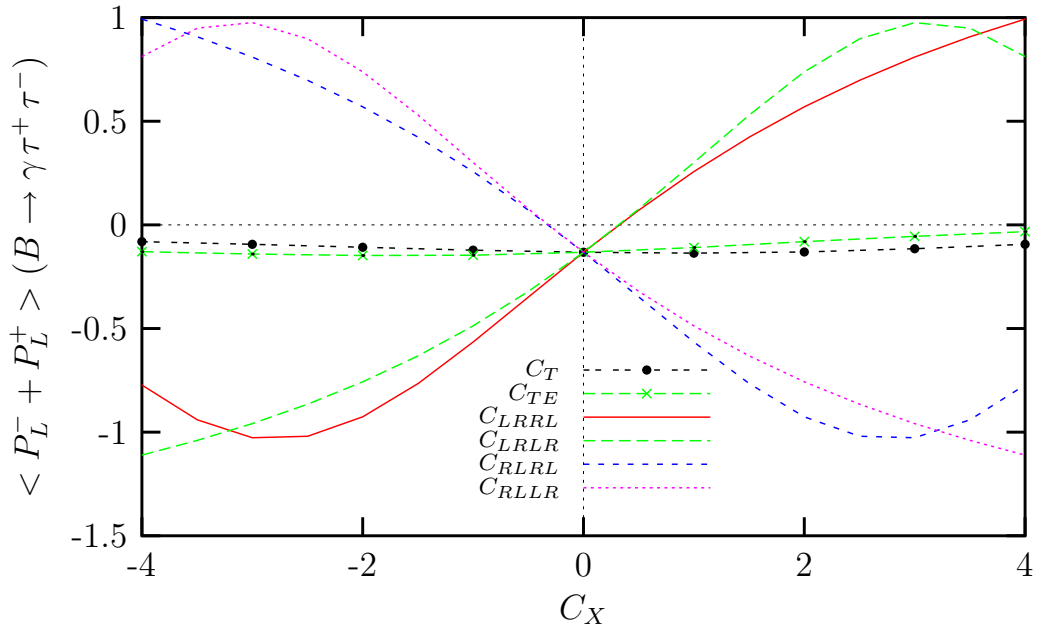


Figure 5.4: The same as Fig.(5.2), but for the $B_s \rightarrow \gamma \tau^+ \tau^-$ decay.

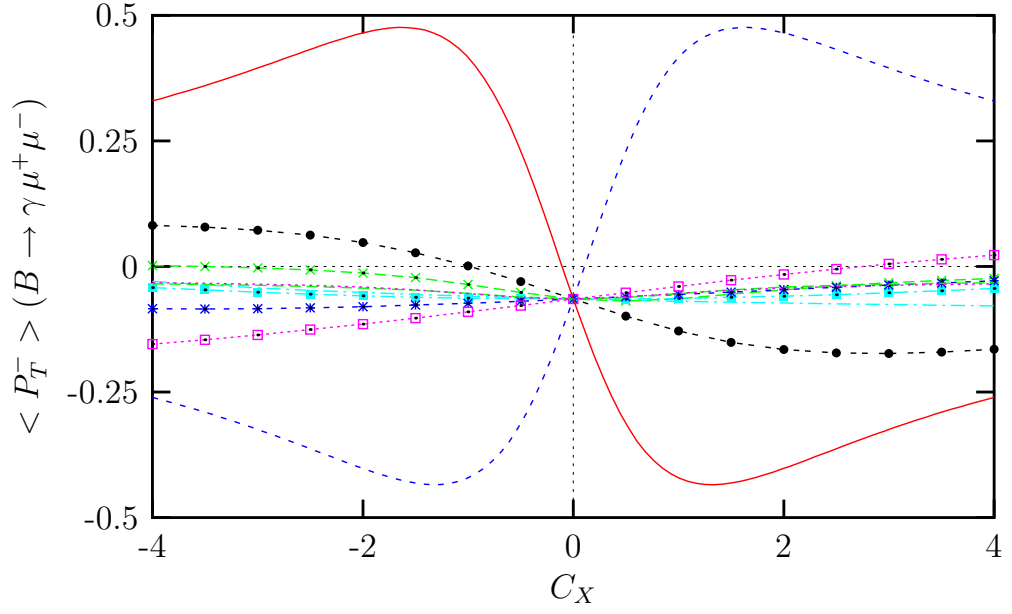


Figure 5.5: The dependence of the averaged transverse polarization $\langle P_T^- \rangle$ of ℓ^- for the $B_s \rightarrow \gamma \mu^+ \mu^-$ decay on the new Wilson coefficients. The line convention is the same as before.

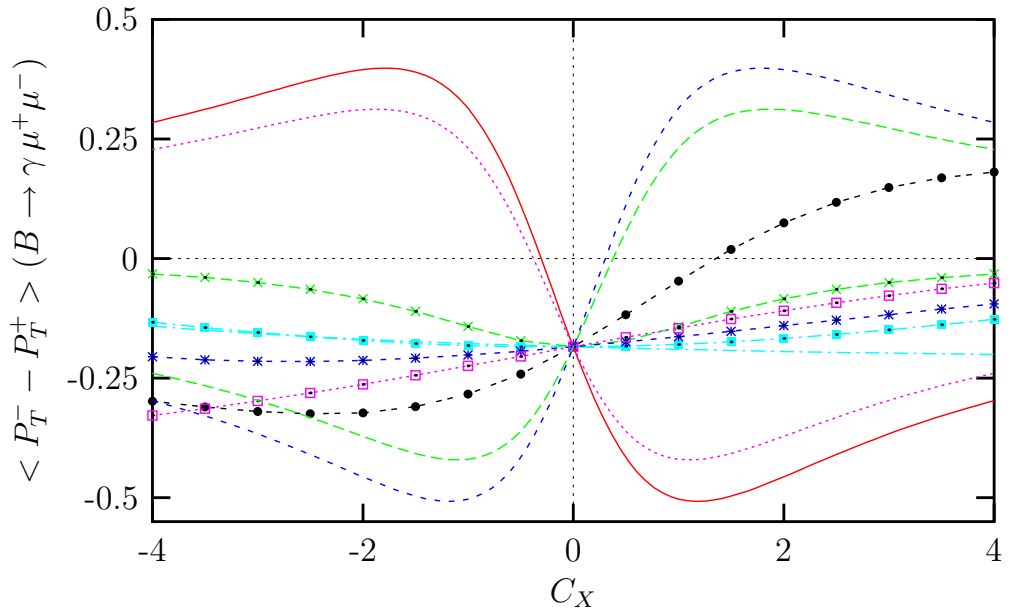


Figure 5.6: The dependence of the combined averaged transverse lepton polarization $\langle P_T^- - P_T^+ \rangle$ for the $B_s \rightarrow \gamma \mu^+ \mu^-$ decay on the new Wilson coefficients. The line convention is the same as before.

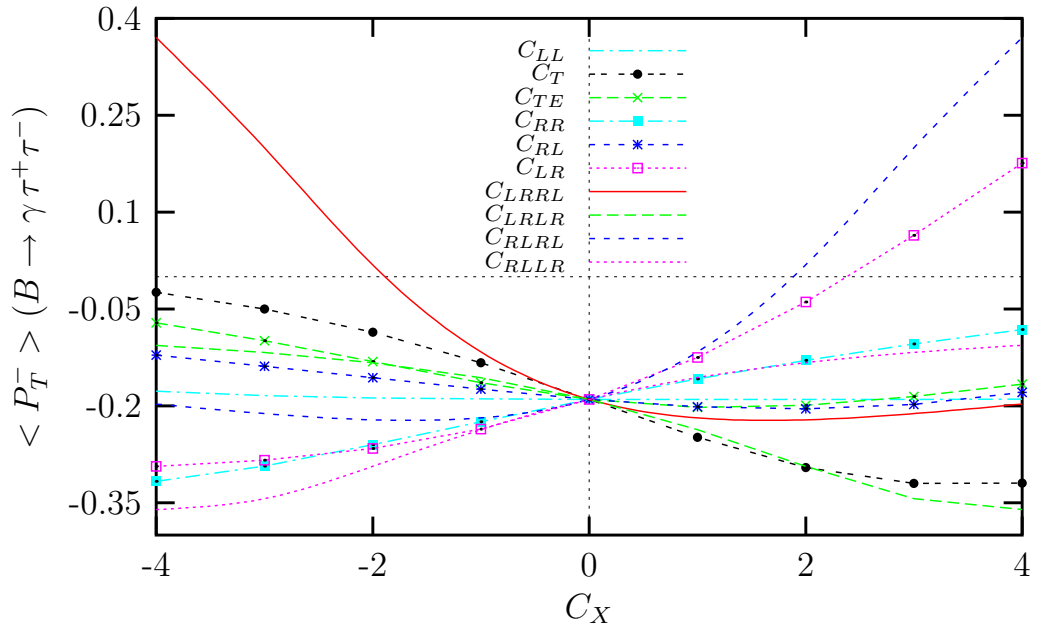


Figure 5.7: The same as Fig.(5.5), but for the $B_s \rightarrow \gamma \tau^+ \tau^-$ decay.

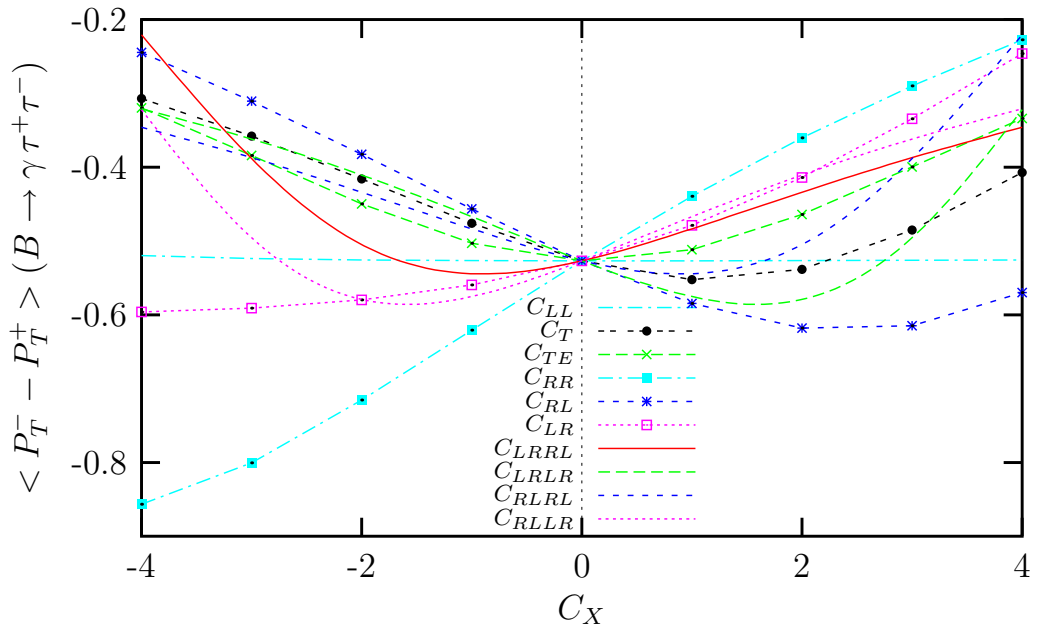


Figure 5.8: The same as Fig.(5.6), but for the $B_s \rightarrow \gamma \tau^+ \tau^-$ decay.

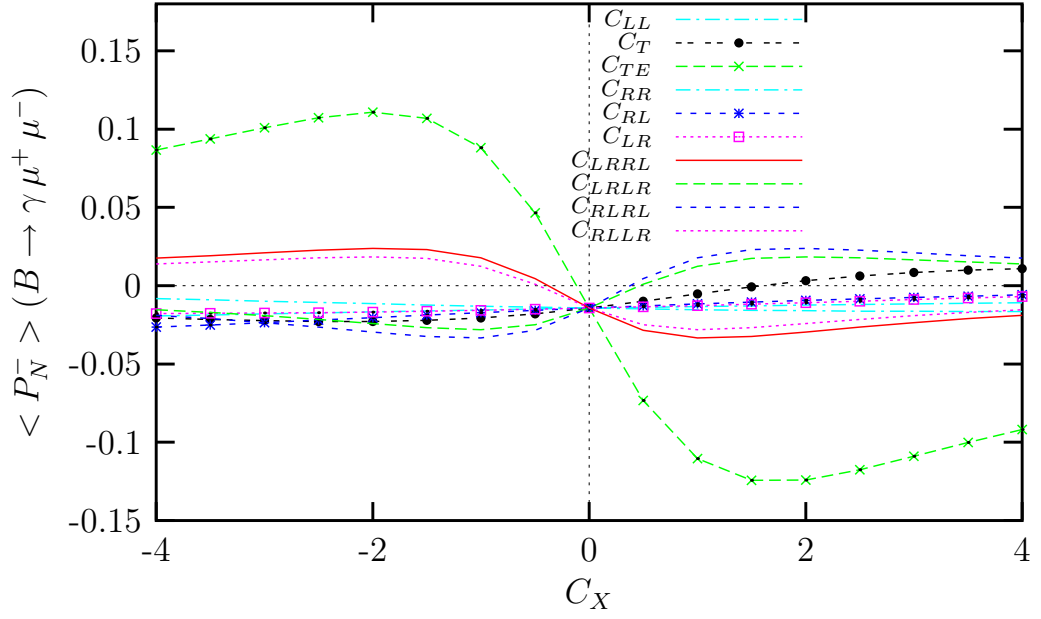


Figure 5.9: The dependence of the averaged normal polarization $\langle P_N^- \rangle$ of ℓ^- for the $B_s \rightarrow \gamma \mu^+ \mu^-$ decay on the new Wilson coefficients .

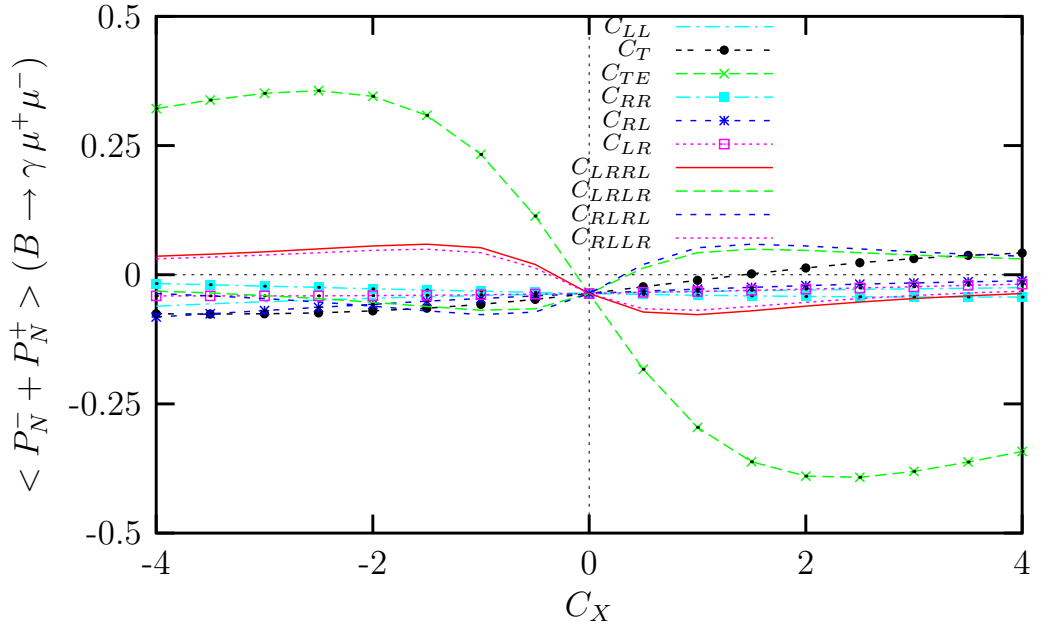


Figure 5.10: The dependence of the combined averaged normal lepton polarization $\langle P_N^- + P_N^+ \rangle$ for the $B_s \rightarrow \gamma \mu^+ \mu^-$ decay on the new Wilson coefficients.

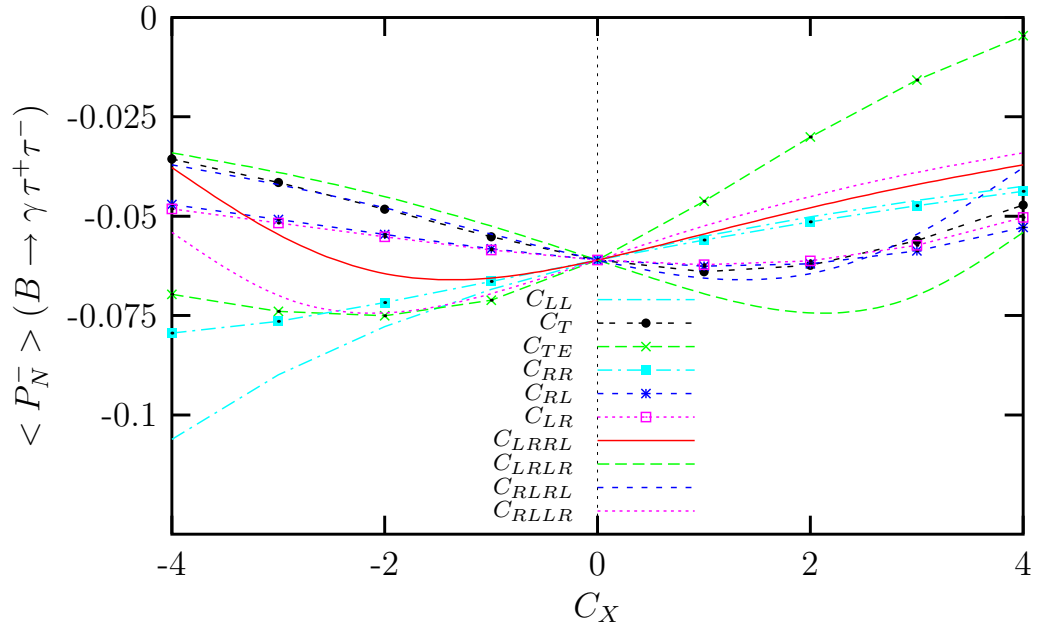


Figure 5.11: The same as Fig.(5.10), but for the $B_s \rightarrow \gamma \tau^+ \tau^-$ decay.

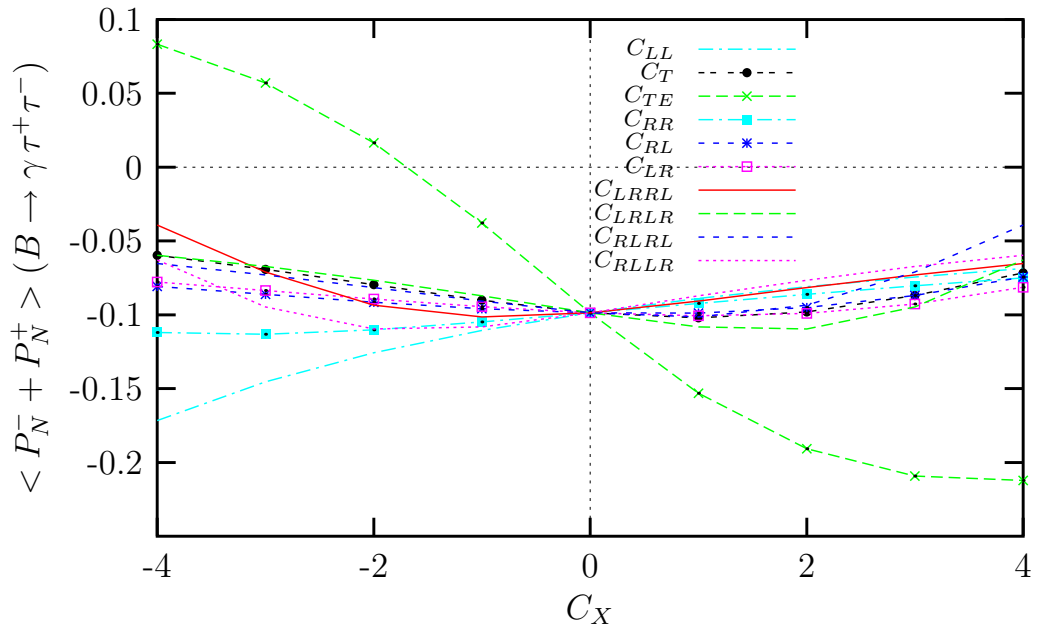


Figure 5.12: The same as Fig. (5.10), but for the $B_s \rightarrow \gamma \tau^+ \tau^-$ decay.

CHAPTER 6

DISCUSSION AND CONCLUSION

It has been realized for a long time that rare B-meson decays induced by the FCNC are one of the most promising fields in particle physics. They comprise very useful probes for obtaining information about the fundamental parameters of the SM and testing its predictions at loop level. At the same time rare decays can also serve as good probes for establishing new physics beyond the SM, such as the 2HDM, minimal supersymmetric extension of the SM, etc., since the contributions from these new models and the SM arise at the same order in perturbation theory.

The experimental situation concerning B-physics is also drastically changing since the first observation of radiative penguin mediated processes, in both the exclusive $B \rightarrow K^*\gamma$ [77] and inclusive $B \rightarrow X_s\gamma$ [78] channels. There are now several B physics experiments running and, in the upcoming years, new facilities will start to measure the decays we have discussed in this work and several others with increasing sensitivity.

Within this thesis, we have studied the radiative rare $B_s \rightarrow \gamma\ell^+\ell^-$ decay by using the most general model independent effective Hamiltonian. Our work mainly consists of two parts: In the first part, we have studied $B_s \rightarrow \gamma\ell^+\ell^-$ decay by taking into account the polarization of final photon. We have investigated the sensitivity of photon polarization asymmetry $H(x)$ to the new Wilson coefficients, in addition to the study of the total and differential branching ratios when the photon is in the positive and negative helicity state, $BR^{(1,2)}$ and $dBR^{(1,2)}(x)/dx$. The second part of the thesis has been devoted to the study of the possible new physics effects in the lepton polarization asymmetries in the $B_s \rightarrow \gamma\ell^+\ell^-$ decay. The sensitivity of the longitudinal, transverse and normal polarizations of the leptons, as well as lepton-antilepton combined asymmetries, on the new Wilson

coefficients have been investigated. The main conclusions that can be extracted from our analysis can be summarized as follows:

- $BR^{(1)}$ and $BR^{(2)}$ are more sensitive to all type of the scalar interactions as compared to the vector and tensor types; receiving the maximum contribution from the one with coefficient C_{RLRL} and C_{LRLR} , respectively. Dependence of $BR^{(2)}$ on all the new Wilson coefficients is symmetric with respect to the zero point, while for $BR^{(1)}$, this symmetry is slightly lifted for the vector type interactions.
- Tensor (scalar) type interactions change the spectrum of $dBR^{(1,2)}(x)/dx$ near the large (small)-recoil limit, $x \rightarrow 1$ ($x \rightarrow 0$). However, the vector type interactions increase the spectrum in the center of the phase space and do not change it at the large or small-recoil limit. When $C_{LL} > 0$, the related vector interaction gives constructive contribution to the SM result, but for the negative values of C_{LL} the contribution is destructive. Therefore, it is possible to get the information about the sign of new Wilson coefficients from measurement of the differential branching ratio.
- Spectrum of H is almost symmetrical with respect to the zero point for all the new Wilson coefficients, except for C_{RL} . The coefficient C_{RL} , when it is between -2 and 0 , is also the only one which gives the constructive contribution to the SM prediction of H , which we find $H(B_s \rightarrow \gamma \mu^+ \mu^-) = 0.74$. This behavior is also seen in the differential photon polarization asymmetry $H(x)$ for the different values of the vector interaction with coefficients C_{RL} . From these considerations we can conclude that performing measurement of H at different photon energies can give information about the signs of the new Wilson coefficients, as well as their magnitudes.
- $\langle P_L^- \rangle$ is strongly dependent on scalar type interactions with coefficients C_{RLRL} and C_{LRLR} , and quite sensitive to the tensor type interactions, while the combined average $\langle P_L^- + P_L^+ \rangle$ is mainly determined by scalar interactions only. The fact that values of $\langle P_L^- \rangle$ become substantially different

from the SM value (at $C_X = 0$) as C_X becomes different from zero indicates that measurement of the longitudinal lepton polarization in $B_s \rightarrow \gamma\mu^+\mu^-$ decay can be very useful to investigate new physics beyond the SM. In addition we have found that $\langle P_L^- + P_L^+ \rangle$ is not sensitive on vector type interactions at all. This is what is already expected since vector type interactions are cancelled when the longitudinal polarization asymmetry of the lepton and antilepton is considered together. We have also noted that $\langle P_L^- + P_L^+ \rangle$ becomes almost zero at $C_X = 0$, which confirms the SM result, and its dependence on C_X is symmetric with respect to this zero point. It is interesting to note also that $\langle P_L^- + P_L^+ \rangle$ is positive for all values of C_{RLRL} and C_{LRRL} , while it is negative for remaining scalar type interactions .

- Similar to the muon case, for τ channel $\langle P_L^- \rangle$ is sensitive to scalar type interactions also, but all type. It is an decreasing (increasing) function of C_{RLRL} and C_{RLLR} (C_{LRRL} and C_{LRLR}). The value of $\langle P_L^- \rangle$ is positive when $C_{RLRL} \lesssim -1$, $C_{RLLR} \lesssim -2$, $C_{LRRL} \gtrsim 1$ and $C_{LRLR} \gtrsim 2$. The behavior of the combined average $\langle P_L^- + P_L^+ \rangle$ for $B_s \rightarrow \gamma\tau^+\tau^-$ decay is different from the muon case in that it changes sign for a given scalar type interaction: e.g., $\langle P_L^- + P_L^+ \rangle > 0$ when $C_{RLRL}, C_{RLLR} \lesssim 0$, while $\langle P_L^- + P_L^+ \rangle < 0$ when $C_{RLRL}, C_{RLLR} \gtrsim 0$. Therefore, it can provide valuable information about the new physics to determine the sign and the magnitude of $\langle P_L^- \rangle$ and $\langle P_L^- + P_L^+ \rangle$.
- For τ channel, $\langle P_T^- \rangle$ strongly depends on the scalar interactions with coefficient C_{RLRL} and C_{LRRL} and quite weakly on all the other Wilson coefficients. It is also interesting to note that $\langle P_T^- \rangle$ is positive (negative) for the negative (positive) values of C_{LRRL} , except a small region about the zero values of the coefficient, while its behavior with respect to C_{RLRL} is opposite. As being different from $\langle P_T^- \rangle$ case, in the combination $\langle P_T^- - P_T^+ \rangle$ there appears strong dependence on scalar interaction with

coefficients C_{RLLR} and C_{LRLR} too, as well as on C_{RLRL} and C_{LRRL} . It is also quite sensitive to the tensor interaction with coefficient C_T .

- As in the muon case, for τ channel too, the dominant contribution to the transverse polarization comes from the scalar interactions, but it exhibits a more sensitive dependence to the remaining types of interactions as well than the muon case. $\langle P_T^- - P_T^+ \rangle$ is negative for all values of the new Wilson coefficients, while $\langle P_T^- \rangle$ again changes sign depending on the change in the new Wilson coefficients: e.g., $\langle P_T^- \rangle > 0$ only when $C_{LRRL} \lesssim -2$ and $C_{RLRL}, C_{LR} \gtrsim 2$. Remembering that in SM in massless lepton case, $\langle P_T^- \rangle \approx 0$ and $\langle P_T^- - P_T^+ \rangle \approx 0$, determination of the sign of these observables can give useful information about the existence of new physics.
- Behavior of both $\langle P_N^- \rangle$ and $\langle P_N^- + P_N^+ \rangle$ are determined by tensor type interactions with coefficient C_{TE} for τ channel. They are both positive (negative) when $C_{TE} \lesssim 0$ ($C_{TE} \gtrsim 0$).

In conclusion, it has been shown that all these physical observables are very sensitive to the existence of new physics beyond the SM and their investigation can give valuable information about its parameters.

REFERENCES

- [1] For a review, see E. S. Abers and B. W. Lee, *Phys. Rep.* **9** (1973) 1; M. Herrero, *hep-ph/98122242*; P. Langacker, Precision Tests of the Standard Electroweak Model, ed. P. Langacker (World, Singapore, 1995), *hep-ph/0304186*.
- [2] CLEO Collaboration, S. Chen, *et al.*, *Phys. Rev. Lett.* **87** (2001) 251807; T. E. Coan, *et al.*, CLEO Collaboration, *Phys. Rev. Lett.* **84** (2000) 5283.
- [3] BaBar Collaboration, B. Aubert, *et al.*, SLAC-PUB-9610, *hep-ex/0207076*; *ibid.* *Phys. Rev. Lett.* **88** (2002) 101905.
- [4] BELLE Collaboration, K. Abe, *et al.*, *Phys. Lett.* **B511** (2001) 151; *ibid.* Belle-CONF-0319.
- [5] C. Jessop, SLAC-PUB-9610 (2002).
- [6] M. Nakao, *Int. J. Mod. Phys.* **A19** (2004) 934.
- [7] BELLE Collaboration, J. Kaneko, *et al.*, *Phys. Rev. Lett.* **90** (2003) 021801; *ibid.* K. Abe *et al.*, *Phys. Rev. Lett.* **88** (2002) 021801.
- [8] BaBar Collaboration, B. Aubert, *et al.*, SLAC-PUB-10100, *hep-ex/0308016*; *ibid.* *hep-ex/0207082*.
- [9] B. Grinstein, R. Springer and M. Wise, *Nucl. Phys.* **B339** (1990) 269; R. Grigjanis, P. J. O'Donnell, M. Sutherland and H. Navelet, *Phys. Lett.* **B213** (1988) 355; Erratum: *ibid* **B286** (1992) 413; G. Cella, G. Curci, G. Ricciardi and A. Viceré, *Phys. Lett.* **B325** (1994) 227; *ibid* *Nucl. Phys.* **B431** (1994) 417.
- [10] M. Misiak, *Nucl. Phys.* **B393** (1993) 23; Erratum: *ibid.* **B439** (1995) 461.
- [11] G. Buchalla, A. Buras, and M. Lautenbacher, *Rev. Mod. Phys.* **68** (1996) 1125.
- [12] T. Inami and C. S. Lim, *Prog. Theor. Phys.* **65** (1981) 297; Erratum: *ibid.* **65** (1981) 1772.
- [13] A. J. Buras and M. Münz, *Phys. Rev.* **D52** (1995) 186.
- [14] A. J. Buras, M. Misiak, M. Münz and S. Pokorski, *Nucl. Phys.* **B424** (1994) 374.

- [15] M. Ciuchini, E. Franco, G. Martinelli, L. Reina and L. Silvestrini, *Phys. Lett.* **B316**(1993)127.
- [16] M. Ciuchini, E. Franco, G. Martinelli and L. Reina, *Nucl. Phys.* **B415**(1994)403.
- [17] M. Ciuchini, E. Franco, G. Martinelli, L. Reina and L. Silvestrini, *Nucl. Phys.* **B421**(1994)41.
- [18] G. Eilam, I. Halperin and R. Mendel, *Phys. Lett.* **B 361**(1995) 137.
- [19] T. Aliev, A. Özpineci and M. Savci, *Phys. Rev.* **D55** (1997) 7059 .
- [20] C. Q. Geng, C. C. Lih and W. M. Zhang, *Phys. Rev.* **D62** (2000) 074017.
- [21] F. Kruger and D. Melikhov, *Phys. Rev.* **D 67** (2003) 034002.
- [22] S. R. Choudhury, N. Gaur, and N. Mahajan, *Phys. Rev.* **D 66** (2002) 054003.
- [23] R. D. Field, *Perturbative QCD*, Addison-Wesley, Redwood City, (1989); F. J. Yndurain, *The Theory of Quark and Gluon Interactions*, Springer-Verlag, Berlin, (1993).
- [24] S. L. Glashow, *Nucl. Phys.* **B22** (1961) 579; S. Weinberg, *Phys. Rev. Lett.* **19** (1967) 1264; A. Salam, in: *Proceedings of the 8th Nobel symposium*, p. 367, ed. N. Svartholm, Almqvist and Wiksell, Stockholm 1968.
- [25] S. L. Glashow, I. Iliopoulos, L. Maiani, *Phys. Rev.* **D2** (1970) 1285.
- [26] N. Cabibbo, *Phys. Rev. Lett.* **10** (1963) 531; M. Kobayashi, K. Maskawa, *Prog. Theor. Phys.* **49** (1973) 652.
- [27] H. Y. Han, Y. Nambu, *Phys. Rev.* **139** (1965) 1006; C. Bouchiat, I. Iliopoulos, Ph. Meyer, *Phys. Lett.* **B138** (1972) 652.
- [28] G. Arnison, *et. al.*, (UA1 Collaboration) *Phys. Lett.* **B122** (1983) 103; P. Bagnaia *et. al.*, (UA2 Collaboration) *Phys. Lett.* **B129** (1983) 130.
- [29] N. Cabibbo *et al.*, *Nucl. Phys.* **B158** (1979), 295.
- [30] R. Barate *et. al.*, *Phys. Lett.* **B565** (2003) 61.
- [31] L.L. Chau and W.-Y. Keung, *Phys. Rev. Lett.* **53** (1984) 1802.
- [32] Particle Data Group, *Phys. Rev.* **D66** (2002) 010001.
- [33] L. Wolfenstein, *Phys. Rev. Lett.* **51** (1983) 1945.
- [34] See f.eg. a recent review by, M. Vysotsky, *Surv. High Energy Phys.* **18** (2003) 19.

- [35] S. King, *Beyond the Standard Model*, Carleton Univ., Ottawa (1992).
- [36] H. E. Haber and G. Kane, *Phys. Rep.* **C117** (1985) 75.
- [37] Super-Kamiokande Collaboration, *Phys. Rev. Lett.* **81** (1998) 1562; SNO Collaboration, *Phys. Rev. Lett.* **89** (2002) 011301.
- [38] J. Lee, *Nucl. Phys. Proc. Suppl.* **93** (2001) 259.
- [39] BABAR Collaboration, *Nucl. Phys. Proc. Suppl.* **93** (2001) 336.
- [40] BELLE Collaboration, *Nucl. Phys. A* **684** (2001) 704.
- [41] CDF and D0 Collaborations, *Nucl. Phys. Proc. Suppl.* **99** (2001) 200.
- [42] LHCb Collaboration, *Nucl. Phys. Proc. Suppl.* **93** (2001) 352.
- [43] BTeV Collaboration, *Nucl. Phys. Proc. Suppl.* **93** (2001) 303.
- [44] N. Isgur and M. B. Wise, *Phys. Lett.* **B232** (1989) 113; *ibid.* **B237** (1990).
- [45] C. Bobeth, M. Misiak and J. Urban, *Nucl. Phys.* **B574** (2000) 291
- [46] P. Gambino, M. Gorbahn and U. Haisch, *Nucl. Phys.* **B673** (2003) 238.
- [47] H. H. Asatryan, H. M. Asatrian, C. Greub and M. Walker, *Phys. Rev.* **D65** (2002) 074004.
- [48] H. H. Asatryan, H. M. Asatrian, C. Greub and M. Walker, *Phys. Rev.* **D66** (2002) 034009.
- [49] A. Ghinculov, T. Hurth, G. Isidori and Y. P. Yao, *Nucl. Phys.* **B648** (2003) 254.
- [50] H. M. Asatrian, K. Bieri, C. Greub and A. Hovhannisyanyan, *Phys. Rev.* **D66** (2002) 094013.
- [51] A. Ghinculov, T. Hurth, G. Isidori and Y. P. Yao, *Nucl. Phys. Proc. Suppl.* **116** (2003) 284.
- [52] A. Ghinculov, T. Hurth, G. Isidori and Y. P. Yao, CERN-TH/2003-132.
- [53] T. Hurth, *Rev. Mod. Phys.* **75** (2003) 1159.
- [54] A. Ali, T. Mannel and T. Morozumi, *Phys. Lett.* **B273** (1991) 505.
- [55] G. Burdman, T. Goldman and D. Wyler, *Phys. Rev.* **D 51** (1995) 111.
- [56] D. Atwood, G. Eilam and A. Soni *Mod. Phys. Lett.* **A11** (1996) 1061.
- [57] P. Colangelo, F. De Fazio, G. Nardulli, *Phys. Lett.* **B372** (1996) 331.

- [58] T. Aliev, A. Özpineci and M. Savcı, *Phys. Lett.* **B393** (1997) 143.
- [59] T. M. Aliev, N. K. Pak, and M.Savcı, *Phys. Lett.* **B 424** (1998) 175.
- [60] C. Q. Geng, C. C. Lih and W. M. Zhang, *Phys. Rev.* **D57** (1998) 5697.
- [61] C. C. Lih, C. Q. Geng and W. M. Zhang, *Phys. Rev.* **D59** (1999) 114002.
- [62] G. P. Korchemsky, Dan Pirjol and Tung-Mow Yan, *Phys.Rev.* **D61** (2000) 114510.
- [63] G. Eilam, C.-D. Lü and D.-X. Zhang, *Phys. Lett.* **B391** (1997)461.
- [64] Z. Xiong and J. M.Yang, *Nucl. Phys.* **B628** (2002) 193.
- [65] S. R. Choudhury, and N. Gaur, *hep-ph/0205076*.
- [66] S. R. Choudhury, and N. Gaur, *hep-ph/0207353*.
- [67] E. O. Iltan and G. Turan, *Phys. Rev.* **D61** (2000) 034010.
- [68] T. M. Aliev, A. Özpineci and M. Savcı, *Phys. Lett.* **B 520** (2001) 69.
- [69] G. Erkol and G. Turan, *Phys. Rev.* **D65** (2002) 094029.
- [70] G. Erkol and G. Turan, *Acta Phys. Pol.* **B33**, No:5, (2002) 1285.
- [71] T. M. Aliev, C. S. Kim and Y. G. Kim, *Phys. Rev.* **D62** (2000) 014026;
T. M. Aliev, D. A. Demir and M. Savcı, *Phys. Rev.* **D62** (2000) 074016;
S. Fukae, C. S. Kim, T. Morozumi and T. Yoshikawa, *Phys. Rev.* **D59**
(1999) 074013.
- [72] B. Sirvanli and G. Turan, *Mod. Phys. Lett.* **A18** (2003) 47.
- [73] V. Halyo, *hep-ex/0207010*.
- [74] Chao-Shang Huang and Xiao-Hong Wu, *Nucl. Phys.* **B665** (2003) 304.
- [75] S. Fukae, C. S. Kim, T. Morozumi and T. Yoshikawa, *Phys. Rev.* **D61**
(2000) 074015.
- [76] T. M. Aliev, M. K. Çakmak and M. Savcı, *Nucl. Phys.* **B 607** (2001) 305;
T. M. Aliev, M. K. Çakmak, A. Özpineci and M. Savcı, *Phys. Rev.* **D64**
(2001) 055007.
- [77] CLEO Collaboration, R. Ammar, *et al.*, *Phys. Rev. Lett.* **71** (1993) 674;
CLEO Collaboration, M. S. Alam, *et all.*, *Phys. Rev. Lett.* **74** (1995) 2885.
- [78] CLEO Collaboration, M. S. Alam, *et al.*, in ICHEP98 Conference 1998;
ALEPH Collaboration, R. Barate *et al.*, *Phys. Lett.* **B429** (1998) 169.

APPENDIX A
INPUT PARAMETERS

$$m_B = 5.28 \text{ GeV}$$

$$m_b = 4.8 \text{ GeV}$$

$$m_\mu = 0.105 \text{ GeV}$$

$$m_\tau = 1.78 \text{ GeV}$$

$$f_B = 0.2 \text{ GeV}$$

$$|V_{tb}V_{ts}^*| = 0.045$$

$$\alpha^{-1} = 137$$

$$G_F = 1.17 \times 10^{-5} \text{ GeV}^{-2}$$

$$\tau_{B_s} = 1.54 \times 10^{-12} \text{ s}.$$

VITA

Personal Details:

Name: Ümit Oktay YILMAZ
Date of Birth: January 15, 1971
Date of Place: Rize, Turkey
Nationality: Turkish
Marital Status: Married
e-mail: uoyilmaz@yahoo.co.uk

Education:

MS, 1997 High Energy Physics
Department of Physics, Middle East Technical University
BS, 1994 Department of Physics, Middle East Technical University

Schools/ Seminars/ Conference Attended:

- * 15th National Physics Congress, Kas, Turkey, September 1995
- * Summer School in High Energy Physics and Cosmology, The Abdus Salam Int. Centre for Theoretical Physics, Trieste, Italy, 29 June- 17 July 1998
- * Summer School in Astroparticle Physics and Cosmology, The Abdus Salam Int. Centre for Theoretical Physics, Trieste, Italy, 12 June- 30 June 2000
- * NATO-Advance Study Institute-2000, Recent Developments in High Energy Physics and Cosmology, Cascais, Portekiz, 26 June-7 July 2000
- * 8th Adriatic Meeting, Particle Physics in New Millennium, Dubrovnik, Croatia, 4-14 September 2001

Publications/ Conference Contributions/ Preprints:

1. Ü. O. Yılmaz, B. B. Şirvanlı, G. Turan, "Model Independent Analysis of the Lepton Polarizations in $B_s \rightarrow \gamma \ell^+ \ell^-$ Decays" Nucl. Phys. B 692 (2004) 249
2. Ü. O. Yılmaz, B. B. Şirvanlı, G. Turan, "New Physics Effects in the Rare $B_s \rightarrow \gamma \ell^+ \ell^-$ Decays" Eur. Phys. J. C 30 (2003) 197
3. S. Atag, A. K. Çiftçi, A. Çelikel, S. Sultansoy, Ü. O. Yılmaz, "The Fourth SM Family, Breaking of Mass Democracy and the CKM Mixings" Phys. Rev. D 54 (1996) 5745
4. "Fourth Family in Standard Model, Breaking of Mass Democracy and CKM Mixings", NATO-Advance Study Institute-2000, Recent Developments in High Energy Physics and Cosmology, Cascais, Portugal, 26 June-7 July 2000
5. "Neutrino Mass Matrix, Lepton Charge Schemes and Oscillation Phenomena", 15th National Physics Congress, Kaş, Turkey, September 1995
6. A. K. Çiftçi, E. Pesen, R. Sever, S. Sultansoy, Ü. O. Yılmaz "Lepton Number Schemes, Neutrino Mass Matrix and Oscillation Phenomena", AU-HEP-96/06, METU-HEP-96/11 (CERN scan-9608063)